

## **Hygrothermal Performance of Hydrophobized Brick and Mortar**

*Energy Renovation Through Internal Insulation - Can Hydrophobization Improve the Moisture Safety?*

Soulios, Vasilis

DOI (link to publication from Publisher):  
[10.54337/aau459966346](https://doi.org/10.54337/aau459966346)

Publication date:  
2021

Document Version  
Publisher's PDF, also known as Version of record

[Link to publication from Aalborg University](#)

Citation for published version (APA):  
Soulios, V. (2021). *Hygrothermal Performance of Hydrophobized Brick and Mortar: Energy Renovation Through Internal Insulation - Can Hydrophobization Improve the Moisture Safety?* Aalborg Universitetsforlag.  
<https://doi.org/10.54337/aau459966346>

### **General rights**

Copyright and moral rights for the publications made accessible in the public portal are retained by the authors and/or other copyright owners and it is a condition of accessing publications that users recognise and abide by the legal requirements associated with these rights.

- Users may download and print one copy of any publication from the public portal for the purpose of private study or research.
- You may not further distribute the material or use it for any profit-making activity or commercial gain
- You may freely distribute the URL identifying the publication in the public portal -

### **Take down policy**

If you believe that this document breaches copyright please contact us at [vbn@aub.aau.dk](mailto:vbn@aub.aau.dk) providing details, and we will remove access to the work immediately and investigate your claim.



# **HYGROTHERMAL PERFORMANCE OF HYDROPHOBIZED BRICK AND MORTAR**

ENERGY RENOVATION THROUGH INTERNAL INSULATION  
– CAN HYDROPHOBIZATION IMPROVE THE MOISTURE SAFETY?

**BY  
VASILIS SOULIOS**

DISSERTATION SUBMITTED 2021



**AALBORG UNIVERSITY**  
DENMARK





# **HYGROTHERMAL PERFORMANCE OF HYDROPHOBIZED BRICK AND MORTAR**

**ENERGY RENOVATION THROUGH INTERNAL  
INSULATION - CAN HYDROPHOBIZATION IMPROVE THE  
MOISTURE SAFETY?**

by

Vasilis Soulios



**AALBORG UNIVERSITY**  
DENMARK

Dissertation submitted 2021

Dissertation submitted: July 1, 2021

PhD supervisor: Senior Researcher Ernst Jan de Place Hansen, PhD  
Aalborg University, Denmark

Assistant PhD supervisor: Research Director Ruut Peuhkuri, PhD  
Aalborg University, Denmark

PhD committee: Senior Researcher Martin Morelli (Chairman)  
Aalborg University

Associate Professor Kurt Kielsgaard Hansen  
Technical University of Denmark

Professor Andra Blumberga  
Riga Technical University

PhD Series: Faculty of Engineering and Science, Aalborg University

Department: Department of the Build Environment

ISSN (online): 2446-1636  
ISBN (online): 978-87-7210-961-9

Published by:  
Aalborg University Press  
Kroghstræde 3  
DK – 9220 Aalborg Ø  
Phone: +45 99407140  
aauf@forlag.aau.dk  
forlag.aau.dk

© Copyright: Vasilis Soulios

Printed in Denmark by Rosendahls, 2021

# BIOGRAPHICAL NOTE



I have been a member of the Department of the Built Environment at Aalborg University since 2018. My main research interest is in building physics. I'm particularly interested in moisture safe energy renovation of the building envelope by applying water repellent agents. The moral of my PhD work is that if you want to insulate your building from the interior, first impregnate the exterior.

Prior to coming to Denmark, I was working as a researcher in the building physics department in KU Leuven in Belgium on the same topic with my PhD in a project named "Hydrophobization and Internal insulation: a match made in heaven or hell?".

My journey in building physics started when I was working in a building materials company named TITAN Cement in Thessaloniki, Greece. While I was working at the company, I had an external collaboration with the building physics department from Eindhoven University of Technology where I co-authored my first journal paper.

I studied urban and spatial planning at the Aristotle University of Thessaloniki in Greece, specializing in the integration of renewables in a smart grid for medium-size cities. Then I completed a Master's degree in energy systems with a specialization in renewables and waste-to-energy technologies.

# PREFACE

This thesis is submitted as a fulfillment of the requirements for the Degree of Doctor of Philosophy at Aalborg University (AAU) in Copenhagen. Laboratory studies were conducted during my stay at KU Leuven, Belgium, at the Danish Technological Institute, Taastrup, Copenhagen, and at Aalborg University in Copenhagen. Funding for this work was provided by Realdania, The National Building Fund, The Danish Landowners Investment Fund, and Aalborg University. The project also had close collaboration with the Horizon 2020 project RIBuild ([www.ribuild.eu](http://www.ribuild.eu)).

First and foremost, I would like to thank my supervisor Ernst Jan de Place Hansen, and my co-supervisor Ruut Peuhkuri for their supervision, guidance, and encouragement during the course of this work.

Many thanks to my former colleague Eva B. Møller for all the discussions we had during the project and the supervising during my special course on the durability of the hydrophobic treatment. Special thanks go to Professor Hans Janssen for his supervision during my stay in Leuven. Many thanks also to Afshin Ghanbari-Siahkali from the Danish Technological Institute for helping me execute the artificial weathering tests. I would furthermore like to thank my wonderful colleagues both from the Dept. of the Built Environment (BUILD) at Aalborg University and from KU Leuven for their support and interest in my project. More specifically Tessa Kvist Hansen, Thomas Cornelius, Maria Saridaki, Nickolaj Feldt Jensen from BUILD, and Chi Feng and Vasileios Metavitsiadis from KU Leuven.

I would especially like to express my gratitude to Jane Dyhr and Maria Jacobsen as well as the whole management team of AAU Copenhagen for the great organization and support in all aspects around the PhD work and the PhD life.

Finally, my deepest gratitude goes to my family, and especially to Irene and Iokasti who were with me in Copenhagen during this amazing journey – thank you for always looking out for me.

Copenhagen, July 2021

Vasilis Soulios

# ENGLISH SUMMARY

**Background:** Improving the energy efficiency of the building stock has been an important goal for the European Union for at least 15 years. Given the vast numbers of existing buildings that need to be renovated, efforts towards improving the energy efficiency of these buildings are expected to be increased. Internal insulation of external masonry walls is often the only alternative in existing buildings to maintain the appearance of the facade. However, internal insulation is not considered a moisture safe renovation measure, and wind-driven rain is a main source of moisture to the masonry. Hydrophobization could be a measure to reduce wind-driven rain load on solid masonry facades. Thus, knowledge regarding the application of water repellent agents to such a building facade is required.

**Objective:** The primary objective of the PhD thesis is to characterize, at the material level, the impact and durability of water repellent agents on building materials used for solid masonry facades: brick and mortar. The secondary objective is to evaluate, at the component level, the impact of water repellent agents on internally insulated solid masonry walls.

**Methods & Results:** The present PhD thesis is based on three journal articles, in the following referred to as Papers I, II, and III. Papers I and II focus on the material level, paper III on the component level.

Paper I determines the hygric properties of hydrophobized brick and mortar samples. The open porosity and pore size distribution were measured with vacuum saturation and mercury intrusion testing respectively, revealing only small changes in the storage properties after impregnation. Transport properties in terms of liquid transport were blocked according to capillary water uptake tests. Vapor transport remained almost the same, according to cup tests. Moreover, liquid water impermeability improved after exposure to water as shown by repeating the capillary water uptake tests. In addition, water uptake tests from the non-impregnated side of the samples showed that the water repellent agent is redistributed inside the material after impregnation.

Paper II illustrates that the hydrophobic layer maintains its very low water absorption performance both in brick and mortar, after artificial aging that includes exposure to water and UV radiation. The samples were treated with two different water repellent agents in different concentrations and capillary water uptake tests were performed. Additionally, the findings showed that the absorption coefficient of hydrophobized brick and mortar samples could be further reduced after aging, due to water exposure. Subsequently, Karsten tube tests on artificially aged samples illustrated the same water repellency performance with mock-up walls exposed to ambient conditions,

after being hydrophobized for six years, also tested with Karsten tube. The beading effect declined with aging, according to contact angle measurements before and after artificial aging. However, the beading effect is just a surface property, affected by UV radiation and does not influence water uptake. Moreover, visual inspection after aging showed that the hydrophobized brick and mortar samples kept their appearance while untreated samples showed signs of efflorescence.

Paper III evaluates the hygrothermal impact of hydrophobization of solid masonry when combined with internal insulation. To predict this effect, it is important to accurately model the hydrophobic layer of the masonry. The developed hydrophobic model was able to predict the hygrothermal behavior of the hydrophobized brick, using experimental results from Paper I. In combination with RH measurements at the interface between masonry and internal insulation of a case study building, simulation results indicated that it is preferable to apply hydrophobization before or at the same time as internal insulation. Otherwise, the desired hygrothermal benefits need more time to be achieved, due to the slower drying of the moisture inside the masonry.

**Conclusion:** The results showed that water repellent agents successfully create a water-tight but vapor-open hydrophobic layer that goes deep into the hydrophobized material, without significantly changing its pore structure. Water uptake of hydrophobized brick or mortar remains very low after aging. Further, it is shown that in combination with either a capillary-active or a water-vapor-tight internal insulation system, hydrophobization can provide a moisture safe energy renovation of solid masonry external walls.

# DANSK RESUME

Baggrund: Forbedring af bygningers energieffektivitet har været et vigtigt mål for Den Europæiske Union i mindst 15 år. I betragtning af det store antal eksisterende bygninger der skal renoveres, forventes indsatsen for at forbedre energieffektiviteten i disse bygninger at blive forøget. Indvendig isolering af murværkets ydervægge er ofte det eneste alternativ i eksisterende bygninger for at opretholde facadens udseende. Indvendig isolering betragtes dog ikke som en fugtsikker renoveringsmetode, og slagregn er en væsentlig kilde til fugt i massivt murværk i historiske bygninger. Derfor er det nødvendigt med viden om effekten af at påføre vandafvisende midler på en sådan bygningsfacade.

Formål: Det primære formål med ph.d.-afhandlingen er på materialeniveau at karakterisere effekten og holdbarheden af vandafvisende midler på byggematerialer, der anvendes til massivt murværk i historiske bygninger, dvs. mursten og mørtel. Det sekundære mål er på komponentniveau at vurdere effekten af vandafvisende midler på indvendigt isolerede ydervægge af massivt murværk.

Metoder og resultater: Denne ph.d.-afhandling er baseret på tre tidsskriftartikler, herefter benævnt artikel I, II og III. Artikel I og II fokuserer på materialeniveauet, artikel III på komponentniveauet.

I artikel I bestemmes de hygrotermiske egenskaber af hydrofoberede mursten og mørtelprøver. Den åbne porøsitet og porestørrelsesfordelingen blev målt med henholdsvis vakuumvandmætning og kviksvølvporøsimetri og afslørede kun små ændringer i lagringsegenskaberne efter imprægnering. Kapillarsugningsforsøg viser, at fugttransport på væskeform blokeres næsten fuldstændigt. Derimod er transport af vanddamp næsten uændret, ifølge kopforsøg. Uigennemtrængeligheden for vand på væskeform øges yderligere efter udsættelse for vand, vist ved gentagelse af kapillarsugningsforsøg. Derudover viste kapillarsugning fra den ikke-imprægnerede side af prøverne, at det vandafvisende middel fordeles inde i materialet efter imprægnering.

Artikel II illustrerer, at det hydrofoberede lag opretholder sin meget lave vandabsorptionsevne både i mursten og mørtel efter kunstig ældning, bestående af eksponering for vand og UV-stråling. Prøverne blev behandlet med to forskellige vandafvisende midler i forskellige koncentrationer, og der blev udført kapillarsugningsforsøg. Derudover viser resultaterne, at absorptionskoefficienten for hydrofoberede murstens- og mørtelprøver reduceres yderligere efter ældning. Endvidere viser forsøg med Karsten målerør på kunstigt ældede prøver den samme vandafvisende ydeevne som for mock-up vægge, eksponeret for vejrliget i seks år efter at være hydrofobert. Perleeffekten aftager med ældning i henhold til målinger

af kontaktvinkler før og efter kunstig ældning. Imidlertid er perleeffekten kun en overfladeegenskab, der er påvirket af UV-stråling og påvirker ikke vandoptagelsen. Desuden viste visuel inspektion efter ældning, at de hydrofoberede mursten og mørtelprøver bevarer deres udseende, mens ubehandlede prøver viser tegn på udblomstring.

I artikel III undersøges den hygrotermiske effekt af hydrofobering af murværk kombineret med indvendig isolering. For at kunne vurdere effekten, er det vigtigt nøjagtigt at kunne modellere det hydrofoberede lag af murværket. Den udviklede model er i stand til at forudsige de hydrofoberede murstens hygrotermiske opførsel ved hjælp af eksperimentelle resultater fra artikel I. Kombineret med RF-målinger af forholdene i laget mellem murværk og indvendig isolering i en casebygning indikerer resultaterne fra simuleringen, at hydrofobering bør ske før eller samtidig med at murværket isoleres, for at opnå hurtigere udtørring af den fugt-I modsat fald behøves mere tid for at opnå den ønskede effekt, fordi udtørringen af murværket sker langsommere.

Konklusion: Resultaterne viser, at vandafvisende midler skaber et vandtæt, men dampåbent, hydrofobert lag, der rækker langt ind i det hydrofoberede materiale, uden at ændre dets porestruktur markant. Vandoptagelsen i hydrofoberede mursten og mørtel forbliver meget lav efter ældning. Det vises også, at kombineret med enten et kapillaraktivt eller et vanddamp-tæt system af indvendig isolering kan hydrofobering give en fugtsikker energirenovring af massive ydervægge af murværk.



# LIST OF APPENDED PAPERS

In the thesis, three journal papers are appended and will be referred to in the text by the Roman numerals I-III.

- I) **V. Soulios**, E. J. de Place Hansen, C. Feng, H. Janssen, Hygric behavior of hydrophobized brick and mortar samples, Build. Environ. 176 (2020) 106843. <https://doi.org/10.1016/j.buildenv.2020.106843>.
  
- II) V. Soulios, E. Jan de Place Hansen, R. Peuhkuri, E. Møller, A. Ghanbari-Siahkali, Durability of the hydrophobic treatment on brick and mortar, Build. Environ. 201 (2021) 107994. <https://doi.org/10.1016/j.buildenv.2021.107994>.
  
- III) **V. Soulios**, E. J. de Place Hansen, R. Peuhkuri, Hygrothermal performance of hydrophobized and internally insulated masonry walls - Simulating the impact of hydrophobization based on experimental results, Build. Environ. 187 (2021) 107410. <https://doi.org/10.1016/j.buildenv.2020.107410>.

# LIST OF OTHER SCIENTIFIC WORK

The following publications/articles have been prepared as additional research for the thesis. Their contents are strongly related with the scope of the thesis and are used as reference where it is needed. They are not appended in the thesis.

- **V. Soulios**, E.J. de Place Hansen, H. Janssen, Hygric properties of hydrophobized building materials, in: MATEC Web Conf., Prague, 2019: pp.1–6.<https://doi.org/https://doi.org/10.1051/mateconf/201928202048>.  
**Short summary:** The aim of the study was to evaluate the hygric properties of hydrophobized building materials and was a precursor of Paper I. The resulting open porosity of hydrophobized brick samples, derived from vacuum saturation test, shows minimal changes in the pore structure. The absorption coefficient of hydrophobized bricks, derived from capillary water uptake test, was close to zero even with low concentration of the active ingredient. Vapor permeability of hydrophobized samples was almost unchanged after cup tests and drying tests.
- **V. Soulios**, E. J. de Place Hansen, R. Peuhkuri, Hygrothermal simulation assessment of internal insulation systems for retrofitting a historic Danish building, in: Cent. Eur. Symp. Build. Phys., 2019: pp. 1–6.  
<https://doi.org/10.1051/mateconf/201928>.  
**Short summary:** The aim of the study was to evaluate with numerical simulations, the combined effect of hydrophobization with internal insulation. The hydrophobic layer was simulated by simply neglecting rain, and the paper is a precursor of Paper II, where the hydrophobic layer is modeled by using experimental input. Numerical results illustrate that hydrophobization is vital in avoiding moisture problems induced when only internal insulation is used.
- T. Kvist Hansen, **V. Soulios**, R. Peuhkuri, Moisture-proof energy renovation of external masonry walls in historic buildings, Copenhagen, 2019. (Internal report)  
**Short summary:** The aim of the study was to provide a guideline for moisture safe internal insulation solutions of a specific historic building in Denmark with plans of installing monitoring equipment to measure the hygrothermal performance. The results based on hygrothermal simulations illustrate that it is moisture safe to internally insulate the building when the facade is not exposed to wind-driven rain or it is hydrophobized.
- H. Janssen, D. Deckers, E. Vereecken, C. Feng, **V. Soulios**, A. Vanek, T.K. Hansen, V. Metavitsiadis, Impact of water repellent agents on hygric

properties of porous building materials, RIBuild Deliverable D2.3 ([www.ribuild.eu](http://www.ribuild.eu)), 2020.

[https://static1.squarespace.com/static/5e8c2889b5462512e400d1e2/t/5eeb67ee2a7db1305c80d34b/1592485898332/RIBuild\\_D2.3\\_final.pdf](https://static1.squarespace.com/static/5e8c2889b5462512e400d1e2/t/5eeb67ee2a7db1305c80d34b/1592485898332/RIBuild_D2.3_final.pdf)

**Short summary:** The aim of the study was to illustrate the impact of water repellent agents on hygric material properties as part of the RIBuild project. The report was a collaboration between AAU, KU Leuven, Technical University of Denmark (DTU) and Introfex. The report consists of a literature study, numerical simulations, laboratory experiments, and field tests. The conclusion based on the results was that hydrophobization blocks the liquid water transport without major alterations in the pore structure, by leaving vapor permeability untouched. Furthermore, in order to assess the combined effect of hydrophobization with internal insulation in real buildings, long monitoring periods were needed.

- E.J. de Place Hansen, T.K. Hansen, **V. Soulios**, Deep renovation of an old single-family house including application of an water repellent agent – a case story, in SBE21 Sustainable Built Heritage: 14-16 April 2021, Bolzano, Italy. IOP Conference Series: Earth and Environmental Science (In Press)

**Short summary:** The aim of the study was to present in-situ measurements of a 145-year-old renovated building involving internal insulation and hydrophobization. Sensors were installed in the interface between masonry and internal insulation to monitor the development of hygrothermal conditions. Measurements show that it takes time to get rid of the built-in moisture due to the application of internal insulation prior to hydrophobization. Simulations show that the order of hydrophobizing the wall and applying internal insulation is important to promote drying of the wall.



# TABLE OF CONTENTS

<b>Chapter 1 Introduction.....</b>	<b>15</b>
1.1 Objectives.....	15
1.2 Outline of the thesis .....	16
1.3 Hypotheses .....	16
<b>Chapter 2 STATE OF THE ART: hydrophobization.....</b>	<b>18</b>
2.1 The nature of water repellency .....	18
2.2 Types of water repellent agents.....	19
2.2.1 Silicon-bearing compounds.....	19
2.2.2 Metal-bearing compounds.....	21
2.2.3 Organic materials .....	21
2.3 Product identification .....	21
2.4 Hygrothermal properties of hydrophobized brick and mortar samples .....	24
2.5 Hydrophobization and Internal insulation .....	26
2.6 Durability of the hydrophobic treatment .....	27
<b>Chapter 3 Methodology .....</b>	<b>28</b>
3.1 Material level: Hydrophobization .....	28
3.1.1 Target building materials .....	28
3.1.2 Classification of commercially available water repellent agents (market overview) .....	29
3.1.3 Selected water repellent agents .....	29
3.1.4 Hydrophobic treatment.....	30
3.1.5 Experimental setup.....	30
3.2 Component level: Hydrophobization and internal insulation.....	34
3.2.1 Hygrothermal simulations .....	34
3.3 Building level: Case study building .....	36
<b>Chapter 4 Results.....</b>	<b>37</b>
4.1 Classification of commercially available water repellent agents .....	37
4.2 Material level: Hydrophobization .....	38
4.2.1 Moisture storage properties .....	38

4.2.2 Transport properties .....	38
4.2.3 Thermal properties .....	41
4.2.4 Impregnation depth .....	42
4.2.5 Durability of the Hydrophobic treatment .....	43
4.3 Component level: Hydrophobization and internal insulation.....	47
4.3.1 Experimental validation of the hydrophobic model .....	47
4.3.2 Simulation study .....	49
4.3.3 Case study building .....	55
<b>Chapter 5 Discussion .....</b>	<b>57</b>
5.1 Main findings .....	57
5.2 Material level .....	57
5.2.1 Hygric properties.....	57
5.2.2 Impregnation depth .....	59
5.2.3 Durability of the hydrophobic treatment .....	59
5.3 Component level .....	61
5.3.1 Hydrophobization and internal insulation .....	61
5.3.2 Energy savings from hydrophobization .....	62
5.3.3 Weak hydrophobic treatment .....	62
5.3.4 Practical recommendations .....	63
<b>Chapter 6 Conclusion .....</b>	<b>64</b>
<b>Chapter 7 Perspective.....</b>	<b>66</b>
<b>References.....</b>	<b>68</b>

# CHAPTER 1 INTRODUCTION

Buildings account for 40% of total energy consumption in E.U. [1] and much of this energy is consumed by old (constructed before 1950), poorly insulated buildings, usually constructed with brick or natural stone [2]. Habitation needs should mainly be covered by existing buildings, as the European building stock increases by 1–1.5% per year [3]. In Denmark, maintaining the cultural heritage is imperative, and the renovation of the building enclosure is an important step [4,5]. Non-insulated buildings account for a big portion of the energy consumption and thermal retrofitting should hence be considered. However, to sustain the architectural and cultural values of historic buildings, thermal retrofit often implies that the facades become internally insulated, although exterior insulation is the most efficient measure [6]. Internal insulation may cause moisture related problems, such as frost damage at the exterior surface, rot of embedded wooden floor beams, or mould growth and interstitial condensation at the interface between masonry and internal insulation [7–9]. Moisture inside the building materials may also have less thermal resistance, thus partially compromising the thermal retrofit that is intended [8–10]. These adverse impacts of moisture on the hygrothermal performance of internally insulated walls are closely connected to the absorption of wind-driven rain at the exterior surface of the wall [8,9,11,12]. Such rainwater absorption can be reduced via various means: a sufficient overhang, an exterior render, or a paint finish. However, such measures typically change the exterior appearance of the building, which often is neither permitted, nor desired. In that case, facade hydrophobization could potentially avoid such moisture problems, minimizing the water absorption by the facade materials [13].

## 1.1 OBJECTIVES

The aim of this PhD study is to evaluate the impact of water repellent agents on the hygrothermal behavior of internally insulated solid masonry walls, both at the material and component levels. In this direction, the primary objectives are as follows:

1. Characterization of the impact of water repellent agents on the hygrothermal properties of building materials used for solid masonry facades (brick/mortar).
2. Long term effectiveness of the hydrophobic treatment in brick and mortar.
3. Investigation of the hygrothermal performance of hydrophobized internal insulated solid masonry walls.

Thus, this PhD thesis screens the market of commercially available water repellent agents to categorize them according to their physical and chemical properties. In addition, laboratory tests to measure the impact of water repellent agents on the hygrothermal properties of brick and mortar, as well as aging tests to ensure the

durability of the treatment and hygrothermal simulations and field tests to investigate the combination of hydrophobization with internal insulation were conducted.

## 1.2 OUTLINE OF THE THESIS

This thesis consists of seven chapters. Chapter 1 describes the motivation behind the thesis and Chapter 2 elaborates the current state-of-the-art about water repellent agents and hydrophobization. Chapter 3 describes the methodologies used in laboratory and numerical investigations, respectively. Chapter 4 presents and Chapter 5 discusses the main findings of the three papers included in this thesis (Papers I-III). Chapter 6 provides conclusions based on the main findings of the thesis. Finally, Chapter 7 provides a perspective on the findings, and suggests the needs for further research.

## 1.3 HYPOTHESES

Internal insulation is often the only thermal retrofit option for historic buildings. However, applying internal insulation to a solid masonry wall can lead to several moisture-related problems. Application of water repellent agents to a building facade (hydrophobization) reduces the water absorption of the materials, which is thus presumed to decrease the moisture level and damage in exposed facades. Thus the main hypothesis in this research work is that the combination of hydrophobization with internal insulation improves the hygrothermal performance of a solid masonry wall.

The following sub-hypotheses (SH) support the answering of the main hypothesis. These sub-hypotheses, hereafter referred to as SH1-SH6, are tested in the papers that encompass this research work.

SH1: By investigating the physical and chemical properties of water repellent agents, it is possible to define indicators that characterize the product (tested in Paper I).

SH2: Hydrophobization does not alternate the moisture storage properties of brick and mortar samples at the material level. It changes the transport properties by eliminating the liquid water absorption; although, it allows vapor transport (tested in Paper I).

SH3: By testing brick and mortar samples, it is possible to define a specific impregnation depth of the hydrophobic treatment (tested in Paper I).

SH4: Hydrophobized brick and mortar samples retain their water repellency performance after aging (tested in Paper II).

SH5: Hydrophobization reduces the moisture related problems induced by internal insulation (tested in Paper III).



SH6: Hydrophobization produces energy savings as a single approach and additional energy savings when it is combined with internal insulation (tested in Paper III).

# CHAPTER 2 STATE OF THE ART: HYDROPHOBIZATION

## 2.1 THE NATURE OF WATER REPELLENCY

Water repellent agents aim at averting liquid water from entering the treated surface [14–16]. While waterproofing makes the treated material completely impermeable to water, water repellency allows the material to be permeable to water vapor [17]. Moisture in porous building materials is a major reason for deterioration. Water repellency should prevent serious moisture related damages at the material and component levels [14].

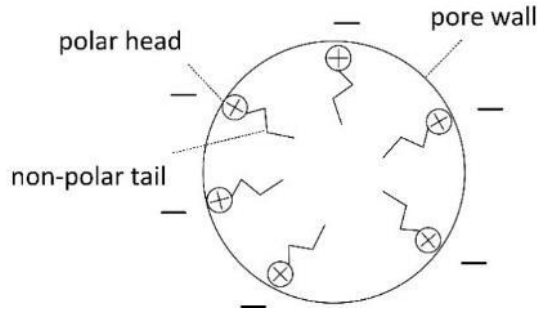


*Figure 2-1 Water repellent molecules have a polar head and a non-polar tail. The polar end attaches itself to the polar pore wall of the substrate, effectively creating a non-polar film, which repels liquid water and allows water vapor diffusion, thus not fully impeding the drying of the material.*

Building materials usually have negative surface charges. Water, being a polar material, is attracted by the hydrophilic surfaces of building materials. Water-repellent molecules have a polar “head” that is attracted by the polar material and a non-polar “tail” that covers the surface. Consequently, the treated surfaces become hydrophobic and do not attract water molecules (see Figure 2-1) [17].

The negative charges of the pore walls of the material and the positive poles of the water molecules create intermolecular electrical forces that induce a surface tension, which in turn forms a meniscus with a contact angle  $\theta < 90^\circ$ , causing capillary rise (Figure 2-2a). When the pore walls are hydrophobized, the non-polar tails of the water repellent molecules force the surface of the material to become hydrophobic. In that case, an inverted meniscus is created with a contact angle  $\theta > 90^\circ$  (Figure 2-2b). Water

is therefore repelled, since there is capillary depression rather than capillary suction [16].

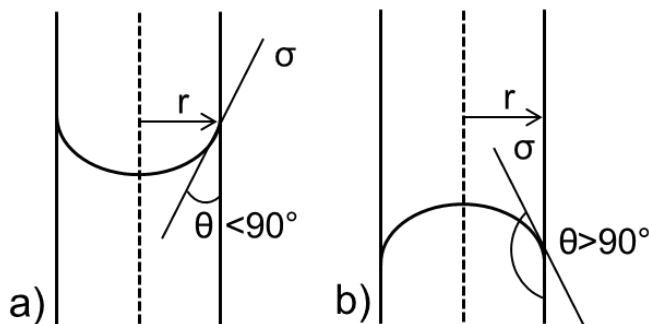


Figure 2-2 Simplified system with cylindrical pore a) Untreated pore - capillary rise with  $\theta < 90^\circ$ . b) Impregnated pore - capillary depression with  $\theta > 90^\circ$ .  $\sigma$ : surface tension,  $\theta$ : contact angle,  $r$ : pore radius.

## 2.2 TYPES OF WATER REPELLENT AGENTS

The commercially available water repellent agents can be divided into three groups, according to the type of the material. These three material groups are: i) silicon-bearing compounds, ii) metal-bearing compounds, and iii) organic materials [17]. It has been mentioned that water repellent products based on nanotechnology could yield better results compared to more traditional products, but as of now, these products are not widely available [10,18,19]. Furthermore, additional studies are needed in order to establish the effectiveness of these nanotechnology-based products.

### 2.2.1 SILICON-BEARING COMPOUNDS

The most common water repellents are silicon-based systems, which can be any product that contains a silicon-oxygen backbone; although, properties between silicon-based products may vary significantly [17]. The silicon-based systems hydrophobize the building material by forming irreversible bonds with the mineral substrate [14,20]. Silicon-based water repellent agents can be classified as silanes, siloxanes, and silicon resins.

#### *Silanes*

Silane molecules contain one silicon atom which is connected to alkyl (-R) and/or alkoxy (-OR) groups (see Figure 2-3a). The alkoxy groups (-OR) are needed for the compound to polymerize and to be chemically linked to the hydroxylated surfaces of siliceous building materials such as brick, mortar, concrete, granite, and sandstone while the hydrophobic properties of the compound are provided by the alkyl groups (-R) [14,17]. Polymerization takes place in two steps: hydrolysis and condensation

reaction. For hydrolysis, water is required as a reactant; a role that can be played by the moisture content of the material. As polymerization continues, longer chains or networks are produced and the viscosity of the product rises. Simple silanes polymerize to siloxanes (between 1 and 5 repeating units) or oligomeric siloxanes (over 6 repeating units) and can be cross-linked to polymeric siloxanes (over 20 repeating units) or silicon resins (over 30 repeating units), as shown in Figure 2-3b [17,21].

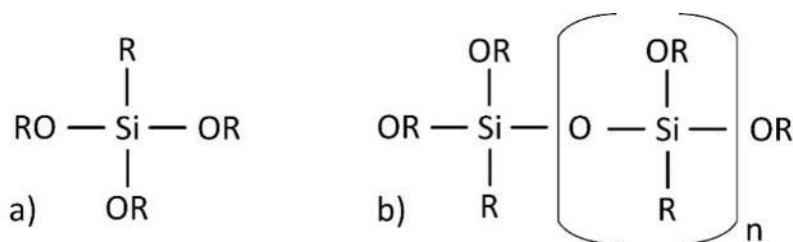


Figure 2-3 Alkyl trialkoxy silane (a) and siloxane (b). Si: Silicon, R: alkyl group (e.g. methyl), OR: reactive alkoxy group (e.g. methoxy).  $n=0$ : silane,  $1 \leq n \leq 5$ : siloxane,  $n \geq 6$ : oligomeric siloxane,  $n \geq 20$ : polymeric siloxane,  $n \geq 30$ : silicone resin.

Silanes can provide sufficient impregnation depths, even in alkaline substrates (e.g. concrete) due to their low reactivity. Their reactivity is determined by the alkoxy group (methoxy, ethoxy) and the functionality (difunctional or trifunctional units). Ethoxy is a larger alkoxy group than methoxy and can be linked easier with the substrate. Difunctional units have two silicon-oxygen backbones and are the basis of higher-molecular chains and cyclic compounds. Trifunctional units have three silicon-oxygen backbones and give rise to three-dimensional crosslinks between the molecules [22]. Existence of longer alkoxy groups and trifunctional functionality increases the reactivity of silanes.

Due to the high volatility of the silanes, high concentrations of active ingredient are needed (25% to 99%), as per the desired outcome [23][24]. The molecular weight of silanes influences their volatility. Shorter alkyl groups like methyl ( $\text{CH}_3$ ) lead to lower molecular weight than larger alkyl groups like iso-octyl ( $\text{C}_8\text{H}_{17}$ ). Siloxanes, which are "pre-cured" silane materials, produce a faster effect compared to silanes because they are larger.

### Siloxanes

Siloxanes are oligomeric or polymeric molecules based on Si-O-Si chains and, therefore, have a more complex molecular structure compared to silanes. Even though their size is comparable to silanes (0.4 to 1.5 nm), it is more difficult for siloxanes (3 to 30 nm) to migrate into the substrate [14,24,25]. Reactivity in siloxanes is higher than in silanes, and siloxane molecules cannot penetrate deep into highly alkaline substrates (e.g. concrete) due to the fast curing process of siloxanes. Consequently,

they are used in less alkaline mineral substrates, such as brick and natural stones [14]. Siloxanes have higher molecular weight and are less volatile than silanes and high concentrations of active ingredient are not needed (usually no more than 10 to 15%). Higher concentrations may also elevate the risk of surface darkening [24].

#### *Silicone resins*

Like siloxanes, the backbone of silicone resins consists of silicon and oxygen atoms, since silicone resins are highly branched poly-siloxanes with high molecular weight [14,22]. In silicone resins, polymerization has already taken place and the only process that occurs after application is the evaporation of the solvent [17]. Silicone resins have poor solubility properties, and can darken the surface [14,17]. To achieve a sufficient penetration depth, silicon resin products should be diluted to 5-10% [14]. Also, it is more difficult for emulsified products to penetrate to the building material, compared to non-emulsified silicone resins products [14].

### **2.2.2 METAL-BEARING COMPOUNDS**

Metal-bearing compounds are not very effective for brick masonry and are mostly used for stone treatments. The most common water repellent agent based on metal-bearing compounds is aluminum stearate, but others exist as well such as titanium stearate and butyl-ortho-titanate, which are used in mixtures with oligomeric siloxanes [17].

### **2.2.3 ORGANIC MATERIALS**

Examples of organic materials that form the basis for hydrophobization agents are acrylics, polyurethanes, and perfluoro-polyethers. Acrylic resins can provide some level of hydrophobicity to the treated material, but they are mainly consolidants. Polyurethanes are polymers that usually have long molecular chains and they are also consolidants that have some hydrophobization properties. Perfluoro-polyethers showcase stability to light, heat, and chemicals, and are transparent, colorless, and permeable to gases [17]. Other organic substances include natural or synthetic waxes, generally used for marble and stone conservation. Waxes have good hydrophobic properties, but are susceptible to mechanical damage and color variations [17,26]. In order to provide both water and oil repellency, some organic materials can be combined with silicon bearing materials [27–29].

## **2.3 PRODUCT IDENTIFICATION**

Silicon-based water repellent agents are categorized according to their active ingredient, form, type of diluent, concentration of active ingredient, alkyl group, and type of substrate that is best suited for application (see Table 2-1) [30]. The characteristics of the active ingredient (silane, siloxane, and silicon resin) were described on the previous section (2.2).

Table 2-1 Product identification (Paper I).

Product characteristic	Description
Active ingredient	Silane - Siloxane - Silicone resins
Product form	Liquid or Cream
Used diluent	Organic solvent - Water emulsion - Water micro-emulsion
Agent concentration	1-100%, Undiluted* or Ready to use
Alkyl group	Octyl or iso-Octyl in commercial products
Intended substrate	Mineral substrate** - Masonry*** - Concrete

\*Undiluted: contain no diluent and must not be diluted before application.

\*\*Mineral substrates: concrete, brick, natural stone, mortar, concrete blocks.

\*\*\*Masonry: brick, mortar, and natural stone, but not for concrete (or concrete blocks).

#### *Influence of the formulation and diluent*

Before usage, some water repellent agents must be diluted with organic solvents [14]. This results in volatile organic compounds (VOC) being released into the atmosphere. In order to avoid that, products with water as diluent have been developed [30]. Since the early 2000s, paste-like or cream products that offer easy application and equivalent performance with liquid products, have been available [10,14,31].

Water repellent agents that contain emulsifiers need longer curing time and tend to show their performance after exposure to rain and solar radiation, while water repellent agents that contain micro-emulsions illustrate their water repellency performance faster (Paper I).

#### *Influence of concentration of the active ingredient*

The performance of the product also depends on the concentration of the active ingredient. Low concentrations typically lead to lower effectiveness of the treatment, [13,31]. The role of the concentration of the active ingredient on the effectiveness, becomes more evident after aging [33].

#### *Influence of the alkyl groups*

The alkyl groups (-R) provide the hydrophobic properties to the silicon based compound. The most popular alkyl groups found in commercial water repellent agents are shown in Figure 2-4.

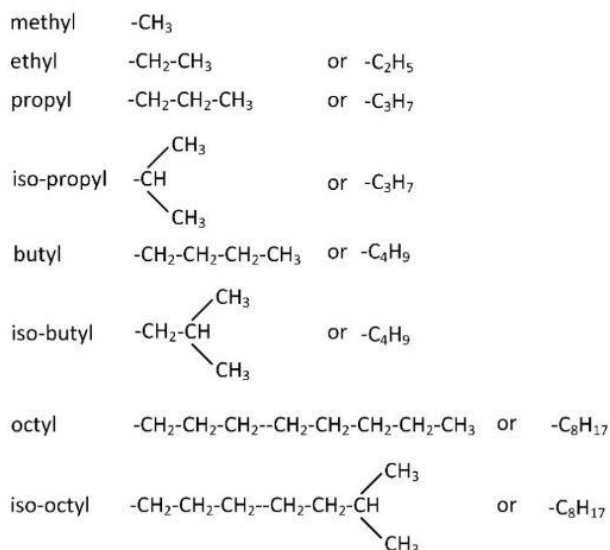


Figure 2-4 Common alkyl groups in commercial water repellent agents.

The chemical bond between the silane and the substrate is not completely stable in an alkaline environment like concrete. Alkyl groups responsible for the hydrophobic nature of the agent keep water molecules away from the reactive OH-groups, which are bonded to the pore wall of the material, and thus, the chemical bond remains dry and stable. Longer and larger alkyl groups like octyl or iso-octyl (see Figure 2-4) ensure that process and provide longer lifetime to the treatment, avoiding hydrolysis and deformation of the hydrophobic layer.

In concrete and in other cementitious materials such as mortar, alkyl groups can play a role in terms of alkali resistance. However, most products today, contain longer alkyl groups and the substrate's alkalinity does not cause stability problems [17,34–36]. As a results, most water repellent agents could be suitable for both concrete and brick.

#### *Influence of the type of substrate*

The pore structure of the material determines the process of polymerization [33]. For that reason, the water repellent agents are classified in relation to their polymer chain length and the pore size of the substrate [15].

## 2.4 HYGROTHERMAL PROPERTIES OF HYDROPHOBIZED BRICK AND MORTAR SAMPLES

Water repellent agents alter the hygric behavior of hydrophobized building materials in such a way that liquid water transfer is impeded and vapor transfer remains possible. Table 2-2 illustrates the difference (in %) in storage and transport properties between treated and untreated brick and mortar samples, including results from both literature and industry. Storage properties are characterized by the moisture content at capillary saturation ( $w_{cap}$ ) while transport properties are characterized by the absorption coefficient at capillary water uptake ( $A_{cap}$ ) and the vapor diffusion resistance factor ( $\mu$ ) as follows.

$$A_{cap} \downarrow (\%) = \frac{A_{cap,untreated} - A_{cap,treated}}{A_{cap,untreated}} \times 100 \quad (1)$$

$$\mu \downarrow (\%) = \frac{\mu_{untreated} - \mu_{treated}}{\mu_{untreated}} \times 100 \quad (2)$$

$$w_{cap} \downarrow (\%) = \frac{w_{cap,untreated} - w_{cap,treated}}{w_{cap,untreated}} \times 100 \quad (3)$$

Table 2-2 Percentage change of hygric properties on hydrophobized brick and mortar samples, involving different concentrations (conc.) of active ingredient,  $A_{cap}$ : Absorption coefficient at capillary water uptake,  $\mu$ : vapor diffusion resistance factor,  $w_{cap}$ : moisture content at capillary saturation, derived from capillary water uptake.

Reference	Type	Conc. (%)	Substrate	$A_{cap} \downarrow$ (%)	$\mu \downarrow$ (%)	$w_{cap} \downarrow$ (%)
Carmeliet [15]	silane	8.53	brick	99.7	-140	28
Sadauskiene [37]	silicon-based	-	brick	99.1	-	-
	silicon-based	-	brick	13.7	-	-
	silicon-based	-	mortar	0.4	-	-
Pavlfk [38]	siloxane	8.32	brick	98.1	-	-
Engel [13]	silane/siloxane	7	brick	98.6	8.6	98.5
	silane/siloxane	10	brick	78.1	-14.9	3
	silane	10	brick	88.8	8.3	12.2
	silane	30	brick	98.9	5.8	97
	silane	40	brick	97.3	6.9	97.5
	silane	50	brick	83	0.9	82.7
	silane	60	brick	98.6	21.4	95.9
Fukui [39]	silane	-	brick	-	0	4.9
Zhao [40]	silicon based	60	brick	-	12.9	98.8



	silicon based	80	brick	-	3.1	98.8
	silane	40	brick	-	3.9	-
	silane	40	mortar	-	0.0	-
Hanssen [41]	silane	-	brick	-	7.9	-
	silane	-	mortar	-	28.6	-
	silane/siloxane	100	brick	-	9.4	-
	silane/siloxane	100	mortar	-	13.0	-
Momentive [42]	silane	40	mortar	93	-	-
Wacker [43]	silane/siloxane	25	brick	95.4	-	-
	silane/siloxane	-	mortar	90	-	-
	siloxane	7	brick	95	-	-
	siloxane	7	brick	92	-	-
Dow [35]	siloxane	7	mortar	96	-	-
	silane/siloxane	10	brick	98	-	-
	silane/siloxane	10	mortar	76	-	-
	silane/siloxane	15	mortar	81.6	-	-

### *Storage properties*

The results presented in Table 2-2 about the moisture storage properties on hydrophobized brick and mortar samples refer to capillary saturation content ( $W_{\text{cap}}$ ) in hydrophobized samples derived from a lengthy water uptake test. It has been suggested that finer pores could be clogged by the polymer network that is created after hydrophobization [15]. In order to examine whether clogging of pores occurs after hydrophobization, vacuum saturation tests are needed to show that the porosity between treated and untreated samples remains unchanged. Similar results from mercury intrusion tests could confirm that the pore structure of the material is not affected by hydrophobization.

### *Transport properties*

Water repellent treatment prevents moisture from penetrating into the material by changing the surface tension of the pore wall of the substrate [40]. Reducing the water uptake can improve the resistance in low temperatures and durability of the brick masonry [37]. When the liquid water transfer is blocked due to capillary forces in the hydrophobic layer, drying becomes possible only via water vapor transfer. However,

vapor transfer is less prominent than liquid transfer and the drying rate can be seriously reduced.

According to [15] some pores can be completely blocked after hydrophobization, and [17] indicates a 5 to 8 % reduction in vapor permeability. On the contrary, according to [22], no clogging occurs in the pores after hydrophobization.

More recent studies provide results showing that vapor permeability remains practically unchanged after hydrophobization [13,39,40]. These results indicate that pores are not completely blocked after hydrophobization.

### *Thermal properties*

Brick and mortar samples illustrate higher values of thermal conductivity when they become wet [10]. This is an indication that hydrophobization can contribute positively to heat loss reduction, by keeping the masonry dry and thus avoiding the increase of thermal conductivity.

## **2.5 HYDROPHOBIZATION AND INTERNAL INSULATION**

Field tests with 60x60 cm<sup>2</sup> walls [44] offer a preliminary insight into the impact of hydrophobization on both uninsulated and internally insulated walls. The results indicate that siloxane impregnation can repel rain water to such an extent that a complete drying (below 1.5 Vol. %) of a masonry wall is possible. The uninsulated masonry needs less than two years to reach a moisture content of 1.5 Vol.-%, from an initial moisture content of around 8 Vol. %, compared to vapor tight insulated test walls, which need more than five years, due the fact that drying could only occur via the external surface.

The first attempts at combining internal insulation and hydrophobization in a simulation environment (WUFI) agree with the statement that the hygrothermal performance of the facade can be improved by hydrophobization [8], [45]. Moreover, in areas with high precipitation, it may not be feasible to install capillary active internal insulation without a hydrophobic protection of the facade, since there is an increased risk of moisture accumulation behind the insulation [8]. Both studies show that the risk of mould growth in internally insulated walls can be eliminated when hydrophobization is applied on the facade.

It should be noted that, in the above-mentioned studies, the hydrophobic layer of the facade was simulated in WUFI by reducing or neglecting completely the wind-driven rain load; a method that produces overly optimistic results. Finken et al. [8], on the other hand, use a weather resistance barrier with a vapor diffusion resistance seven times greater than the one of the untreated brick [8]. In real conditions, the liquid water transfer in the hydrophobic layer is partially or completely blocked, while vapor permeability remains unchanged. Experimental studies indicate no difference in vapor

diffusion resistance values between treated and untreated brick samples [13,39,40]. Therefore, the approach of using a barrier with a high vapor diffusion resistance [8] reverses the actual drying behavior of a hydrophobized facade by impeding vapor transfer and leaving liquid transfer unchanged. Determining the hygric properties experimentally is crucial for representing the hydrophobic layer in a simulation environment.

The combination of hydrophobization with internal insulation, when applied at the same time, can be positive for the hygric performance of the wall, shown by testing mock-up walls with different insulation systems in a container using cream water repellent agent (Remmers FC cream 40%) [46] and in a test house using liquid water repellent agent (Wacker SMK 2100) [47]. But the combined effect of hydrophobization with internal insulation should be also tested in real inhabited buildings where the condition of the facade and the moisture loads may differ.

## **2.6 DURABILITY OF THE HYDROPHOBIC TREATMENT**

Although results from hydrophobized walls have been very promising, it is important to ensure that hydrophobized walls can keep their hydrophobic properties for a long time. Also, it is important to understand which factors (e.g. concentration of active ingredient) can play a role in ensuring the longevity of hydrophobization. When the right product is correctly applied, the literature indicates a good durability of hydrophobization, which may remain efficient for up to 30 years [48]. The general trend in the literature has been to suggest testing a specific type of product to a specific type of substrate, in order to assure the effectiveness and durability of the hydrophobic treatment. Moreover, there is not a single water repellent agent or a type of water repellent agents that behaves better than others for building materials (brick, mortar, and natural stone). [17,30] Nowadays, considerable attention has been paid to cream products, due to the workability and easy application, but there is no data concerning the durability of the hydrophobic treatment.

## CHAPTER 3 METHODOLOGY

This chapter provides information on the methods used in the present PhD study. The investigations were conducted as a mix of laboratory and simulation studies at the material and component levels along with field measurements at building level. In laboratory settings, investigations were made on how silicon based water repellent agents influence on the hygrothermal properties of brick and mortar samples, as well as the impregnation depth of the treatment. This part of the study involved the different silicon based water repellent agents that exist on the market. Further, analysis was conducted investigating the durability of the hydrophobic treatment in brick and mortar samples through artificial aging. Numerical simulations were performed investigating the potential match between hydrophobization and internal insulation, using as input the values derived from the laboratory tests and validated with field measurements. In the field, additional analyses were conducted investigating the relative humidity in the interface between masonry and internal insulation, in a high-risk case of a Danish building where the insulation was installed two years prior to hydrophobization. In addition, analyses of the durability of the treatment through Karsten tube tests conducted in brick/mortar mock-up walls to connect the artificial aging results at the material level with actual wall configurations at the component level.

### 3.1 MATERIAL LEVEL: HYDROPHOBIZATION

#### 3.1.1 TARGET BUILDING MATERIALS

Internal insulation combined with hydrophobic impregnation is an alternative retrofit measure in cases where external insulation is not a feasible solution due to the architectural or cultural value of the facades. These facades are often made of solid masonry consisting of ceramic brick and lime mortar. This study including three types of ceramic brick and three types of mortar also involves modern materials (R brick and C mortar) shown in Table 3-1.

*Table 3-1 Building materials used in the current study, characterized by their capillary water uptake ( $A_{cap}$ ) and water content at capillary saturation ( $w_{cap}$ ) untreated samples, i.e. before hydrophobization)*

Name	Description	$A_{cap}$ [kg/m <sup>2</sup> ·s]	$w_{cap}$ [kg/m <sup>3</sup> ]
R brick	Robusta Vandersanden Belgian Brick	0.607 (0.02)	208 (2.3)
H brick	Historic Danish Brick from an old building in Copenhagen (1944)	0.399 (0.023)	249 (3.9)
Y brick	Yellow soft-moulded Danish brick from Helligsø Teglværk	0.310 (0.046)	276 (19.3)

L mortar	Carbonated hydrolic lime mortar	0.258 (0.02)	227 (6.6)
AL mortar	Carbonated air lime mortar with aggregates of 0-4 mm grain size (7.7%)	0.156 (0.006)	177 (5.87)
C mortar	Cement mortar with aggregates of 0-4 mm grain size (Wewers)	0.152 (0.009)	177 (0.66)

$A_{cap}$  and  $w_{cap}$  derived from water uptake test (each result is an average based on five samples. The values in () correspond to the standard deviation.

### 3.1.2 CLASSIFICATION OF COMMERCIALY AVAILABLE WATER REPELLENT AGENTS (MARKET OVERVIEW)

The existing distributors of water repellent agents provide an array of products that are characterized according to the type of active ingredient, formulation, concentration and type of substrate, as explained in Section 2 (see also Paper I).

In this study, 77 commercially available products suitable for mineral substrates have been identified from 13 distributing companies, including five big silicon-producing companies: Wacker, Dow, BlueStar, Sika, and Momenive. Companies that do not produce silicon products, make their formulations using silicon products from the big silicon-producing companies.

In-plant impregnations for cement, products used for wood or against rising damp, and products that are used as admixtures in coatings are excluded, since the main focus is water repellent agents for façade impregnation against wind-driven rain (Paper I).

### 3.1.3 SELECTED WATER REPELLENT AGENTS

The basic variations available on the market of silicon-based water repellent agents are represented by the water repellent agents shown in Table 3-2, according to the characterization shown in Table 2-1. These water repellent agents include different active ingredients, in liquid or cream form, water or solvent-based, with different concentrations, and recommended for different types of substrate. A detailed description of the water repellent agents referred in Table 3-2 can be found in Paper I.

*Table 3-2 Water repellent agents used in the current study, including the concentrations used (not in all cases as recommended by the producer)*

Product	Company	Type	Form	Diluent	Concentration	Substrate
SMK 2101	Wacker	90% silane	Liquid	Water	6, 10, 25** %	Concrete
SMK 1311	Wacker	90% siloxane	Liquid	Water	6, 10, 25** %	Mineral
SMK 2100	Wacker	Silane/siloxane	Liquid	Water	2*, 6, 10, 25** %	Mineral
SNL	Remmers	Siloxane	Liquid	Solvent	7 %	Mineral

WS	Remmers	Silane/siloxane	Liquid	Water	10 %	Mineral
FC	Remmers	Silane	Cream	Water	10,* 20, 40, 80 %	Mineral
BS C	Wacker	Silane	Cream	Water	80 %	Concrete

Information derived from the technical data sheets of the products.

\*Concentration lower than recommended.

\*\*Concentration higher than recommended.

### 3.1.4 HYDROPHOBIC TREATMENT

The substrate should be cleaned from dirt, dust, and possible efflorescence before impregnation, as dictated by the technical data sheets of the water repellent agents used in this study [23,49,50]. In real buildings, the facade is cleaned by sweeping, compressed air, or even sandblasting.

For the current study, the samples were washed with deionized water and were cleaned with a brush. Then, the samples were stored in an oven (55 °C) for drying. After drying the samples were cooled in room temperature (T) and relative humidity (RH). For impregnation with cream products 150-200 ml/m<sup>2</sup> were applied with a brush (minimum recommended amount) [51]. For the impregnation process using liquid water repellent agents, please see Paper I. After impregnation the samples were maintained in a climatic chamber (21 °C, 53% RH) for one month before any experiment took place.

### 3.1.5 EXPERIMENTAL SETUP

Six main factors that characterize the hydrophobic layer: i) change in the open porosity ( $\Phi$ ) and the pore volume distribution ( $f_v$ ) (moisture storage), ii) reduction of the water absorption coefficient ( $A_{cap}$ ) (moisture transport), iii) change of vapor diffusion resistance factor ( $\mu$ ) (moisture transport), iv) change in the thermal conductivity, v) impregnation depth ( $d_p$ ), and vi) change of absorption coefficient as well as contact angle and discoloration after aging (durability) were investigated as presented in Table 3- 3 and described in Papers I-III.

Table 3- 3 Laboratory experiments.

Properties	Experiments
<b>Moisture storage</b>	
Open porosity ( $\Phi$ )	Vacuum saturation test
Pore volume distribution ( $f_v$ )	Mercury intrusion test
<b>Moisture transport</b>	
Capillary absorption coefficient ( $A_{cap}$ )	Capillary water uptake test
Vapor diffusion resistance factor ( $\mu$ )	Cup test

Thermal properties	
Thermal conductivity ( $\lambda$ )	Heat-flow meter
Impregnation depth	
Impregnation depth ( $d_p$ )	Visual inspection Water uptake from non-impregnated side
Durability	
Capillary absorption coefficient ( $A_{cap}$ )	Artificial aging, water uptake
Contact angle ( $\gamma$ )	Artificial aging, contact angle measurement
Discoloration	Visual inspection

### Moisture storage

Open porosity ( $\Phi$ ), which is proportional to vacuum saturated moisture content  $w_{sat}$  [52,53], was calculated via a vacuum saturation test, according to [54] (ASTM C1699-09, 2009). For each test, dry samples were placed in a vacuum desiccator, before being immersed in water.

$$\Phi(\%) = \frac{M_{sat, in air} - M_{dry}}{M_{sat, in air} - M_{sat, in water}} \times 100 \quad (4)$$

$M_{dry}$  is the mass of the dry sample,  $M_{sat, in air}$  is the mass of the saturated sample measured in air and  $M_{sat, in water}$  is the mass of the sample, measured when immersed in water.

A mercury intrusion test was carried out to determine the pore volume distribution of hydrophobized brick and mortar according to [55]. According to [56], assuming a cylindrical pore shape (radius  $r$ ) and based on the capillary pressure curve, the pore volume distribution ( $f_v$ ) can be determined as follows:

$$f_v(r) = - \frac{\partial w}{\partial \log_{10}(p_c(r))} \quad (5)$$

where  $w$  is the moisture content and  $p_c(r)$  is the capillary pressure, according to the Young-Laplace equation:

$$p_c = \frac{2\sigma \cos(\theta)}{r} \quad (6)$$

where  $\sigma$  is the surface tension [N/m],  $\theta$  is the contact angle [ $^\circ$ ] and  $r$  is the pore radius [m] [53].

### Moisture transport

The water absorption coefficient ( $A_{cap}$ ) was obtained through water uptake tests, in accordance with [57], as described in [52,58]. The time intervals for the measurement

were 10', 30', 1h, 1h 30', 2h, 3h, 4h, 7h, 9h, and 24h. The duration of the water uptake test for the impregnated samples was 24 hours because impregnation decreases the rate of capillary water uptake significantly [15]. When the graph of water uptake does not produce a straight line but a curve of some form,  $A_{cap}$  is defined as the increase in weight ( $\Delta m$ ) at 24h divided by  $\sqrt{86400}$  [57]. The water uptake tests are repeated to check the water repellency performance after water exposure.

$$A_w = \frac{\Delta m}{\sqrt{86400}} \quad (7)$$

In order to determine the water vapor diffusion resistance factor ( $\mu$ ), cup tests were conducted in accordance with [59]. The samples were pre-conditioned, enclosed in the lids attached to cups containing saturated salt solutions and placed in a climatic chamber with relative humidity of 53.5 % and temperature of 21 °C. The samples were weighed two times per week for four weeks and the  $\mu$ -value was calculated as follows:

$$\mu = - \frac{\delta_{air} \cdot \Delta p}{d \cdot g} - \frac{d_{air}}{d} \quad (8)$$

where  $\mu$  is the water vapor resistance factor [-],  $\delta_{air}$  the water vapor permeability of still air [ $\text{kg} \cdot \text{m}^{-1} \cdot \text{s}^{-1} \cdot \text{Pa}^{-1}$ ],  $\Delta p$  the pressure difference between inside and outside the cup [Pa],  $d$  the sample thickness [m],  $g$  the density of water vapor flow rate [ $\text{kg} \cdot \text{m}^{-2} \cdot \text{s}^{-1}$ ], and  $d_{air}$  the distance between the sample and the salt solution inside the cup [m].

#### *Thermal properties*

In order to showcase the potential energy savings due to hydrophobization, the thermal conductivity of dry and saturated brick samples was measured. Three types of brick and one type of mortar were put in a heat flow meter in dry and capillary saturated conditions in accordance with [60] and the thermal conductivity of each sample was calculated following Equation (9) [61], where  $\lambda$  stands for the thermal conductivity of the sample [ $\text{W}/(\text{m} \cdot \text{K})$ ],  $q$  for the heat flux through the sample [ $\text{W}/\text{m}^2$ ],  $d$  for the thickness of the sample [m], and  $T_{hot} - T_{cold}$  for the temperature difference between the hot and cold plates [K]:

$$\lambda = q \cdot \frac{d}{T_{hot} - T_{cold}} \quad (9)$$

For the capillary saturated condition, the samples were immersed in water for 24 hours and for the dry condition, the samples were kept in an oven at 70 °C until their weight was stabilized.

#### *Impregnation depth*

The impregnation depth was measured by visual inspection (i.e. as the length of the area that becomes darker due to impregnation, measured perpendicularly to the surface), immediately after the impregnation and one month after the impregnation. As the water repellent agent is redistributed and spread inside the specimens, water



uptake tests were also conducted from the non-impregnated side of the samples. Hydrophobization creates a first, strongly hydrophobized layer and a second, partly hydrophobized layer further away from the surface [62] (see Paper I). In this study, “impregnation depth” refers to both the strongly hydrophobized region along with the partly hydrophobized region.

### *Durability*

The methodology to evaluate the durability of the hydrophobic surface treatment of brick and mortar samples is based on artificial aging with Atlas Ci 4000 weatherometer, conducted at the Danish Technological Institute (Taastrup), according to ISO 4892-2 as described in Paper II. The results of water absorption measurements are expressed as water absorption coefficient ( $A_{\text{cap}}$ ) and derives from capillary uptake tests. Capillary uptake tests are carried out before and after artificial aging for the untreated samples. For the treated samples the water absorption coefficient was measured: a) one month after the application of the water repellent agent, b) during artificial aging (every two weeks), and c) after artificial aging. The total artificial aging procedure consists of 635 cycles. Capillary water uptake measurements were carried out after 165, 335, 482, and 635 cycles. One cycle (two hours) consists of:

-102 min.: Lamp: Xenon

Irradiance level: 0.5 W/m<sup>2</sup> at 340 nm (UV)

Back panel temperature: 63 °C

Chamber temperature: 38 °C

Relative humidity: 50%

Specimen spray: off

Back spray: off

-18 min.: Specimen spray: on

The rest of the weathering test conditions remain the same

The Karsten tubes are 10 cm in height (15 ml volume) and are placed on the substrate vertically and horizontally after sealed with plasticine. The water level is recorded every minute for 11 minutes, and water absorption in ml/min is calculated using the average of the last ten measurements. Water is added every time 1 ml of water is absorbed in order to sustain a steady water pressure [63] (see also Paper II).

Contact angle measurements took place to check the beading effect. The measurements used 3  $\mu\text{L}$  droplets placed on the treated surface of the materials. The droplet images were recorded with a CCD camera, and the results were analyzed by DropSnake, a plugin for ImageJ software, similarly to [64].

After the artificial aging, the samples were inspected for possible discoloration.

## 3.2 COMPONENT LEVEL: HYDROPHOBIZATION AND INTERNAL INSULATION

### 3.2.1 HYGROTHERMAL SIMULATIONS

#### *Hydrophobic model*

The hygrothermal properties measured as described in section 3.1 were used as input for the hydrophobic model developed in Delphin (as it is shown in Table 3- 4), resulting in adjusted versions of the moisture retention and permeability curves as well as the vapor permeability and thermal conductivity curves. The minimum impregnation depth reported in Paper I is used as base case. 1D simulations were decided as sufficient since the impregnated brick and mortar samples illustrate similar values of absorption coefficient.

*Table 3- 4 Material properties of Y brick in untreated (Untd) and hydrophobized condition (FC 40 %) based on own measurements (Paper III).*

Material property (Y brick)	Untd	FC 40%
Saturation moisture content ( $W_{\text{sat}}$ ) [ $\text{m}^3/\text{m}^3$ ]	0.290	0.290
Capillary absorption coefficient ( $A_{\text{cap}}$ ) [ $\text{kg}/\text{m}^2\text{s}^{0.5}$ ]	0.32	0.0009
Vapor resistance factor ( $\mu$ ) [-]	11.9	13.7
Dry thermal conductivity ( $\lambda_{\text{dry}}$ ) [ $\text{W}/(\text{m K})$ ]	0.63	0.63
Thermal conductivity at capillary saturation ( $\lambda_{\text{wet}}$ ) [ $\text{W}/(\text{m K})$ ]	1.47	1.47
Bulk density ( $\rho$ ) [ $\text{kg}/\text{m}^3$ ]	1643	1643
Specific heat capacity ( $C_p$ ) [ $\text{J}/(\text{kg K})$ ]	942	942

### *Experimental validation of the hydrophobic model*

The hydrophobic model was validated first at the material level by comparing the water uptake and drying curves obtained by experiments and duplicated in a simulation environment in order to capture the wetting and drying behavior.

The hydrophobic model was also validated at the component level, comparing the relative humidity and temperature at the interface between masonry and internal insulation (iQ-Therm) of a mock-up wall constructed with Y brick and air lime mortar in a container segment at the Technical University of Denmark (DTU), with a 1D model constructed in Delphin software to simulate the container mock-up wall as described in Figure 3- 1. The hydrophobization (FC 40%) was applied in the same period as the internal insulation (March 2015). The hydrophobized brick was modeled as a separate material as described in Paper III.

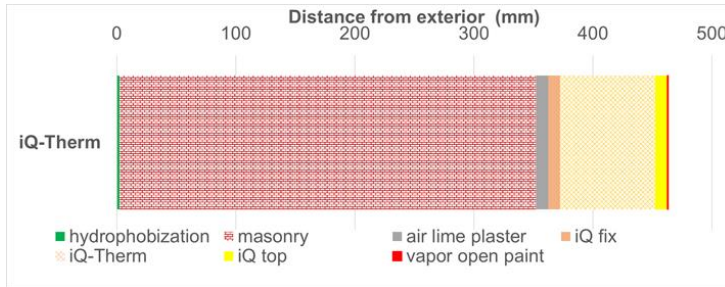


*Figure 3- 1 Configuration of the container mock-up wall. Hydrophobization: 2.4 mm impregnation depth, masonry (Y brick): 350 mm, air lime mortar: 10 mm, iQ fix (adhesive mortar): 10 mm, iQ-therm (PUR-foam based insulation): 80 mm, iQ top (render): 10 mm, vapor open paint:  $sd = 0.01$  m.  $sd$ : equivalent air layer thickness ( $\mu * \text{material thickness}$ ) (Paper III).*

### *Simulation input*

Three different wall configurations were studied as a base case scenario as presented in Figure 3- 2. Based on three indicators: the average moisture content in the masonry, the mould growth at the interface between masonry and internal insulation, and the heat loss.

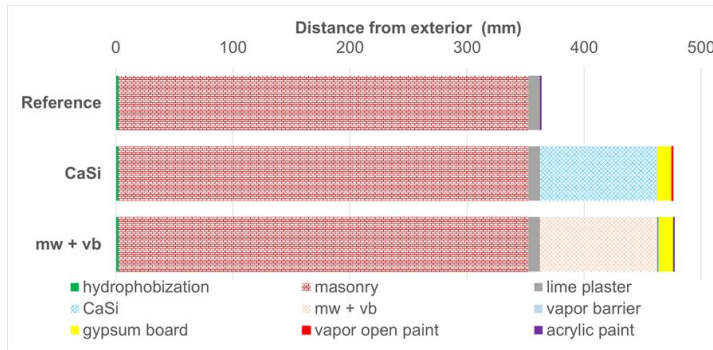


*Figure 3- 2 Wall configuration without (reference) and with internal insulation. Hydrophobization: 2.4 mm impregnation depth, masonry (Y brick): 350 mm, lime mortar: 10 mm, insulation system: 100 mm (mineral wool or CaSi), gypsum board: 12.5 mm, vapor open paint with  $sd = 0.01$  m, vapor barrier (vb)  $sd = 70$  m (only for the mineral wool (mw) system) and acrylic paint  $sd = 0.18$  m.  $sd$ : equivalent air layer thickness ( $\mu \cdot$  material thickness) (Paper III).*

#### Parametric analysis

A parametric analysis was conducted with different orientations (N, E, W, S, SW), climates (Copenhagen, Munich, Milan), masonry thicknesses (350, 590, 710 mm) insulation thicknesses (60, 100, 300 mm), insulation systems (CaSi, mineral wool + vapor barrier, iQ-Therm, XPS, Multipor, Kingspan), impregnation depths (2.4 and 40 mm), impregnation strengths (characterized by  $A_{cap}$  using 0.0009 and 0.033 [ $\text{kg/m}^2\text{s}^{0.5}$ ]), and hydrophobization before or after internal insulation represented by initial moisture content in the wall (see Paper III).

### 3.3 BUILDING LEVEL: CASE STUDY BUILDING

The case study building is a recently renovated old two-story farm house, built in 1875 and located on the coast of northern Zealand in Denmark. During the refurbishment of the house, internal insulation and afterwards, hydrophobization were applied. The relative humidity in the interface between masonry and internal insulation (iQ-Therm), which was installed in 2016, was studied on different wall orientations where the hydrophobization installed in 2018 (see also Paper III).

## CHAPTER 4 RESULTS

This chapter will present the main findings from Papers I-III.

### 4.1 CLASSIFICATION OF COMMERCIALY AVAILABLE WATER REPELLENT AGENTS

Almost all companies provide silicon-based water repellents, covering 80 % of the market, half of them being mixtures of silanes and siloxanes, while less than 20 % are based on organic or metal-bearing materials (see Figure 4-1). Most water repellent agents are in liquid form. Also, most of the products use water as a diluent, especially if they are in cream form (see Figure 4-2 left). The majority of the products are generally recommended for mineral substrates, but some products are specifically recommended for application in concrete and cementitious materials (see Figure 4-2 right and Paper I).

These results led to the selection of the water repellent agents used in the research, since non-silicon based products were excluded. However, regarding the product form, special attention was given to cream products due to their easy application, despite there being fewer on the market compared to liquid products.

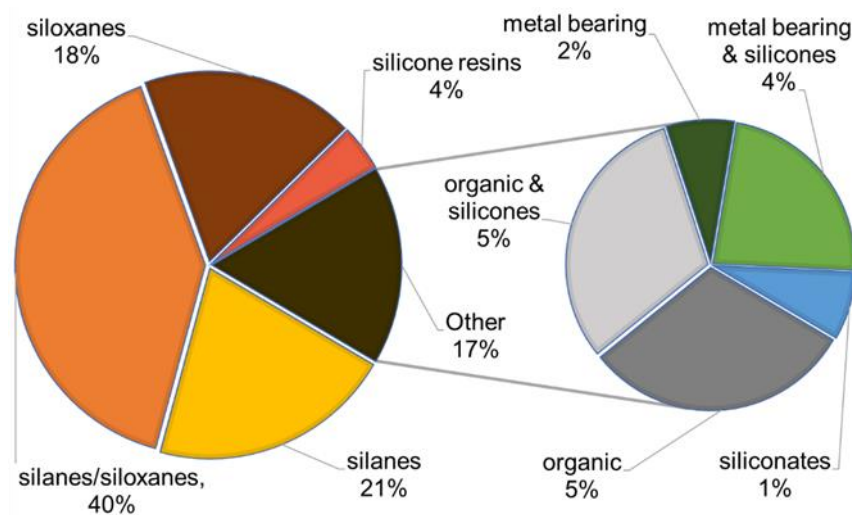


Figure 4-1 Types of commercially available water repellent agents. Data from 77 listed products (Paper I).

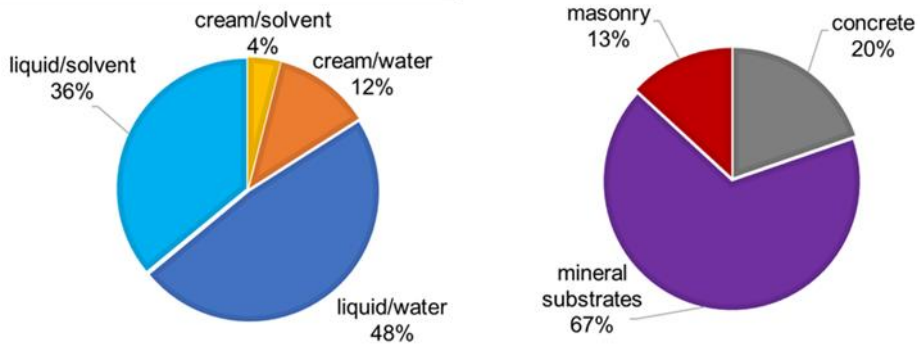


Figure 4-2 Form/diluent of water repellent agents (left), Type of substrate (right). Data from 77 listed products (Paper I).

## 4.2 MATERIAL LEVEL: HYDROPHOBIZATION

### 4.2.1 MOISTURE STORAGE PROPERTIES

Hydrophobic impregnation can induce minor changes in the open porosity ( $\Phi$ ) and vacuum saturation moisture content ( $w_{\text{sat}}$ ), as seen in Figure 4-3 (left), for both R brick and L mortar. After mercury intrusion test, the pore volume distribution in Figure 4-3 (right) shows that the available pore volume space in the hydrophobized materials did not change significantly, but L mortar was influenced slightly more compared to R brick due to its finer pores.

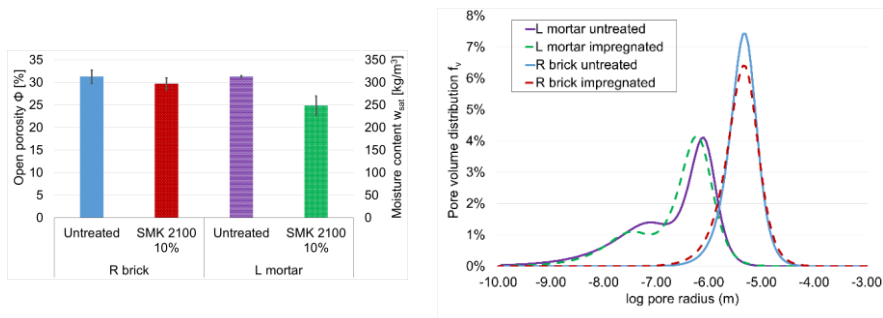


Figure 4-3 Open porosity and moisture content at vacuum saturation (left) and pore volume distribution (right), R brick and L mortar, untreated and impregnated with SMK 2100 10 %. Each result is an average based on five samples, error bars correspond to standard deviation, for exact values see Paper I (Paper I).

### 4.2.2 TRANSPORT PROPERTIES

#### Capillary water absorption

Hydrophobization significantly reduces the capillary water absorption in all the treated substrates as presented in Figure 4-4. The effect is less obvious in the case of cement mortar, but after repeating the capillary water uptake test, as shown in Figure 4-5, the water repellency performance reaches the same level as the rest of the substrates.

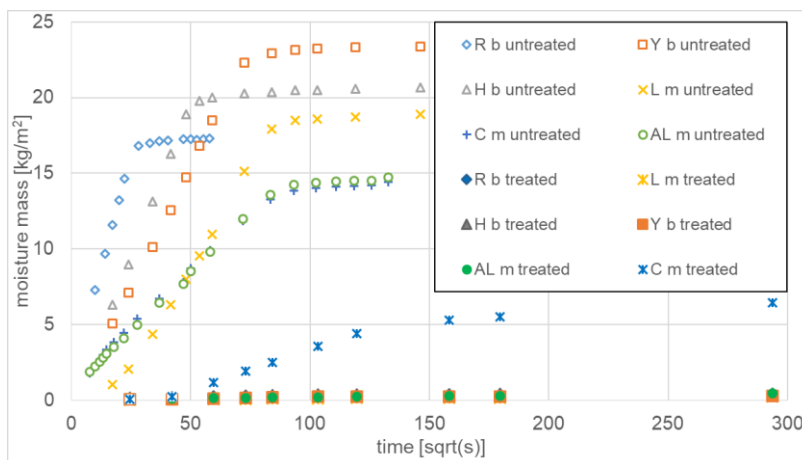


Figure 4-4 Capillary water uptake. R brick, H brick, Y brick, L mortar, C mortar, AL mortar, untreated and impregnated with FC 40%. 300 sqrt(s) corresponds to 25 hours. The data points for the treated Y brick, H brick, R brick, L mortar, and AL mortar samples fall very close. Each point of each curve is the average value of the respective measurements of three different samples.

Water exposure after treatment and a longer curing time increase the water repellency performance in all types of water based silicon agents tested in Paper I. The water absorption coefficient ( $A_{cap}$ ) is negligible compared to untreated samples regardless of the concentration of the active ingredient, the diluent, the percentage of silane/siloxane, the application time (10 sec, 5 min, 80 min) for liquid products, inner/weathered surface, and duration of capillary water uptake, cf. Paper I.

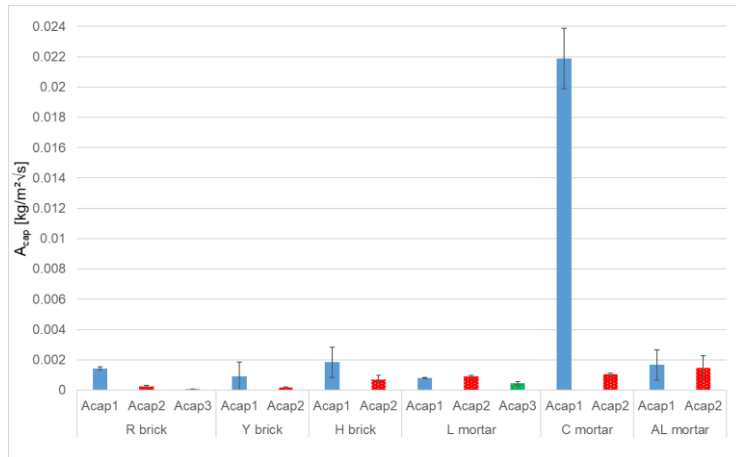


Figure 4-5 Influence of water exposure after treatment. R brick, H brick, Y brick, L mortar, C mortar, and AL mortar impregnated with FC 40%. Water absorption coefficient at first ( $A_{cap1}$ ), second ( $A_{cap2}$ ), and in some cases third ( $A_{cap3}$ ) water uptake test. Between the water uptake tests the samples were dried in an oven at 55°C and then cured at room temperature and RH. Each result is an average based on three samples, error bars correspond to standard deviation.

#### Water vapor diffusion

Hydrophobization does not block the vapor transport, cf. Figure 4-6. Although there was a small increase of vapor diffusion resistance factor at the first cup test with treated samples (red columns) compared to untreated (blue), the increase becomes less obvious after immersing the samples for 24 hours in water and repeat the cup test (green).



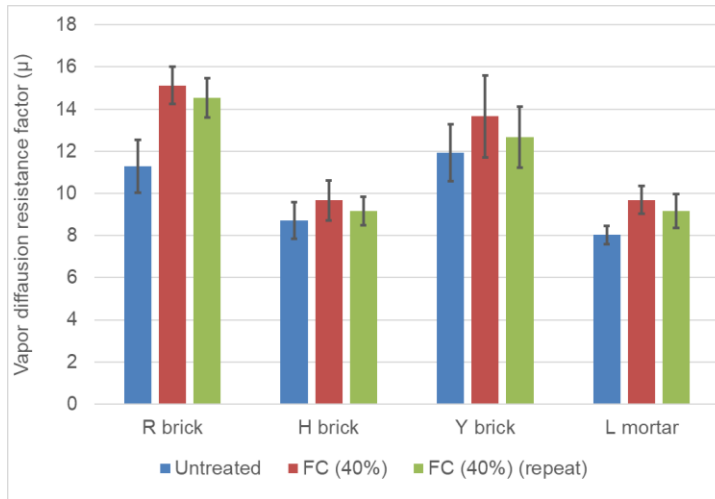


Figure 4-6 Water vapor diffusion resistance factor ( $\mu$ ) of R brick, L mortar, H brick and Y brick, untreated and impregnated with FC 40%. Each result is an average based on four samples, error bars correspond to standard deviation.

### 4.2.3 THERMAL PROPERTIES

The thermal conductivity of the tested brick and mortar types is affected by the moisture content and becomes more than twice as high in capillary saturated state compared to dry state in all tested materials (see Figure 4-7). This reveals potential energy savings as a result of hydrophobization by keeping the building materials in a dry state.

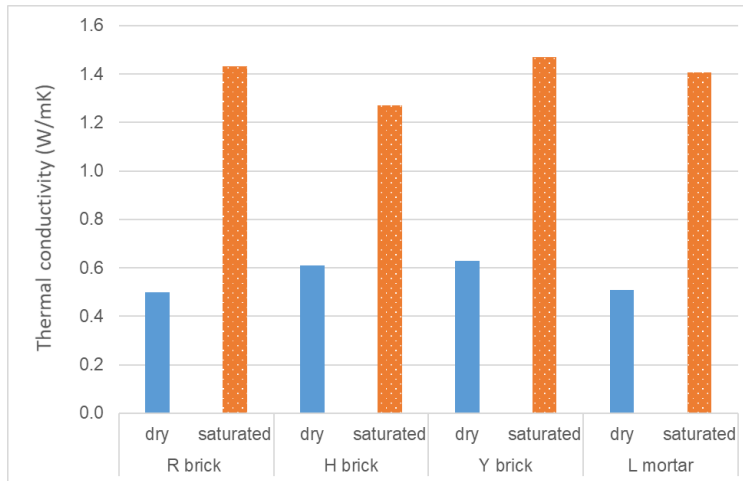


Figure 4-7 Thermal conductivity in dry and capillary saturated building materials: R brick, H brick, Y brick, and L mortar.

#### 4.2.4 IMPREGNATION DEPTH

Paper I reveals that there is not a specific type of water repellent agent that penetrates deeper in a specific building material. However, all the water repellent agents tested tend to penetrate deeper to brick than mortar, the active ingredient continues to spread inside the material, and the water exposure after treatment contributes to a larger impregnation depth. Brick and mortar samples illustrate water repellency performance even at 8 cm depth, which becomes better by repeating the water uptake test from the non-impregnated side (see Figure 4- 8). Hydrophobization creates a strongly hydrophobized layer and a larger area that is partially hydrophobized where the active ingredient would spread deeper with time and water exposure (Paper I).

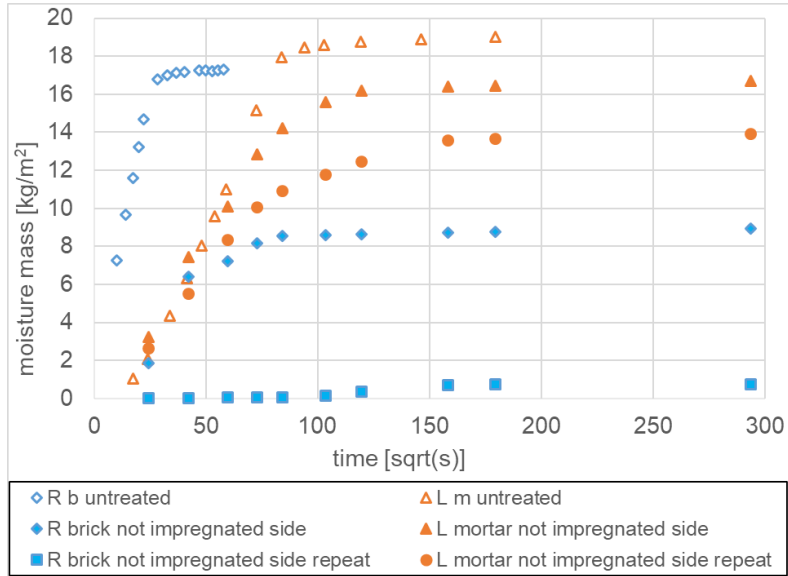


Figure 4- 8 Capillary water uptake test of R brick and L mortar, in untreated state, and in treated state from the not impregnated side of the sample including a repeated test after drying in the oven at 55°C and one month curing at room temperature and RH. Impregnated with FC 40%. Each point at each curve is the average value of the respective measurements of three different samples.

#### 4.2.5 DURABILITY OF THE HYDROPHOBIC TREATMENT

##### *Capillary water uptake test during artificial aging*

Hydrophobization retains the water repellency performance during artificial aging as presented in Figure 4- 9 where the water uptake before aging, during aging, and after aging of all the tested brick and mortar samples is negligible compared to the water uptake of untreated samples.

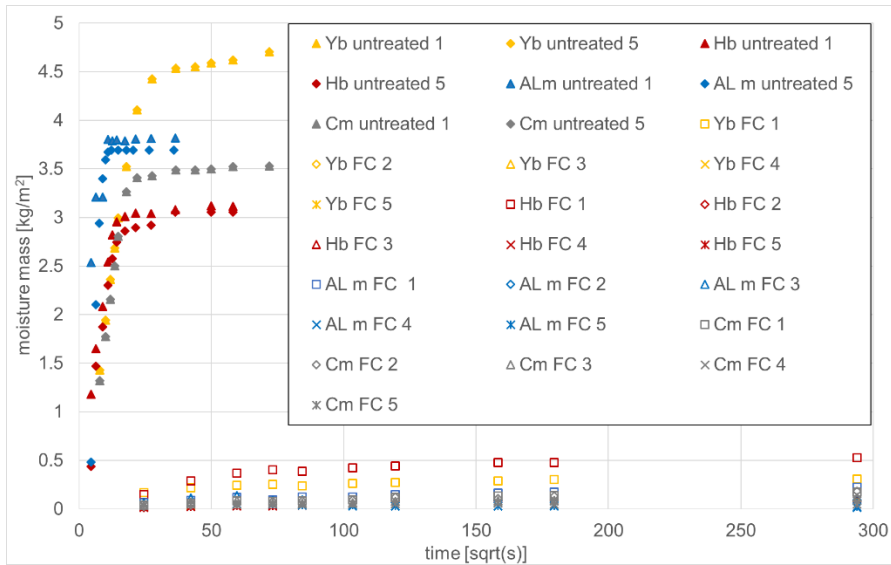


Figure 4- 9 Capillary water uptake of Y brick, H brick, C mortar, AL mortar, untreated and impregnated with FC 40%. 1: 1<sup>st</sup> water uptake before artificial aging, 2: 2<sup>nd</sup> water uptake after 165 cycles of artificial aging, 3: 3<sup>rd</sup> water uptake test after 335 cycles of artificial aging, 4: 4<sup>th</sup> water uptake after 482 cycles of artificial aging, 5: 5<sup>th</sup> water uptake after 635 cycles of artificial aging. Each point of each curve is the average value of the respective measurements of three different samples.

Figure 4- 10 indicates that weathering reduces further the water uptake of the impregnated brick and mortar samples. For bricks, reduction is mainly seen at 2<sup>nd</sup> water uptake, while a more gradual reduction is seen for mortars.

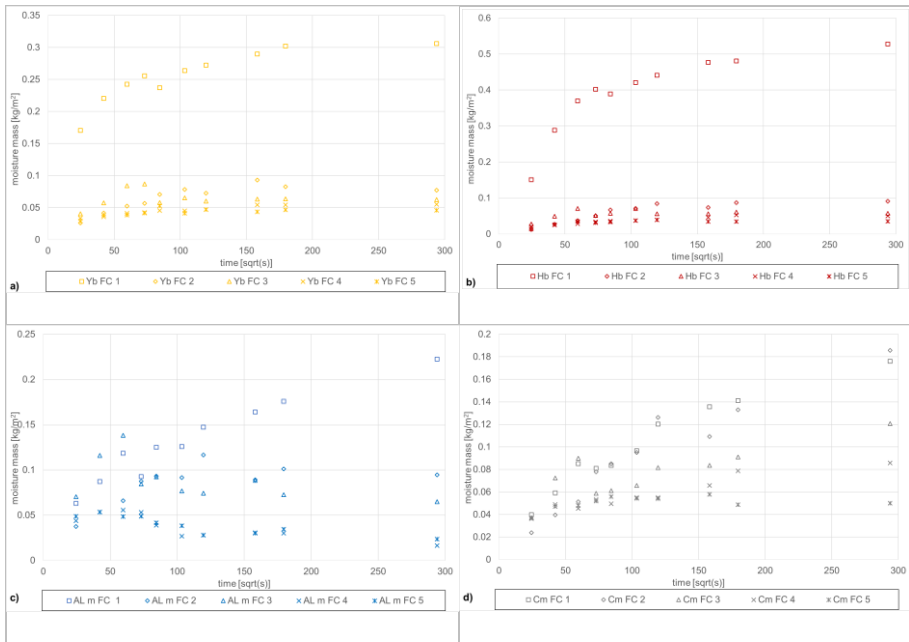


Figure 4- 10 Capillary water uptake of a) Y brick, b) H brick, c) C mortar, d) AL mortar, impregnated with FC 40%. 1: 1<sup>st</sup> water uptake before artificial aging, 2: 2<sup>nd</sup> water uptake after 165 cycles of artificial aging, 3: 3<sup>rd</sup> water uptake test after 335 cycles of artificial aging, 4: 4<sup>th</sup> water uptake after 482 cycles of artificial aging, 5: 5<sup>th</sup> water uptake after 635 cycles of artificial aging. Each point of each curve is the average value of the respective measurements of three different samples.

#### Karsten tube measurements

Karsten tube tests also showed that hydrophobization could block liquid water transport in brick and mortar samples after aging and in brick and mortar joints of a mock-up wall treated with water repellent agents six years ago (see Figure 4- 11).

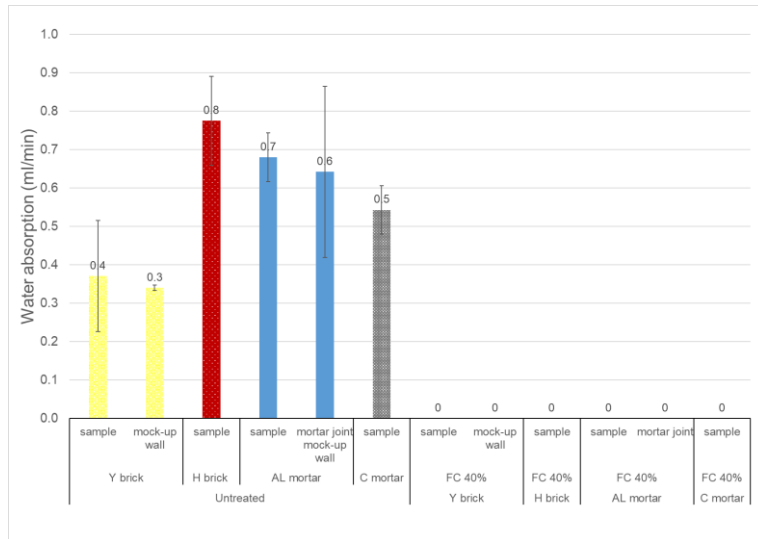


Figure 4- 11 Water absorption by Karsten tube test, Y brick, H brick, AL mortar, C mortar, and mock-up wall, untreated and impregnated with Remmers FC cream 40%. “Sample” refers to samples from artificial aging, “wall” and “mortar joint” refer to mock-up wall measurements on brick and mortar joints respectively. Each result is an average based on three measurements, error bars correspond to standard deviation (Paper II).

#### Contact angle measurements

Contact angle determines the hydrophobic behavior of building materials surface. The surfaces of hydrophobized brick and mortar samples had similar contact angles, which were reduced after artificial aging. In C mortar and AL mortar impregnated with FC 40%, the contact angle was reduced to the point that it was difficult to be measured (see Table 4- 1).

Table 4- 1 Contact angle measurements before and after artificial aging.

	Y brick	H brick	C mortar	AL mortar
<b>Before aging (<math>\gamma^\circ</math>)</b>	130 (8)	124 (3)	130 (5)	132 (9)
<b>After aging (<math>\gamma^\circ</math>)</b>	104 (4)	91 (15)		

Each result is an average based on three samples. The values in () correspond to the standard deviation

#### Discoloration

Hydrophobization keeps the exterior appearance of the brick and mortar samples tested in the Atlas Weather-Ometer while all the untreated tested materials reveal white stains after artificial aging (see Figure 4- 12). The white stains are more evident in the Y brick compared to the rest of the building materials.

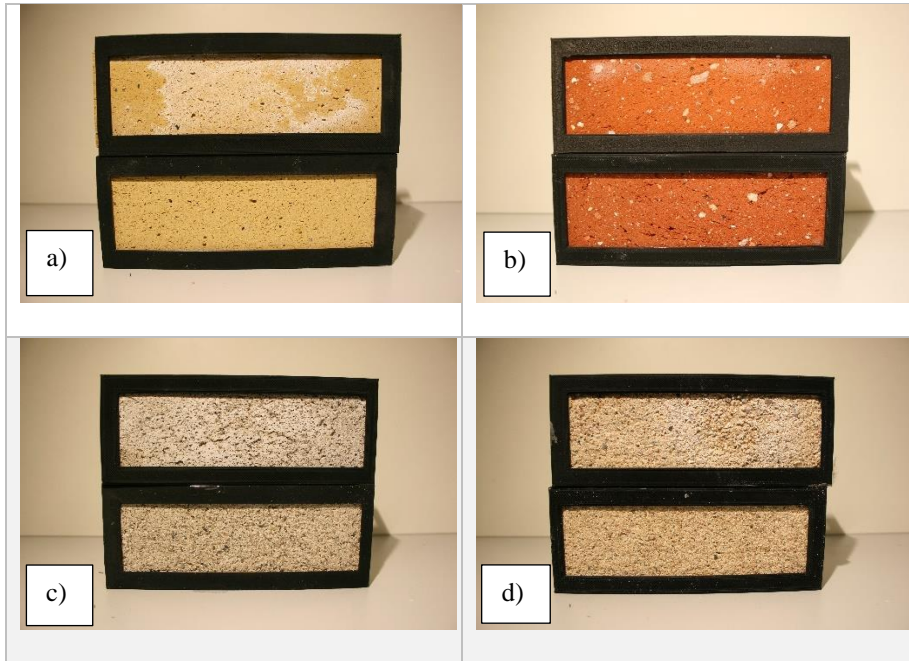


Figure 4- 12 Untreated (above) and impregnated (below): a) Y brick, b) H brick, c) C mortar, d) AL mortar, impregnated with FC 40% after 635 cycles of artificial aging.

## 4.3 COMPONENT LEVEL: HYDROPHOBIZATION AND INTERNAL INSULATION

### 4.3.1 EXPERIMENTAL VALIDATION OF THE HYDROPHOBIC MODEL

#### *Material level*

The hydrophobic model captures the basic characteristics of wetting and drying at the material level as illustrated in Figure 4- 13. The simulation results of the drying test are on the safe side and the small difference compared to experimental results is explained in Paper III.

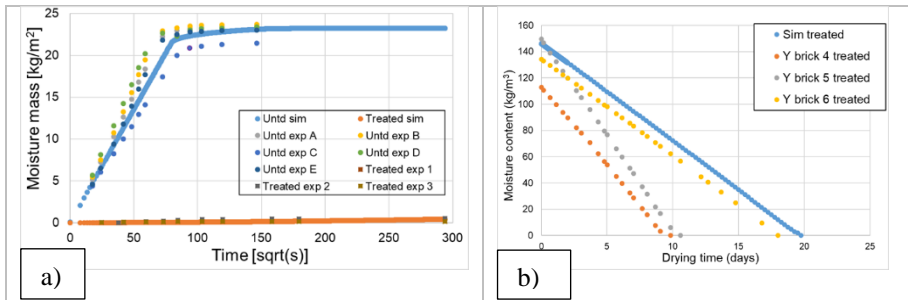
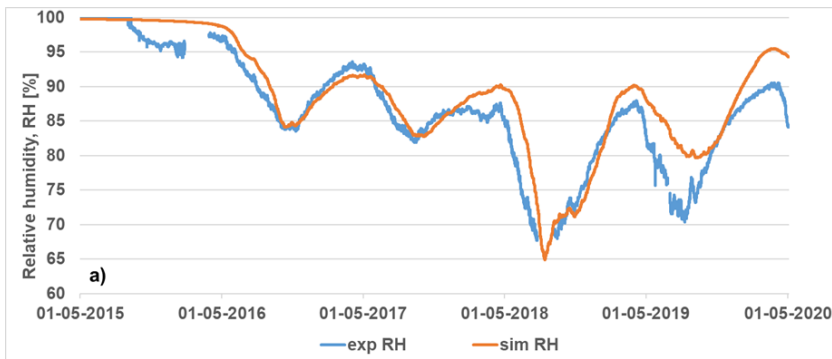


Figure 4- 13 Comparison of experimental (Y brick) impregnated with FC 40% and simulation (Sim) results. Water uptake (a). Drying test (b) (Paper III).

### Component level

The results indicate an agreement between the measured and predicted values, as the model predicts the peaks and troughs of both temperature and relative humidity (see Figure 4- 14 and Paper III).





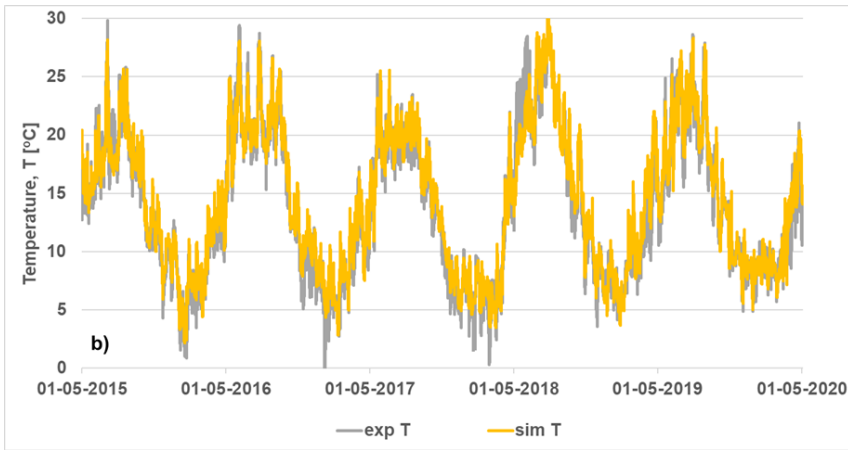


Figure 4- 14 Relative humidity (a) and temperature (b) in the interface between hydrophobized (FC 40%) masonry and internal insulation (IQ-therm). Comparison of experimental (exp) and simulation (sim) results (Paper III).

#### 4.3.2 SIMULATION STUDY

##### *Average moisture content in the masonry*

Adding internal insulation to the masonry significantly increases the average moisture content. When hydrophobization is applied prior to or at the same time as internal insulation, it can sustain the average moisture content at very low levels (see Figure 4- 15). However, when hydrophobization is applied after internal insulation in our case five years after, the average moisture content needs some time to reach very low levels (see Figure 4- 16). It needs additional time to be eliminated, depending on, among other parameters, the insulation system and the impregnation depth of the treatment. Vapor tight insulation systems like mineral wool with vapor barrier and deeper impregnation depths increase the time needed for moisture to be eliminated. Hydrophobization blocks liquid transport, which results in a reduced drying rate, and moisture remains inside the masonry for a longer period when the hydrophobic layer spreads deeper into the masonry (40 mm) compared to the impregnation depth of 2.4 mm. Since hydrophobization blocks water liquid transport, drying mainly occurs through water vapor transport. The longer the distance water vapor has to travel, the slower the process of drying becomes.

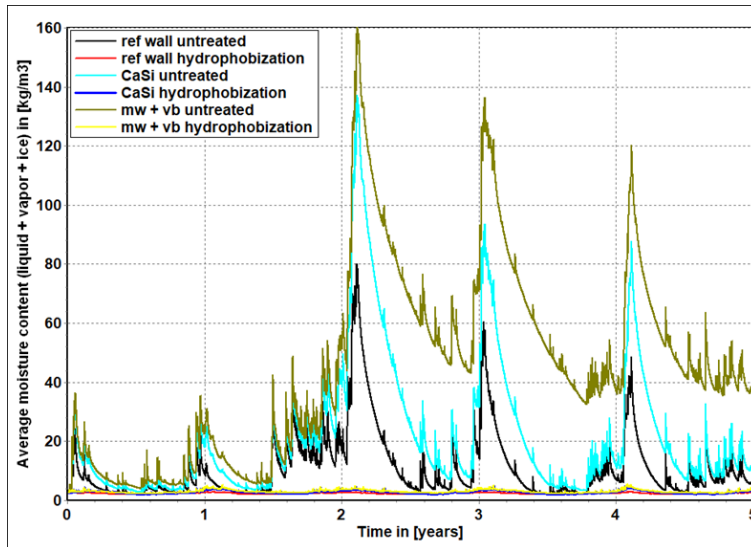


Figure 4- 15 Average moisture content in the masonry in SW-oriented wall configurations, including a reference wall (ref wall), a wall internally insulated with calcium silicate (CaSi), and a wall internally insulated with mineral wool and a vapor barrier (mw+vb). In all three cases with or without hydrophobization. Impregnation depth 2.4 mm based on the lowest reported value of impregnation depth in Y brick from Paper I. Simulation based on climate data for Copenhagen 2020-2024 (Paper III).

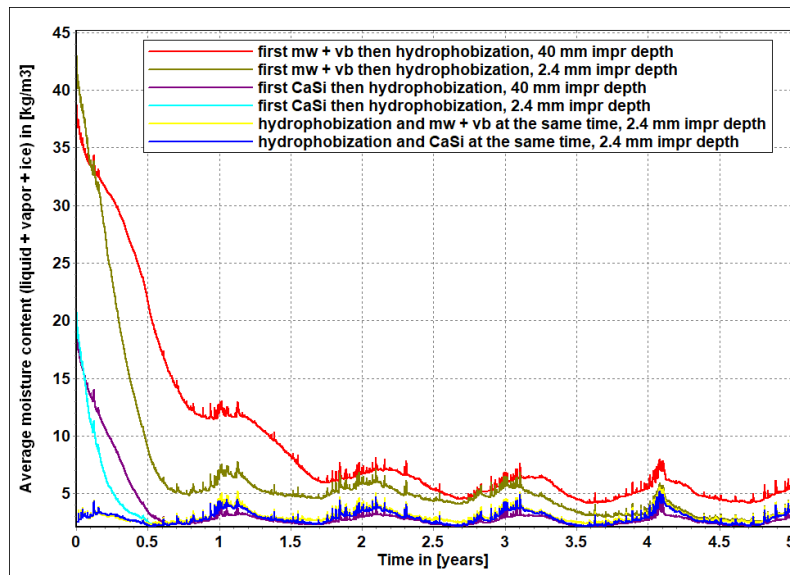
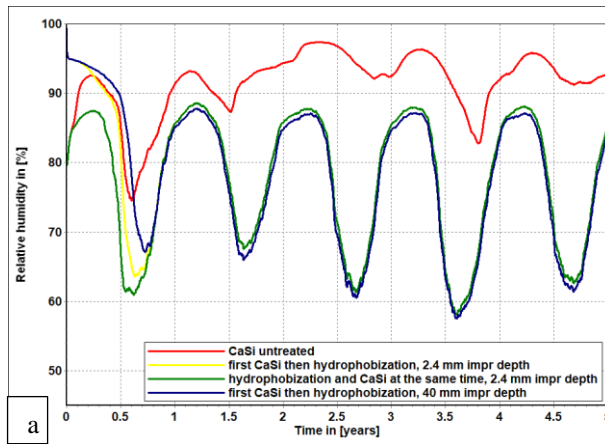


Figure 4- 16 Average moisture content in the masonry in SW-oriented wall configurations, in the case of applying a water repellent agent at the same time as internal insulation (as in Figure 4- 15) or five years after. Yellow and blue curves are the same as in Figure 4- 15,

while olive and turquoise curves are the continuation of curves in Figure 4- 16. Impregnation depth 2.4 mm or 40 mm based on impregnation depth values reported from Paper I. The configurations include a wall internally insulated with calcium silicate (CaSi) and a wall internally insulated with mineral wool and a vapor barrier (mw+vb). Simulation based on climate data for Copenhagen 2020-2024 (Paper III).

#### *Relative humidity between masonry and internal insulation*

Relative humidity on the interface between masonry and internal insulation follows the trends of average moisture content in the masonry. It is influenced, among other parameters, by the insulation system, the sequence of applying hydrophobization, internal insulation, and the impregnation depth. For the vapor-open capillary-active internal insulation (CaSi), the effect that the sequence of applying hydrophobization and internal insulation as well as the impregnation depth have on the relative humidity between masonry and internal insulation, is practically insignificant, as shown in Figure 4- 17 (a) . The situation changes dramatically for a vapor and water tight internal insulation, such as mineral wool plus vapor barrier, for which RH stays at high levels, similar to the case where hydrophobization is applied five years after internal insulation. In the case of 2.4 mm impregnation depth, RH reaches the same level with the case of applying hydrophobization and internal insulation at the same time after four years. However, in the case of 40 mm impregnation depth, the RH remains at high levels after five years, as shown in Figure 4- 17 (b).



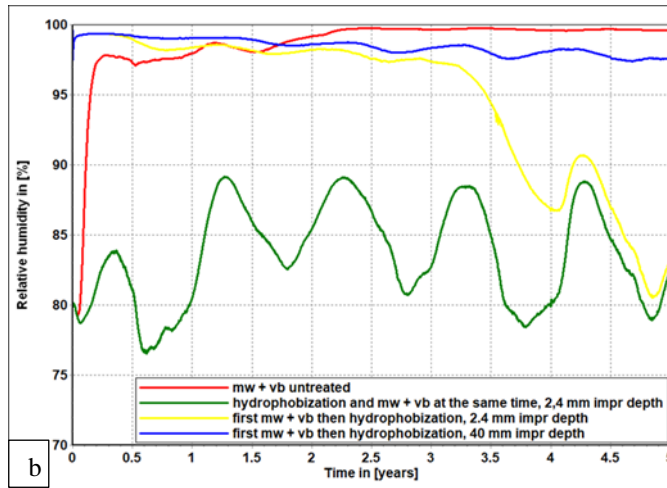


Figure 4- 17 Relative humidity at the interface between masonry and internal insulation in a SW-oriented wall configurations, in the case of applying a water repellent agent at the same time as internal insulation or five years after. Impregnation depth 2.4 mm or 40 mm based on impregnation depth values reported from Paper I. The configurations include a wall internally insulated with a wall internally insulated with calcium silicate (CaSi) (a), mineral wool and a vapor barrier (mw+vb) (b). Simulation based on climate data for Copenhagen 2020-2024.

#### *Mould growth in the interface between masonry and internal insulation*

A frequent problem in buildings in Denmark is the risk of mould growth in the interface between masonry and internal insulation, which is significantly reduced by hydrophobization (see Figure 4- 18).

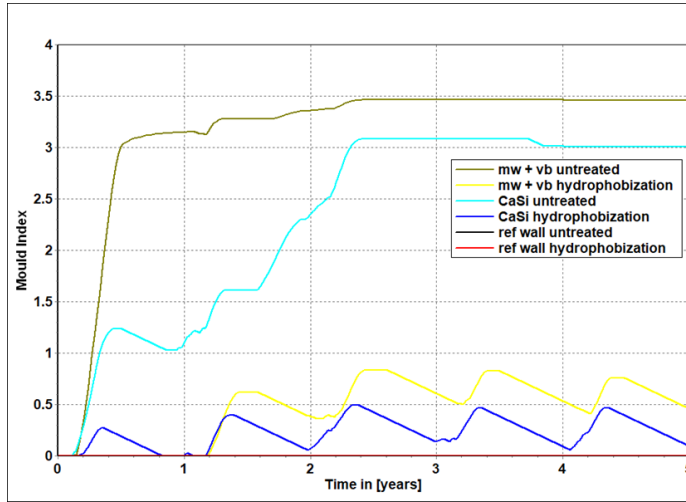


Figure 4- 18 Mould growth expressed as mould index in the interface between masonry and internal insulation in SW-oriented wall configurations, including a reference wall (ref wall), a wall internally insulated with calcium silicate (CaSi) and a wall internally insulated with mineral wool and a vapor barrier (mw+vb). In all three cases with or without hydrophobization (applied at the same time as internal insulation). Impregnation depth 2.4 mm based on the lowest reported value of impregnation depth in Y brick from Paper I. Simulation based on climate data for Copenhagen 2020-2024 (Paper III).

#### Moisture safe energy savings

Figure 4- 19 illustrated the accumulated heat loss after five years of simulation. Hydrophobization has the potential of further reducing the heat losses for both uninsulated and internally insulated walls.

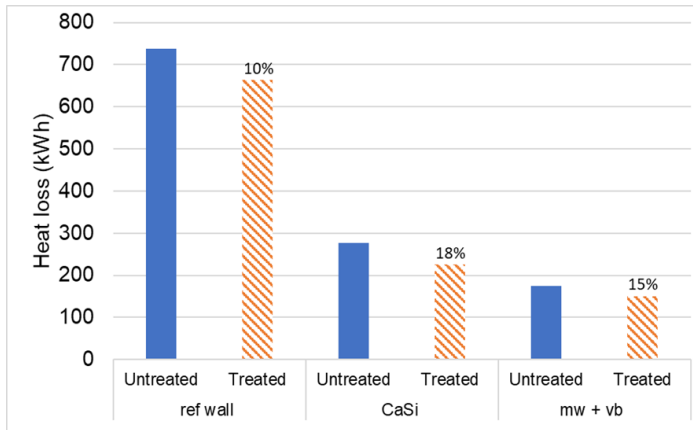


Figure 4- 19 Accumulated heat loss in SW-oriented wall configurations, including a reference wall (ref wall), a wall internally insulated with calcium silicate (CaSi), and a wall internally insulated with mineral wool and a vapor barrier (mw+vb). In all three cases without (untreated) and with (treated) hydrophobization, applied at the same time as internal insulation. Impregnation depth 2.4 mm based on the lowest reported value of impregnation depth in Y brick from Paper I. Simulation based on climate data for Copenhagen 2020-2024. The percentages indicate the additional energy savings due to hydrophobization (Paper III).

#### Weak hydrophobic layer

Previous sections reported the potential benefits of applying hydrophobization and the combined effect with internal insulation. However, in case of a hydrophobic treatment that remains weak in terms of absorption coefficient ( $A_{cap}$ ) in the long-run, the hygrothermal performance of the wall configuration may worsen, as shown in Figure 4- 20.

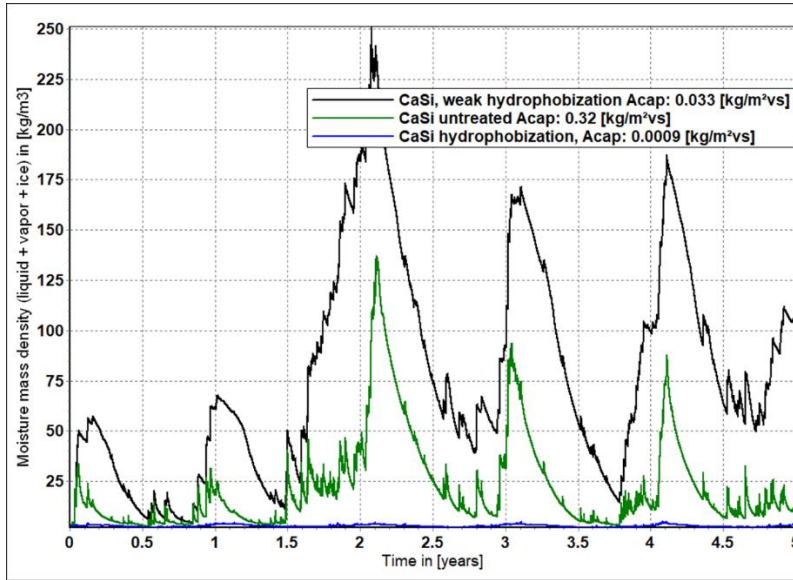


Figure 4- 20 Average moisture content in a SW-oriented wall internally insulated with calcium silicate (CaSi). Weak hydrophobization is based on the highest  $A_{cap}$  reported in hydrophobized samples which becomes lower after repeating the capillary water uptake test in Paper I. Impregnation depth 2.4 mm based on the lowest reported value of impregnation depth in Y brick from Paper I. Simulation based on climate data for Copenhagen 2020-2024.

### 4.3.3 CASE STUDY BUILDING

Figure 4- 21 shows four years of relative humidity at the interface between masonry and internal insulation in the case building. Hydrophobization lowers RH peaks, but for RH to reach lower levels, more time is needed because of the built-in moisture caused by applying internal insulation two years before hydrophobization. The west-oriented RH sensor at the interface between masonry and internal insulation (green curve) is the only sensor that does not illustrate any reduction in relative humidity, but its accuracy is questioned since the sensor in the window sill at the same orientation illustrates a significant reduction in relative humidity (red curve) (Paper III).

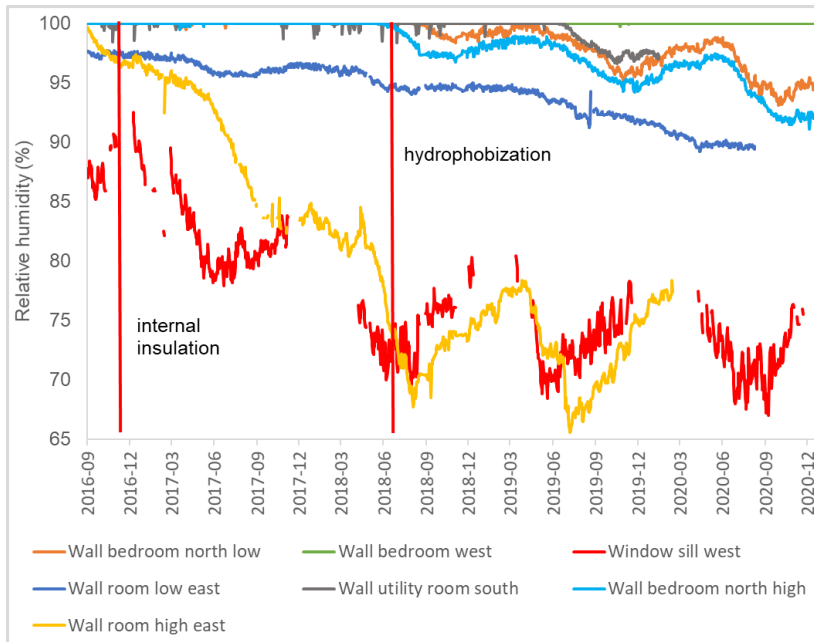


Figure 4- 21 Relative humidity during a four-year-period (Sep 2016 – Dec 2020) in the interface between masonry and internal insulation (iQ-Therm) in a case building. West (green), South (grey), North (orange and light blue), and East (blue and yellow) oriented wall configurations and in the window sill West (red).



# CHAPTER 5 DISCUSSION

## 5.1 MAIN FINDINGS

The present thesis examined the effect of water repellent agents on different types of brick and mortar, both at the material and at the component levels. Water repellent agents significantly alternate the hygrothermal behavior of brick and mortar samples as well as hydrophobized internally insulated walls. They can create a layer impermeable to liquid water that keeps both its performance and its appearance but loses its beading effect after aging, without notable change in the pore structure of the material. The layer is still permeable to water vapor with an increasing impregnation depth over a period of time after hydrophobization through the redistribution of the active ingredient. Further, the combination of hydrophobization and internal insulation can create a moisture safe construction with reduced risk of moisture-related damage and increased energy saving by keeping the moisture content and thereby the thermal conductivity of the wall materials low. The hygrothermal benefits of hydrophobization in combination with internal insulation can reveal faster when hydrophobization is applied prior or at the same time with internal insulation. The before-mentioned results are going to be discussed in the following sections of the discussion.

## 5.2 MATERIAL LEVEL

### 5.2.1 HYGRIC PROPERTIES

#### 5.2.1.1 Storage properties

Defining the storage properties of hydrophobized building materials faces a challenge since liquid water transport is impeded. Results based on the current experimental procedures should be interpreted with care, as these experiments were developed for hydrophilic building materials. In some studies, the capillary moisture content is defined from a free capillary water uptake (see Table 2-2). In those cases where a significant reduction of the value is reported [13,40], it is coming from the first stage of the capillary water uptake curve, because a second stage cannot be defined in a strong hydrophobic layer. On the other hand, those reports of a small reduction in capillary moisture content, and who are able to define a second stage [15,39], possibly refer to a incorrectly applied hydrophobic layer or more probably to a hydrophobic layer that needs water exposure after treatment and longer curing time to show an improved water repellency performance (Paper I). If they repeated the capillary water uptake test, they would be unable to define a second stage. In a material with a strong hydrophobic layer, the capillary moisture content is difficult to define with the current experimental techniques designed for hydrophilic porous building materials.

The open porosity should be defined in a hydrophobized material, but the results are not fully reliable as water needs a longer time to fill the pores of the material, even with the absence of air in a vacuum saturation test. The most reliable of the current experimental procedures to provide information about the storage properties of hydrophobized building materials is the mercury intrusion porosimetry test (MIP) where you intrude mercury into the pores of the material using overpressure, and therefore the results are not affected by the hydrophobicity of the material. The results concerning open porosity and pore volume distribution of brick and mortar samples (see Figure 4-3 and [65]) agree that there is no significant change in the pore structure of the material. Some small changes can occur in mortar samples due to finer pores. The small reduction of the open porosity is also responsible for the small increase of the vapor diffusion resistance factor presented in Figure 4-6 and some of the references of Table 2-2 [13,40,41]. But after storing the hydrophobized samples in water and repeating the cup test, the vapor diffusion resistance factor decreases and comes even closer to the result of the untreated samples (see Figure 4-6). By combining the latter with the increased water repellency performance after water exposure (see Papers I and II) and the redistribution of the active ingredient (water uptake from the not impregnated side, Figure 4- 8), we can conclude that the hydrophobic film is attached to the pore walls of the building material. Then after water exposure and longer curing time, the active ingredient reacts again and forms new bonds, and is spreading deeper without losing its water repellency performance after aging (see Figure 4- 9).

### 5.2.1.2 Transport properties

It is possible to determine the transport properties of hydrophobized porous building materials, i.e. capillary absorption coefficient and vapor diffusion resistance factor, but – as for the storage properties – the absorption coefficient faces a challenge due to the very low water uptake, which means that the results are dependent on the accuracy of the measurements. Also, since a second stage in the capillary water uptake curve cannot be reached, we define the capillary absorption coefficient according to [57]. However, the clear message in this PhD thesis is that silicon based water repellent agents tested in brick and mortar samples show significant reduction of the absorption coefficient ( $A_{cap}$ ) when comparing untreated and treated samples (98.8 %) and when the water uptake test is repeated (99.8 %), cf. Paper I, supporting previous findings (Table 2-2, average reduction 92.5 %). The silicon based water repellent agents even retain the low level of  $A_{cap}$  after aging, according to Paper II. On the contrary, vapor diffusion resistance factor remains almost unchanged with a slight increase in both brick and mortar tested with liquid and cream water repellent agents. The determination of transport properties ( $A_{cap}$  and  $\mu$ -value) are relevant for the hydrophobized building materials, but it is advisable to repeat the tests since these properties can change after water exposure (see Figure 4-5, Figure 4-6, and Figure 4-10).

It is generally agreed in the literature and in the technical data sheets of water repellent agents that specific types of water repellent agents are suitable for specific types of substrates. Nonetheless, silane water repellent agents originally recommended for concrete (SMK 2101 liquid, BS creme C) perform exceedingly well in both mortar and brick, although they may need longer curing time and after-treatment water exposure compared to siloxanes, especially in bricks. Silanes need longer time when applied to brick, compared to siloxanes, in order for hydrolysis and polycondensation to occur and start the formation of longer molecules to effectively cover the larger pores of brick.

### 5.2.2 IMPREGNATION DEPTH

Brick and mortar illustrate similar levels of  $A_{cap}$  reduction after impregnation with silicon based water repellent agents; however, the impregnation depth is higher in the different types of brick than in the mortar types. Both in brick and in mortar, hydrophobization creates a first strongly hydrophobized layer as well as a larger volume that is partly hydrophobized [40] (see also Paper I). Water uptake tests from the non-impregnated side are particularly interesting in view of extending and challenging our understanding of a specific impregnation depth reported in the technical data sheets of water repellent agents [43]. Since water uptake from the non-impregnated side in brick becomes negligible after longer curing time and water exposure (see Figure 4- 8), it can be assumed that the active ingredient is distributed deeper and reaches the opposite side (8 cm), even by applying the minimum recommended amount for cream products (150-200 ml/m<sup>2</sup>). In other words, the whole sample becomes hydrophobized. In samples with larger heights, the active ingredient could have been spread even deeper probably. In mortar samples the active ingredient did not reach the opposite side (8 cm), although the  $A_{cap}$  was lowered on the second water uptake tests from the non-impregnated side compared to the first, leading to the conclusion that the active ingredient spreads deeper compared to the initial observations. It should be noted that water uptake tests from the non-impregnated side aim not to define a specific impregnation depth but to investigate the redistribution of the active ingredient. Moreover, it is interesting to note that both in liquid and cream products, the water repellent agent is absorbed faster in brick than in mortar. The impregnation depth might be increased by applying larger amounts of the agent and/or increasing the amount of the active ingredient by using higher concentrations. These actions could result in a higher impregnation depth both in brick and mortar, further ensuring water repellency (see Paper I).

### 5.2.3 DURABILITY OF THE HYDROPHOBIC TREATMENT

Hydrophobization creates a layer impermeable to liquid water that penetrates deep into the material, cf. sections 4.2.2 and 4.2.4, but the durability of this layer in terms of water repellency is very important to know. The artificial aging results (Figure 4-9) contribute to existing research on the durability of hydrophobization in brick

samples [30] and extend this perspective to mortar samples impregnated with cream water repellent agents. The tested concentrations of 40 and 80 %, which are typical concentrations for cream agents [39,40], keep the water repellency performance through artificial aging both in brick and mortar samples. The water repellency performance of all the tested samples is improved after aging (see Figure 4- 9 and Paper II), supporting the findings that rain exposure contributes positively to a strong hydrophobic layer. Moreover, air lime mortar had the risk of being insufficiently impregnated due to the chemical composition (not hydroxylated surfaces) being different from cement and hydraulic lime mortar. But it seems that the active ingredient of the cream agents is able to form irreversible bonds with the pore walls of the air lime mortar, as the level of water repellency of the air lime mortar samples was similar to the samples of cement mortar and the brick types in the first water uptake before the artificial aging. Further, the water repellency performance of air lime mortar follows exactly the same trend of improvement like the rest of the building materials during artificial aging.

#### **5.2.3.1 Beading effect**

The four tested substrates showed a tendency of contact angle reduction after artificial aging which means that the beading effect (droplet formation on the facade during rain events) had declined (Table 4- 1). In the area that was covered by the sample holders and thus was not exposed to UV radiation, the contact angle was not reduced after artificial aging in any sample. This leads to the assumption that UV radiation was responsible for the reduction of the beading effect after aging, since the whole surface of all samples was exposed five times to water during water uptake tests. UV radiation can cause the formation of molecules with an excess of electrons (i.e. free radicals), which facilitates the degradation of polymeric surfaces [66]. In concrete, UV light is known to break the chemical bonds between hydrophobic molecules and the substrate [67]. Nevertheless, because UV light cannot penetrate deep into the material, this only takes place at the outermost layer of the substrate [68], and therefore water absorption performance was not worsened [67] (see Figure 4- 9 and Figure 4- 11). Although the beading effect is not an important indicator in terms of overall efficiency of the hydrophobic treatment and not necessarily desirable for the building owner, it could remain for longer by applying a higher percentage of siloxane and higher concentrations of the active ingredient (see Paper II).

#### **5.2.3.2 Discoloration through aging**

The artificial aging reveals an additional benefit of hydrophobization as hydrophobized samples keep their appearance after artificial aging while the untreated samples reveal white stains (efflorescence). Both brick and mortar samples were sprayed with deionized water during the artificial aging, so the migration of salts to the exterior surface occurs from salts present in the materials. Efflorescence may not

be a major structural problem of the construction, but it is an aesthetic problem to the prestige of the building that should be avoided.

## **5.3 COMPONENT LEVEL**

### **5.3.1 HYDROPHOBIZATION AND INTERNAL INSULATION**

The building materials tested for artificial aging were selected to represent a typical Danish historic building (bricks and air lime mortar) and the type of cement mortar used for mortar joints repointing. The performance of these building materials after hydrophobization seems quite promising at the material level, but it is equally important to know their hygrothermal performance at the component level, especially when combined with internal insulation, since it induces moisture problems to the construction. Finding a solution to the moisture problems induced by internal insulation is one of the greatest challenges faced by building practitioners today.

Numerical simulations support the view that a hydrophobic layer with properties derived from the experimental section of the thesis improves the hygrothermal behavior of internally insulated walls. More specifically, the numerical simulations illustrate that hydrophobization is able to reduce the moisture content considerably in the masonry and also the risk of mould growth formation in the interface between masonry and internal insulation when applied before or at the same time as internal insulation. This is observed regardless of the insulation thickness, masonry thickness, climate, and orientation. However, when internal insulation is installed prior to hydrophobization, moisture starts to accumulate in the masonry. The accumulation of moisture depends on the insulation system, the duration of time before hydrophobization is applied, the hygric properties of the masonry, the climate, the wall orientation, the insulation thickness, and on the seasonal wetting and drying. When hydrophobization is applied, it may allow vapor diffusion but impedes liquid transport in the hydrophobized part of the masonry which slows down the drying. On one hand, the wind-driven rain load is eliminated; on the other hand, the built-in moisture dries out at a slower rate. When hydrophobization is applied in an internally insulated wall, for a period of time, the hygrothermal performance of the wall configuration can illustrate a poorer performance compared to the untreated wall (see Figure 4- 16 and Figure 4- 17). This period could last from months in a wall configuration with a vapor open and capillary active insulation system, such as CaSi, to years with a vapor and water tight insulation system, such as mineral wool with a vapor barrier, or XPS (see Figure 4- 16 and Paper III).

If a solid, south-west oriented masonry facade in Denmark or similar climate with high rain load, which is internally insulated with more than 100 mm mineral wool and a vapor barrier and stands for more than five years without hydrophobization, it should be expected that the built-in moisture would need more than two years to dry out from the moment that the water repellent agent is applied (see Figure 4- 16 ). Eventually,

the built-in moisture dries out and, at the same time, there is no new entry of moisture from rain events, resulting in very low levels of average moisture content inside the masonry. Therefore, even when hydrophobization is applied after internal insulation, the long-term hygrothermal performance would be positive.

The monitoring results from the case study building where hydrophobization was applied two years after internal insulation are in line with the numerical simulation results. RH in the interface between masonry and internal insulation gradually declines from a high level following the seasonal wetting and drying.

The probability of mould formation and interstitial condensation at the interface between masonry and internal insulation is affected from the sequence of applying hydrophobization and internal insulation, but the wind-driven rain is not the only source of moisture at that point. RH in the interface between masonry and internal may reach high levels due to i) wind-driven rain transported by liquid transfer, ii) outdoor RH, and iii) indoor RH transported via diffusion and air leakages. In a North European climate, in the case of an exceedingly high outdoor RH during winter or/and high internal moisture load, RH in the interface between masonry and internal insulation can reach high values even when hydrophobization has eliminated the incoming wind-driven rain load (see also Paper III).

### **5.3.2 ENERGY SAVINGS FROM HYDROPHOBIZATION**

The difference in thermal conductivity measured in dry and capillary saturated samples illustrates a potential for energy savings when applying water repellent agents, as shown in Figure 4-7. In Southern European countries, hydrophobization should be mainly used for building maintenance of the structure and to avoid discoloration. But numerical simulations illustrate that in North European countries with high rain loads, hydrophobization could be considered as an energy-saving measure both as a single approach and when it is combined with internal insulation, providing additional energy savings by keeping the wall elements dry.

### **5.3.3 WEAK HYDROPHOBIC TREATMENT**

However, it is very important to note that in order for the hydrophobized internally insulated wall to maintain a high level of hygrothermal performance, the hydrophobic layer should be durable in terms of a low absorption coefficient. A weak hydrophobic layer that allows part of the wind-driven rain to penetrate may reverse the positive impact of hydrophobization and worsen the hygrothermal behavior of the wall (see Figure 4- 20). The weak impregnation reported in Figure 4- 20 derives from water repellent agents that improve the water repellency performance with longer curing time and after-treatment water exposure. So, the actual absorption coefficient for that impregnation would be much lower, resulting in a hydrophobic layer impermeable to liquid water as it is shown after repeating the water uptake. Moreover, it is very

important that the artificial aging indicates that the brick and mortar could maintain their water repellency performance during aging, as a declined performance could threaten the long-term effectiveness of hydrophobization when combined with internal insulation.

### 5.3.4 PRACTICAL RECOMMENDATIONS

The current PhD thesis illustrates that a strong hydrophobic layer in terms of water repellency could be beneficial for the hygrothermal performance of internally insulated solid walls constructed with brick and mortar. For other types of material, such as natural stone, not included in this study, it is recommended to extract a sample from the masonry and first impregnate it and test at least the absorption coefficient before impregnating the whole building to ensure a low absorption coefficient of the treated building material.

Further considerations to be taken into account when starting a hydrophobization project in order to ensure a sufficient strong hydrophobic layer are as follows:

- ❖ not to leave untreated parts of the facade such as art details, window sills, roof corners, and overhangs constructed from porous building materials,
- ❖ to give extra attention when treating close to windows and doors,
- ❖ to repair visible cracks before impregnation, and
- ❖ to clean the substrate with sandblasting or brushing and water.

For the cream products, rain events that occur a few hours after the treatment could be harmful as they can remove the freshly applied cream. However, rain events that take place after a couple of days could enhance the hydrophobic treatment, in terms of lowering further the absorption coefficient, by washing of the emulsifiers that permit the active ingredient of the water repellent agent to form additional bonds with the pore wall of the building material. The findings of the current thesis suggest testing the water repellency performance after one month of curing and then checking after some months of rain events for improved water repellency performance. If the water repellency on some parts of the wall is not sufficient, the treatment should be repeated [67].

## CHAPTER 6 CONCLUSION

The numbers correspond to the previously stated hypotheses in section 1.3 Hypotheses:

SH1) It was hypothesized that the water repellent agents available on the market can be identified by studying their physical and chemical properties. This is proven to be true since silicon based water repellent agents can be identified through their active ingredient, their form, the type of diluent, the concentration of the active ingredient, the alkyl group, and the type of substrate recommended for application.

SH2) It was hypothesized that hydrophobization does not alternate the moisture storage properties of brick and mortar samples in the material level, but changes the transport properties by eliminating the capillary liquid water absorption although it allows vapor transport. This is proven to be true since hydrophobization creates a layer impermeable to liquid water but still permeable to water vapor, without major alterations in the pore structure, according to experimental results from water uptake tests (absorption coefficient), cup tests ( $\mu$  value), vacuum saturation tests (open porosity), and mercury intrusion tests (pore volume distribution).

SH3) It was hypothesized that by testing brick and mortar samples, a specific impregnation depth of the treatment can be defined. This was in fact proven to be untrue since the depth of the hydrophobized layer increases for a period of time after hydrophobization through the redistribution of the active ingredient, resulting in a non-homogenous hydrophobic layer with a strong hydrophobized area and a larger area that is partially hydrophobized. This was tested by investigating the absorption coefficient from the non-impregnated side.

SH4) It was hypothesized that hydrophobized brick and mortar samples retain their water repellency performance after aging. This is proven to be true since after artificial aging (water spray and UV radiation) the absorption coefficient remains at low levels in four types of building materials (air lime mortar, cement mortar, and two types of brick) impregnated with cream products. After-treatment water exposure contributes to further reduction of the absorption coefficient, and the UV radiation is responsible for the declined beading effect. Furthermore, in all cases, the untreated building materials suffered from efflorescence after artificial aging while in the hydrophobized cases they did not.

SH5) It was hypothesized that hydrophobization reduces the moisture related problems induced by internal insulation. This is supported by the numerical simulations that illustrate a lower risk for moisture related problems in hydrophobized internally insulated walls. When you apply hydrophobization before or at the same time as internal insulation, you get all the advantages of a moisture safe construction



immediately. If instead you apply hydrophobization after internal insulation, you need some time to achieve a moisture safe construction. This was also shown in a case building where internal insulation was installed two years prior to hydrophobization and high RH values were measured in the interface between masonry and internal insulation. However, there is gradual decline of relative humidity peaks after hydrophobic treatment following the wetting (winter) and drying (summer) period.

SH6) It was hypothesized that hydrophobization yields energy savings as a single approach and additional energy savings when combined with internal insulation. True. This is supported by numerical simulations illustrating that hydrophobization shows the potential to be considered as an energy-saving measure, especially in a North European country with high rain loads like Denmark. Hydrophobization reduces the heat losses of the wall configurations by keeping the building materials dry and thus keeping a low thermal conductivity, as a single approach, and further reduces heat loss when it is combined with internal insulation.

As an overall conclusion, this work has confirmed the main hypothesis that hydrophobization improves the hygrothermal performance of an internally insulated solid masonry wall.

## CHAPTER 7 PERSPECTIVE

The current thesis presents an in-depth analysis of water repellent agents and their impact on brick/mortar samples at the material level and on brick/mortar walls at the component level. But there is still work to be done in order to achieve a better overview of hydrophobization and the combined effect with internal insulation to produce robust guidelines targeting a moisture safe renovation of the existing building stock. Initially, at the material level, the durability of the hydrophobic treatment tested at artificial aging in the Atlas Weather-Ometer with water spray and UV radiation, the temperature in the cabinet was set at 38 °C. There was no exposure to lower temperatures, i.e. the risk of frost damage after hydrophobic treatment is an area still in need of research. Furthermore, the present study focuses on different types of brick and mortar, but other building materials like natural stone, wood, and concrete should be tested as well as, because they are usually found in buildings and since they are also porous building materials, hydrophobization may be effective in terms of lowering the absorption coefficient.

The existing experimental procedures that measure the hygric properties of porous building materials are based on the principle that liquid water is being absorbed by capillary uptake. Hydrophobization proved to impede this liquid water transport heavily, giving rise to thoughts that new experimental procedures should be developed to better characterize the hygric properties of hydrophobized building materials which should also target defining the moisture retention and moisture permeability curves. The moisture retention and permeability curves are important to fully characterize the hydrophobic building material and to create accurate models of the materials for hygrothermal simulations. This is a field of study that is in the process of development at the Building Physics department in KU Leuven.

The first extension of the present thesis at the component level should be Karsten tube measurements of hydrophobized buildings in order to build more confidence about the durability of the hydrophobic treatment. Hydrophobization blocks the wind-driven rain from entering the facade. But moisture coming from the ground advances additional risks for the construction that should be further investigated with in-situ measurements in real buildings and numerical simulations. The same level of water repellency between hydrophobized brick and mortar samples gave us the opportunity to perform 1D simulations of hydrophobized internally insulated wall configurations. However, the facade consists of both brick and mortar, and 2D simulations could provide higher accuracy especially on the percentage of energy savings derived from hydrophobization in the comparison with untreated samples, but also on internal transport inside the masonry, including how the impregnation depth in a brick masonry wall develops and especially at the interface between brick and mortar.

Even though the present thesis reports monitoring measurements of an inhabited building, further monitoring of hydrophobized buildings with various insulation systems and further testing of the moisture and heat flow should be considered to define the energy saving in a real case scenario of hydrophobization as a single approach and in combination with internal insulation. The technical data sheets of the water repellent agents mention to repoint all the visible cracks before impregnation. However, repointing the mortar joints and replacing the damaged bricks is a time-consuming and capital-intensive procedure. It should be worthy to test the effect of repointing the mortar joints before hydrophobization on the effectiveness of the hydrophobic treatment and to investigate the possible cracks after treatment.

After the hygrothermal assessment of hydrophobization in combination with internal insulation presented in the current thesis, a life cycle assessment as well as life cycle cost assessment will contribute towards a holistic view of hydrophobization.

Last but not least, taking into consideration the results of the current study and the proposed perspectives, guidelines of how to combine hydrophobization with internal insulation should be issued targeting to improve the energy performance of the building by keeping it dry.

## REFERENCES

- [1] C.A. Balaras, A.G. Gaglia, E. Georgopoulou, S. Mirasgedis, Y. Sarafidis, D.P. Lalas, European residential buildings and empirical assessment of the Hellenic building stock, energy consumption, emissions and potential energy savings, *Build. Environ.* 42 (2007) 1298–1314. <https://doi.org/10.1016/j.buildenv.2005.11.001>.
- [2] M. Jerman, I. Palomar, V. Kočí, R. Černý, Thermal and hygric properties of biomaterials suitable for interior thermal insulation systems in historical and traditional buildings, *Build. Environ.* 154 (2019) 81–88. <https://doi.org/10.1016/j.buildenv.2019.03.020>.
- [3] EC Adhoc Industrial Advisory Group, Energy efficient buildings Public-Private Partnership (PPP): Multi annual roadmap and longer term strategy, Brussels, 2010. <https://doi.org/doi:10.2777/10074>.
- [4] M. Morelli, T.R. Nielsen, S. Svendsen, Development of a method for holistic energy renovation, Technical University of Denmark, 2013. [http://orbit.dtu.dk/en/publications/development-of-a-method-for-holistic-energy-renovation\(2a7f7eae-1627-46eb-b0fc-74616eaa9b6b\).html](http://orbit.dtu.dk/en/publications/development-of-a-method-for-holistic-energy-renovation(2a7f7eae-1627-46eb-b0fc-74616eaa9b6b).html).
- [5] M. Morelli, M. Harrestrup, S. Svendsen, Method for a component-based economic optimisation in design of whole building renovation versus demolishing and rebuilding, *Energy Policy*. 65 (2014) 305–314. <https://doi.org/10.1016/j.enpol.2013.09.068>.
- [6] M. Guizzardi, D. Derome, R. Vonbank, J. Carmeliet, Hygrothermal behavior of a massive wall with interior insulation during wetting, *Build. Environ.* 89 (2015) 59–71. <https://doi.org/10.1016/j.buildenv.2015.01.034>.
- [7] E. Vereecken, Hygrothermal Analysis of Interior Insulation for renovation projects, KU Leuven, 2013.
- [8] G.R. Finken, S.P. Bjarløv, R.H. Peuhkuri, Effect of façade impregnation on feasibility of capillary active thermal internal insulation for a historic dormitory - A hygrothermal simulation study, *Constr. Build. Mater.* 113 (2016) 202–214. <https://doi.org/10.1016/j.conbuildmat.2016.03.019>.
- [9] E. Vereecken, L. Van Gelder, H. Janssen, S. Roels, Interior insulation for wall retrofitting - A probabilistic analysis of energy savings and hygrothermal risks, *Energy Build.* 89 (2015) 231–244. <https://doi.org/10.1016/j.enbuild.2014.12.031>.

- [10] J. MacMullen, Z. Zhang, E. Rirsch, H.N. Dhakal, N. Bennett, Brick and mortar treatment by cream emulsion for improved water repellence and thermal insulation, *Energy Build.* 43 (2011) 1560–1565. <https://doi.org/10.1016/j.enbuild.2011.02.014>.
- [11] H. Janssen, B. Blocken, S. Roels, J. Carmeliet, Wind-driven rain as a boundary condition for HAM simulations: Analysis of simplified modelling approaches, *Build. Environ.* 42 (2007) 1555–1567. <https://doi.org/10.1016/j.buildenv.2006.10.001>.
- [12] A. Erkal, D. D'Ayala, L. Sequeira, Assessment of wind-driven rain impact, related surface erosion and surface strength reduction of historic building materials, *Build. Environ.* 57 (2012) 336–348. <https://doi.org/10.1016/j.buildenv.2012.05.004>.
- [13] J. Engel, P. Heinze, R. Plagge, Adapting hydrophobizing impregnation agents to the object, *Hydrophobe VII7th Int. Conf. Water Repel. Treat. Prot. Surf. Technol. Build. Mater.* 20 (2014) 141–150. <https://doi.org/https://doi.org/10.12900/rbm14.20.6-0042>.
- [14] M. Roos, F. König, S. Stadtmüller, B. Weyershausen, Evolution of silicone based water repellents for modern building protection, *5th Int. Conf. Water Repel. Treat. Build. Mater.* 16 (2008) 3–16. [http://www.hydrophobe.org/pdf/bruxelles/V\\_01.pdf](http://www.hydrophobe.org/pdf/bruxelles/V_01.pdf).
- [15] J. Carmeliet, G. Houvenaghel, J. Van Schijndel, S. Roels, Moisture phenomena in hydrophobic porous building material Part 1: Measurements and physical interpretations / Wechselwirkung hydrophobierter poröser Werkstoffe des Bauwesens mit Feuchtigkeit, Teil 1: Messungen und physikalische Interpretationen, *Restor. Build. Monum.* 8 (2002) 165–183. <https://doi.org/https://doi.org/10.1515/rbm-2002-5660>.
- [16] E.B. Møller, C. Rode, Hygrothermal Performance and Soiling of Exterior Building Surfaces, Technical University of Denmark, 2004. <https://orbit.dtu.dk/files/5285541/byg-r068.pdf>.
- [17] A.E. Charola, Water-Repellent Treatments for Building Stones: A Practical Overview, *APT Bull. J. Preserv. Technol.* 26 (1995) 10–17. <https://doi.org/10.2307/1504480>.
- [18] B. Lubelli, R.P.J. van Hees, Evaluation of the effect of nano-coatings with water repellent properties on the absorption and drying behaviour of brick, in: *Hydrophobe VI Proc. 6th Int. Conf. Water Repel. Treat. Build. Mater.*, 2011: pp. 125–135. [http://www.hydrophobe.org/pdf/rome/VI\\_12.pdf](http://www.hydrophobe.org/pdf/rome/VI_12.pdf).

- [19] M. Stefanidou, A. Karozou, Testing the effectiveness of protective coatings on traditional bricks, *Constr. Build. Mater.* 111 (2016) 482–487. <https://doi.org/10.1016/j.conbuildmat.2016.02.114>.
- [20] K. Ren, D. Kagi, Evaluation of an oil and water repellent on masonry substrates, in: *Hydrophobe VIII*, Hongkong, 2017: pp. 44–52. <http://www.hydrophobe.org/pdf/hongkong/A-1-3.pdf>.
- [21] A. Selander, *Hydrophobic Impregnation of Concrete Structures*, Royal Institute of Technology, 2010.
- [22] H. Mayer, Masonry protection with silanes, siloxanes and silicone resins, *Surf. Coatings Int.* 81 (1998) 89–93. <https://doi.org/10.1007/BF02692337>.
- [23] Wacker Chemie AG, Silres® bs smk 2101, Technical data sheet, (2014) 3–4. [https://www.brenntag.com/media/documents/bsi/product\\_data\\_sheets/material\\_science/wacker\\_silicone\\_resins/silres\\_bs\\_smk\\_2101\\_pds.pdf](https://www.brenntag.com/media/documents/bsi/product_data_sheets/material_science/wacker_silicone_resins/silres_bs_smk_2101_pds.pdf).
- [24] A. Syed, M. Donadio, Silane Sealers / Hydrophobic Impregnation - The European Perspective, (2013) 1–6. [https://cdn.ymaws.com/www.icri.org/resource/resmgr/crb/2013septoct/CRB\\_SeptOct13\\_Syed-Donadio.pdf](https://cdn.ymaws.com/www.icri.org/resource/resmgr/crb/2013septoct/CRB_SeptOct13_Syed-Donadio.pdf).
- [25] Sika Services AG, Refurbishment Sika Technology and Concepts for Hydrophobic Impregnations, (2017) 1–20.
- [26] T. Szymura, D. Barnat-hunek, Protection of Stone Building Structures Against Corrosion Caused by Moisture, in: 2013: pp. 65–76. [http://br.wsia.edu.pl/zeszyty/pdfs/br32\\_07szymura.pdf](http://br.wsia.edu.pl/zeszyty/pdfs/br32_07szymura.pdf).
- [27] Wacker Chemie AG, Silres® bs 38, Technical data sheet, (2011) 1–2. [https://www.brenntag.com/media/documents/bsi/product\\_data\\_sheets/material\\_science/wacker\\_silicone\\_resins/silres\\_bs\\_38\\_pds.pdf](https://www.brenntag.com/media/documents/bsi/product_data_sheets/material_science/wacker_silicone_resins/silres_bs_38_pds.pdf).
- [28] Technichem S.A., Technisil Hydro Plus, W.T.C.B., (2005) 1–2.
- [29] Rewah N.V, OLEOFUGE F, Technical data sheet, (2018) 1–3. <http://www.rewah.com/images/products/166/technicalsheet.pdf?refresh=1572963183>.
- [30] E. de Witte, H. De Clercq, R. De Bruyn, A. Pien, Systematic Testing of Water Repellent Agents, *Restor. Build. Monum.* 2 (1996) 133–144. <https://doi.org/https://doi.org/10.1515/rbm-1996-5093>.

- [31] A.E. Charola, Water Repellents and Other “ Protective ” Treatments : A Critical Review, in: *Hydrophobe III. 3rd Int. Conf. Surf. Technology with Water Repel. Agents. Aedif. Publ.*, 2001: pp. 3–20. [http://www.hydrophobe.org/pdf/hannover/III\\_01.pdf](http://www.hydrophobe.org/pdf/hannover/III_01.pdf).
- [32] H. Kober, Water thinnable silicone impregnating agents for masonry protection, in: *Hydrophobe I Delft*, 1995: pp. 1–13. [http://www.hydrophobe.org/pdf/delft/I\\_3.pdf](http://www.hydrophobe.org/pdf/delft/I_3.pdf).
- [33] H. De Clercq, E. De Witte, Effectiveness of commercial silicon based water repellents applied under different conditions, *Restor. Build. Monum. an Int. J. = Bauinstandsetz. Und Baudenkmalpfl. Eine Int. Zeitschrift.* 8 (2002) 149–164. <https://doi.org/https://doi.org/10.1515/rbm-2002-5659>.
- [34] Rewah N.V, ARTISIL B10, Technical data sheet, (2016) 1–2. <http://www.rewah.com/images/products/12/technicalsheet.pdf>.
- [35] D. Corning, Dow Corning® Z-6689 Water Repellent, Safety data sheet, (2017) 1–4. <https://www.dow.com/en-us/pdp.dowsil-z-6689-water-repellent.04023290z.html>.
- [36] Hilde De Clercq, RC 805 ECO REYNCHÉMIE NV, Test report, (2004) 1–10. <http://www.reynchemie.com/Content/Bestanden/20123-RC805ECO-KIK-nl.pdf>.
- [37] J. Šadauskienė, J. Ramanauskas, V. Stankevičius, Effect of Hydrophobic Materials on Water Impermeability and Drying of Finish Brick Masonry, in: *Issn Mater. Sci.*, 2003: pp. 1392–1320. [https://www.researchgate.net/profile/Jolanta\\_Sadauskiene/publication/237779777\\_Effect\\_of\\_Hydrophobic\\_Materials\\_on\\_Water\\_Impermeability\\_and\\_Drying\\_of\\_Finish\\_Brick\\_Masonry/links/53fb1c580cf27c365cf06ef8.pdf](https://www.researchgate.net/profile/Jolanta_Sadauskiene/publication/237779777_Effect_of_Hydrophobic_Materials_on_Water_Impermeability_and_Drying_of_Finish_Brick_Masonry/links/53fb1c580cf27c365cf06ef8.pdf).
- [38] Z. Pavlík, M. Keppert, ... M.P., Investigation of the Effectiveness of Siloxane Hydrophobic Injection for Renovation of Damp Brick Masonry, *Int. J. Chem. Mol. Nucl. Mater. Metall. Eng.* 6 (2012) 123–126. <https://pdfs.semanticscholar.org/e581/93b1a954364e330dc0eca284f6d7699a aa89.pdf> (accessed November 12, 2019).
- [39] K. Fukui, C. Iba, S. Hokoi, Moisture behavior inside building materials treated with silane water repellent, *Energy Procedia.* 132 (2017) 735–740. <https://doi.org/10.1016/j.egypro.2017.10.018>.
- [40] J. Zhao, F. Meissener, Experimental investigation of moisture properties of historic building material with hydrophobization treatment, in: *Energy*

- Procedia, Elsevier Ltd, 2017: pp. 261–266.  
<https://doi.org/10.1016/j.egypro.2017.09.716>.
- [41] T.K. Hansen, S.P. Bjarløv, R.H. Peuhkuri, K.K. Hansen, Performance of hydrophobized historic solid masonry – Experimental approach, *Constr. Build. Mater.* 188 (2018) 695–708.  
<https://doi.org/10.1016/j.conbuildmat.2018.08.145>.
- [42] Momen AG, Silblock wms Technical data sheet, (2011) 1–4.  
[https://www.momentive.com/docs/default-source/productdocuments/silblock-wms/silblock-wms-mb-indd.pdf?sfvrsn=d50e61c\\_14](https://www.momentive.com/docs/default-source/productdocuments/silblock-wms/silblock-wms-mb-indd.pdf?sfvrsn=d50e61c_14).
- [43] Wacker Chemie AG, Hydrophobic impregnation with Silres BS, (2014) 1–22.
- [44] H.M. Künzle, K. Kiehl, Drying of brick walls after impregnation, *Bauinstandsetzen*. 2 (1996) 87–100. <https://wufi.de/literatur/Künzel, Kiehl 1996 - Drying of brick walls.pdf>.
- [45] A. Abdul Hamid, P. Wallentén, Hygrothermal assessment of internally added thermal insulation on external brick walls in Swedish multifamily buildings, *Build. Environ.* 123 (2017) 351–362.  
<https://doi.org/10.1016/j.buildenv.2017.05.019>.
- [46] N. Feldt Jensen, S.P. Bjarløv, C. Rode, E.B. Møller, Hygrothermal assessment of four insulation systems for interior retrofitting of solid masonry walls through calibrated numerical simulations, *Build. Environ.* 180 (2020) 107031.  
<https://doi.org/10.1016/j.buildenv.2020.107031>.
- [47] H. Janssen, D. Deckers, E. Vereecken, C. Feng, V. Soulios, A. Vanek, T.K. Hansen, V. Metavitsiadis, Impact of water repellent agents on hygric properties of porous building materials, 2020.  
[https://static1.squarespace.com/static/5e8c2889b5462512e400d1e2/t/5eeb67ee2a7db1305c80d34b/1592485898332/RIBuild\\_D2.3\\_final.pdf](https://static1.squarespace.com/static/5e8c2889b5462512e400d1e2/t/5eeb67ee2a7db1305c80d34b/1592485898332/RIBuild_D2.3_final.pdf) (accessed October 26, 2020).
- [48] R.P.J. van Hees, The performance of surface treatments for the conservation of historic brick masonry, *Compat. Mater. Prot. Eur. Cult. Herit. [Volume 2]*. (1998) 279–287.
- [49] Rewah NV, GELIFUGE NEW, Technical data sheet, (2016) 1–3.  
<http://www.rewah.com/images/products/121/technicalsheet.pdf>.
- [50] Remmers AG, Funcosil WS, Technical data sheet, (2016) 1–2.

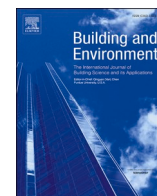


[http://www.bg.remmers.com/fileadmin/dam/produkte/tm/TM1\\_0614\\_EN.pdf](http://www.bg.remmers.com/fileadmin/dam/produkte/tm/TM1_0614_EN.pdf).

- [51] Remmers AG, Funcosil FC, Technical data sheet, (2016) 1–3. [https://www.introflex.dk/images/pdf/DK\\_0711\\_-\\_08\\_13.pdf](https://www.introflex.dk/images/pdf/DK_0711_-_08_13.pdf).
- [52] C. Feng, H. Janssen, Y. Feng, Q. Meng, Hygric properties of porous building materials: Analysis of measurement repeatability and reproducibility, *Build. Environ.* 85 (2015) 160–172. <https://doi.org/10.1016/J.BUILDENV.2014.11.036>.
- [53] J. Todorović, H. Janssen, The impact of salt pore clogging on the hygric properties of bricks, *Constr. Build. Mater.* 164 (2018) 850–863. <https://doi.org/10.1016/j.conbuildmat.2017.12.210>.
- [54] ASTM C1699-09, Standard Test Method for Moisture Retention Curves of Porous Building Materials Using Pressure Plates, (2015). <https://doi.org/10.1520/C1699-09R15>.
- [55] ASTM D4404-18, Standard Test Method for Determination of Pore Volume and Pore Volume Distribution of Soil and Rock by Mercury Intrusion Porosimetry, (2018). <https://doi.org/10.1520/D4404-18>.
- [56] J. Carmeliet, S. Roels, Determination of the Isothermal Moisture Transport Properties of Porous Building Materials, *J. Therm. ENV.&BLDG. SCI.* 24 (2001) 183–210. <https://doi.org/10.1106/Y6T2-9LLP-04Y5-AN6T>.
- [57] ISO 15148: 2002, Hygrothermal performance of building materials and products Determination of water absorption coefficient by partial immersion, English version of DIN EN ISO 15148, (2003) 1–14.
- [58] C. Feng, H. Janssen, Hygric properties of porous building materials (III): Impact factors and data processing methods of the capillary absorption test, *Build. Environ.* 134 (2018) 21–34. <https://doi.org/10.1016/j.buildenv.2018.02.038>.
- [59] ISO 12572, Hygrothermal performance of building materials and products - transmission properties -Cup method, (2016) 1–5. <https://www.sis.se/api/document/preview/920749/>.
- [60] ASTM Int., C518-15: Standard Test Method for Steady-State Thermal Transmission Properties by Means of the Heat Flow Meter Apparatus, ASTM Int. 04 (2015) 1–15. <https://doi.org/10.1520/C0518-10.2>.

- [61] W. de Van Walle, H. Janssen, Prediction of the Effective Thermal Conductivity of Porous Building Blocks Based on Their Pore Structure, KU Leuven, 2019. <https://bwk.kuleuven.be/bwf/PhDs/phdvandewalle>.
- [62] J. Zhao, F. Meissener, Experimental investigation of moisture properties of historic building material with hydrophobization treatment, *Energy Procedia*. 132 (2017) 261–266. <https://doi.org/10.1016/j.egypro.2017.09.716>.
- [63] TQC, Karsten tube penetration test II7500, manual, (2020) 1–4. <https://mk0tqcsheendm9hfmnd0.kinstacdn.com/wp-content/uploads/2016/05/karsten-tube-penetration-test-li7500-m44.pdf>.
- [64] M. Rahimi, P. Fojan, L. Gurevich, A. Afshari, Effects of aluminium surface morphology and chemical modification on wettability, *Appl. Surf. Sci.* 296 (2014) 124–132. <https://doi.org/10.1016/j.apsusc.2014.01.059>.
- [65] C. Feng, H. Janssen, Impact of water repellent agent concentration on the effect of hydrophobization on building materials, *J. Build. Eng.* 39 (2021) 102284. <https://doi.org/10.1016/j.jobbe.2021.102284>.
- [66] R. Asmatulu, G.A. Mahmud, C. Hille, H.E. Misak, Effects of UV degradation on surface hydrophobicity, crack, and thickness of MWCNT-based nanocomposite coatings, *Prog. Org. Coatings*. 72 (2011) 553–561. <https://doi.org/10.1016/j.porgcoat.2011.06.015>.
- [67] L. Courard, V. Lucquiaud, O. Gérard, M. Handy, F. Michel, Evaluation of the Durability of Hydrophobic Treatments on Concrete Architectural Heritage, in: *Hydrophobe VII*, 2014: pp. 29–38. [http://www.hydrophobe.org/pdf/lisboa/VII\\_03.pdf](http://www.hydrophobe.org/pdf/lisboa/VII_03.pdf).
- [68] I.J. De Vries, Hydrophobic Treatment, *Constr. Build. Mater.* 11 (1997) 259–265. <https://pdf.sciencedirectassets.com/271475/1-s2.0-S0950061800X00207/1-s2.0-S0950061897000469/main.pdf?X-Amz-SecurityToken=IQoJb3JpZ2luX2VjEBQaCXVzLWVhc3QtMSJHMEUCIA RwT9fI%2B%2F4uPdWTTbOmg1eV6XRFxUtnG8%2FzFyEcre0AiEAg7sLvd7Qk7XT7eGJ2ow1dtVV%2B0TguOBef45L>.





# Hygic behavior of hydrophobized brick and mortar samples

Vasilis Soulios<sup>a,\*</sup>, Ernst Jan de Place Hansen<sup>a</sup>, Chi Feng<sup>b</sup>, Hans Janssen<sup>c</sup>

<sup>a</sup> Department of the Built Environment, Aalborg University, Denmark

<sup>b</sup> School of Architecture and Urban Planning, Chongqing University, Chong Qing, 400045, PR China

<sup>c</sup> KU Leuven, Department of Civil Engineering, Building Physics Section, Kasteelpark Arenberg 40, 3001, Leuven, Belgium

## ARTICLE INFO

### Keywords:

Hygic properties  
Hydrophobization  
Water repellent agents  
Ceramic brick  
Carbonated lime mortar  
Impregnation depth

## ABSTRACT

Moisture that penetrates into porous building materials is a major reason for their deterioration and the subsequent failure of the whole structure. Water repellency treatment could prevent serious damages to materials and components. Hydrophobization is a method with a long tradition for protecting buildings from wind-driven-rain-induced moisture absorption. Nonetheless, it remains an ambiguous practice. To understand the nature of water repellency it is important to examine how hydrophobization works, how the existing products differ from one another, and how the hygic response of the substrate changes after treatment. The aim of this article is to characterize the impact of water repellent agents on the properties of building materials mostly used in old facades: clay brick and lime mortar.

The resulting open porosity and pore size distribution, determined with vacuum saturation and mercury intrusion testing respectively, reveal only minimal change in the overall pore structure after impregnation. Our findings also show that hydrophobic treatment is nearly impermeable to liquid water, by evaluating the samples with capillary absorption tests, but still permeable to water vapour, by testing the samples with cup tests. Moreover, the water impermeability grows after exposure to water. In addition, the water repellent agent appears to spread progressively in the material for a long time after the hydrophobic treatment, yielding high final impregnation depths. These findings confirm that water repellent agents successfully hydrophobize the tested materials, with a water-tight but vapour-open hydrophobic layer that goes deep into the material, without notably changing its pore size distribution though.

## 1. Introduction

### 1.1. General background

Existing buildings will have to cover human habitation needs for many years to come, as the European building stock increases solely by 1–1.5% per year [1]. Historic buildings, most commonly with brickwork or natural stone facades, account for 10–40% of the building stock and their conservation is therefore crucial [2]. They are responsible for a sizable fraction of the energy consumption by the built environment, because they typically lack insulation. Thermal retrofitting should hence be considered, for which exterior insulation is the most efficient measure. However, to sustain the architectural and cultural values of the edifice, thermal retrofits of such historic buildings often imply internally insulating the facades [3]. Internal insulation may yield moisture problems though, such as frost damage at the exterior surface, rot of embedded wooden floor beams, or mould growth at interior surfaces

[4]. Applying water repellent agents on the facades could potentially avoid such moisture problems, since it minimizes the water absorption by the facade materials [5]. However, it should be carefully examined as it is an irreversible technique [6].

### 1.2. Literature overview

To thoroughly investigate the behaviour of a hydrophobized masonry facade, we should define the moisture storage and transport properties of its components (brick and mortar), as well as the impregnation depth of the hydrophobic treatment.

Previous studies provide experimental results on impregnation depth of brick and mortar [7–10]. Additionally, the existence of a first strongly hydrophobized and a second partly hydrophobized region in brick samples has already been established [11,12]. However, the influence of several characteristics of the water repellent agents, such as the different percentage of silane/siloxane and different percentages of active

\* Corresponding author.

E-mail address: [vsou@build.aau.dk](mailto:vsou@build.aau.dk) (V. Soulios).

<https://doi.org/10.1016/j.buildenv.2020.106843>

Received 11 November 2019; Received in revised form 23 March 2020; Accepted 25 March 2020

Available online 9 April 2020

0360-1323/© 2020 Elsevier Ltd. All rights reserved.

ingredient, on the impregnation depth of brick and mortar samples and the extent of the redistribution of the active ingredient needs to be further investigated. Whereas some previous studies examine moisture storage properties (maximum moisture content), which derives from free water uptake, on hydrophobized brick samples [5,8,11,13], the present study defines the open porosity and the pore volume distribution in order to investigate the effects of hydrophobic impregnation on the pore structure of both brick and mortar.

The most crucial function of hydrophobization is to reduce, or avoid, the spontaneous capillary absorption of wind-driven rain, which forms an important moisture source for facades [14,15]. Hydrophobization has shown to be very efficient in reducing the capillary suction of bricks [5,8,10,11,16–18], as well as cement mortars [10,19], commonly expressed by their capillary absorption coefficient ( $A_{cap}$ ). However, there is a lack of similar studies on lime mortar. The question of whether hydrophobization can eliminate driving-rain absorption by providing the same level of water repellency in both brick and mortar still remains. Also, the influence of the active ingredient, the form, the diluent, and the concentration of the water repellent agent on the capillary suction, as well as the water exposure after treatment, are factors that all need to be investigated. Moreover, several researchers use different application times and curing periods during the impregnation process in lab conditions [7,8,11,17,20] and there has been relatively little analysis on the effect they have on the water repellency and the impregnation depth of the hydrophobic treatment.

Opposed to the change in the capillary suction, there seems to be no significant change in the vapour diffusion resistance factor ( $\mu$ -value) of both brick and mortar, however both increases and decreases between untreated and treated samples are reported [5,7,9–11,13,21]. The question of whether and to what extent hydrophobization can influence the vapour permeability of brick and mortar requires an answer. Moreover, whether different forms of water repellent agents (liquid or cream) give different behaviors in the vapour permeability of hydrophobized materials should be investigated both in brick and mortar.

### 1.3. Aim and outline

The main aim of this article is to characterize the impact of water repellent agents on the hygric behavior of building materials most often used in historic facades: brick and mortar. Serving the above-mentioned aim, the first section describes the physical and chemical properties of the water repellent agents and screens the market of commercially available products. The article continues by comparing the impregnation depth between bricks and mortar and indicating the redistribution of the water repellent agent after treatment. It also considers the influence of hydrophobic impregnation on the open porosity and the pore size distribution of brick and mortar. Subsequently, it is investigated how various water repellent agents employed on different bricks and mortar affect the impregnation strength, quantified by calculating the capillary absorption coefficient. The article concludes by studying the vapour transport with cup tests.

## 2. Water repellent agents

### 2.1. The nature of water repellency

The main function of water repellent agents is to prevent liquid water from entering the impregnated surface [8,22,23]. Water is a polar material since it has a positive charge at the hydrogen ends and a negative charge at the oxygen end. Inorganic building materials, such as brick, usually have negative surface charges and therefore attract the positive end of the water molecules (i.e. they are hydrophilic). A water-repellent molecule has a polar “head” and a non-polar “tail”. The polar “heads” are attracted by the polar material and the non-polar “tails” cover the surface. In that way, the surface becomes non-polar and as a result, no longer attracts water molecules (i.e. surface becomes hydrophobic)

[21].

### 2.2. Types of water repellent agents

Water repellent agents that are available on the market, are primarily based on the following types of materials: i) silicon-bearing compounds, ii) metal-bearing compounds and iii) organic materials [21]. Although not widely available yet, water repellent products based on nanotechnology claim to produce better results compared to the more traditional products [24–26]. However, further studies are needed first to conclude on the effectiveness and efficiency of these nanotechnology-based products.

#### 2.2.1. Silicon-bearing compounds

Silicon-based systems are the most popular water repellents in use. Generally, all products that contain a silicon-oxygen backbone can be referred to as silicones, but their properties can vary significantly [21]. When applied, the silicon-based systems form irreversible bonds with the mineral substrate and hydrophobize the building material [22,27]. A simple classification of silicon-based water repellent agents would include silanes, siloxanes and silicon resins.

**2.2.1.1. Silanes.** Silanes are monomeric low-weight molecules that contain one silicon atom which is connected to alkyl (-R) and/or alkoxy (-OR) groups. These alkoxy groups (-OR) permit the compound to polymerize and to link chemically to the hydroxylated surfaces of siliceous building materials (e.g. brick, concrete, granite, sandstone), providing anchorage between hydrophobic film and building substrate [21,22]. The alkyl groups (-R) take no part in the polymerization but they provide the hydrophobic properties to the compound.

The low reactivity of silanes often gives great impregnation depths, even in alkaline substrates such as concrete. Silanes are highly volatile though and therefore high concentrations of active content are required, ranging from 25% up to 99% (almost pure silane) [28], according to the preferred use and the desired performance [29].

**2.2.1.2. Siloxanes.** Siloxanes are similar in nature to silanes, but their molecular structure is more complex, since they are oligomeric or polymeric molecules based on Si–O–Si chains. Due to this complexity, siloxanes more difficultly migrate into the substrate, although their dimensions are comparable to those of silanes [22,29]. The size of silanes is 0.4–1.5 nm and of siloxanes 3–30 nm [30]. Siloxanes are more reactive compared to silanes. In fact, the fast curing process on highly alkaline substrates (e.g. concrete) does not permit siloxane molecules to penetrate deep into the substrate. For that reason, they are mostly used in more porous and more neutral mineral substrates (e.g. brick, natural stones, and aged concrete) [22]. Due to their higher molecular weight, siloxanes are less volatile than silanes, and consequently the needed active content is usually no more than 10–15%. Also, higher concentrations encompass the risk of darkening the surface [29].

**2.2.1.3. Silicone resins.** Silicone resins are highly branched polysiloxanes with high molecular weight, with a backbone consisting of silicon and oxygen atoms [22,31]. Silicone resins are already polymerized and the evaporation of the solvent is the only process that takes place after application [21]. However, silicone resins have poor solubility properties, can darken the surface and provide a beading effect, which is not always desirable [21,22]. Silicon resin products should be diluted to 5–10% solids in solvents to achieve a better penetration depth [22].

#### 2.2.2. Metal-bearing compounds

Metal-bearing compounds are mainly based on aluminum stearate, the most popular hydrophobization agent of this kind. Metal-bearing compounds are mostly used for stone treatments, not being effective

for brick masonry. Other metal-organic compounds, such as titanium stearate and butyl-ortho-titanate are used in mixtures with oligomeric siloxanes [21].

### 2.2.3. Organic materials

Hydrophobization agents that are based on organic materials include acrylics, polyurethanes and perfluoro-polyethers. Waxes are also organic substances of either natural or synthetic origin and they are generally used for the conservation of materials such as marble and stone. Although waxes have good hydrophobic properties, they can easily suffer from mechanical damage and color variations [21,32]. Some organic materials are also used in combination with silicon bearing materials in order to provide both water and oil repellency [33–35].

## 2.3. Product identification

Silicon-based water repellent agents, which are the most popular in practice, can be identified through their active ingredient, the form, the type of diluent, the concentration of the active ingredient, the alkyl group and the type of substrate that is recommended for application (see Table 1) [36].

### 2.3.1. Influence of the formulation and diluent

During the previous decades, combination products of both silanes and siloxanes have been marketed as more broadly applicable water repellent agents as they combine the penetration power of silanes and the reactivity of siloxanes. In order to be prepared as ready-to-use, these products have to be diluted with white spirits or alcohols, in various concentrations according to the product and the substrate [22]. However, volatile organic compounds (VOC) are released to the atmosphere when silanes, siloxanes or silicone resins are dissolved in organic solvent. For that reason, more environmentally friendly products based on water as diluent were developed [36]. Paste-like or cream products, developed since the early 2000s, provide alternative treatment methods, easy to apply and with good water repellence characteristics [22,25,37].

Water-based emulsions and creams contain emulsifiers to keep the reactive material stable in a water environment [10]. These products perform better after rain exposure and solar radiation. Solar radiation increases the temperature and consequently the reactivity, while rain exposure “washes off” the emulsifiers that impede reactions with water. Micro-emulsions do not contain classical emulsifiers and can immediately demonstrate their performance. However, micro-emulsion products should be applied within 24 h after dilution, so there would be no reactions between active ingredients and water (personal communication with Hamont, Corne Van, Wacker’s representative).

### 2.3.2. Influence of concentration of the active ingredient

The concentration of the active ingredient is important for the performance of the product. Lower concentrations generally decrease the effectiveness of the treatment, which may lead to faster drying though

[5,37]. De Clercq and De Witte [20] show that the influence of concentration on the effectiveness of the treatment becomes more important after ageing.

### 2.3.3. Influence of the alkyl groups

The alkyl groups (-R) attached to silane, siloxane and silicone resin take no part in the polymerization but provide the hydrophobic properties to the compound. Some studies have shown that long alkyl groups are not more effective than methyl groups and that the nature of the substrate played a more significant role in the performance of the treatment [21]. However, longer alkyl chains provide good resistance against alkalinity as they create a steric shield for the Si-O-Si bonds which are prone to hydrolysis [22].

If the hydrophobic compound is composed only of methyl groups, the alkaline stability may not be very strong. The influence of the alkyl group, in terms of alkali resistance, is more notable in cementitious substrates. For brick this influence may not be that important, because brick is a more neutral material than concrete with respect to alkalinity. In masonry walls the length of the alkyl group may influence the treatment, since mortar is an alkaline material. However, most formulations nowadays contain longer alkyl groups so that the alkalinity of mortar cannot cause stability problems [21,38–40].

### 2.3.4. Influence of the type of substrate

Compatibility between pore structure and polymer chain length can play an important role in the effectiveness of the hydrophobic treatment and the hygric behavior of the impregnated substrate. De Clercq and De Witte [20] indicate that the pore structure of the substrate is the key factor that determines the process of polycondensation. For that reason, the water repellent agents should be classified according to their polymer chain length in relation to the pore size of the substrate that will be impregnated [8]. Thus, different water repellent agents are suitable for different types of substrates.

## 2.4. Classification of commercially available water repellent agents

In order to select the products that will be used in the laboratory experiments, it is important to obtain an overview of the commercially available water repellent agents so that selected agents will represent a wide spectrum of the existing products. There are several distributors of water repellent agents, and they all provide a spectrum of products that can be categorized according to several characteristics: type of active ingredient, formulation, concentration and type of substrate, explained in Section 2.3.

Water repellent agents from thirteen distributing companies were classified, including five big silicon-producing companies: Wacker, Dow, BlueStar, Sika, and Momenite. The rest of the water repellent agents are selected from non-silicon-producing companies. These companies developed their own formulations using silicones from the above-mentioned silicon producing companies (see Table A 1 Appendix). In total, 77 commercially available products suitable for mineral substrates have sufficient information to be identified, although there are more products on the market.

This study focuses on water repellent agents that are used as brick masonry impregnation against wind-driven rain. This means that products against rising damp, in-plant impregnations for cement, products used for wood and products that are used as admixtures in paints or coatings, are not included.

Almost all companies use silicon-based repellents, while some of them also provide agents based on organic or metal-bearing materials which may or may not contain silicones. Almost half of the silicon-based products are mixtures of silanes and siloxanes (see Fig. 1). The majority of water repellent agents are in liquid form. Most products use water as a diluent, especially if they are in the cream form (see Fig. 2 left). Although some products are recommended only for application in concrete and cementitious materials, most products are recommended for

**Table 1**  
Product identification.

Product characteristic	Description
Active ingredient	Silane - Siloxane - Silicone resins
Product form	Liquid or Cream
Used diluent	Organic solvent - Water emulsion - Water microemulsion
Agent concentration	1–100%, Undiluted <sup>a</sup> or Ready to use
Alkyl group	Octyl or iso-Octyl in commercial products
Intended substrate	Mineral substrate <sup>b</sup> - Masonry <sup>c</sup> - Concrete

<sup>a</sup> Undiluted: contain no diluent and must not be diluted before application.

<sup>b</sup> Mineral substrates: concrete, brick, natural stone, mortar, concrete blocks.

<sup>c</sup> Masonry: brick, mortar and natural stone, but not for concrete (or concrete blocks).

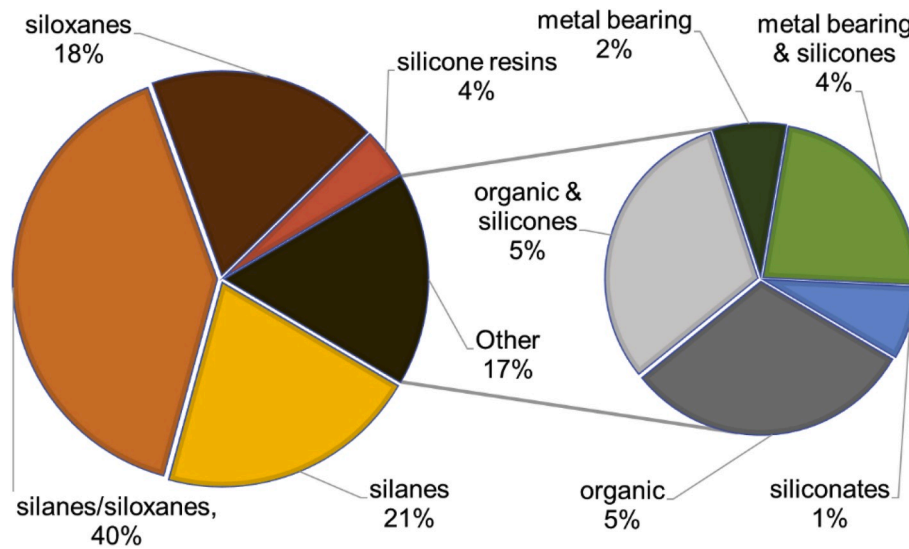


Fig. 1. Types of water repellent agents. Data from 77 listed products.

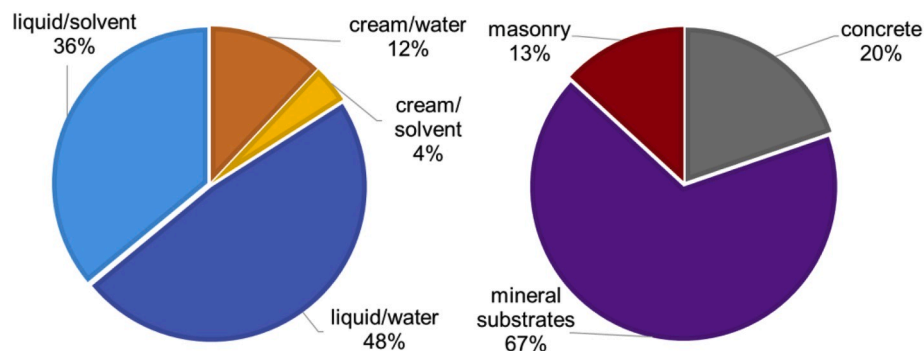


Fig. 2. Form and diluent of water repellent agents (left), Type of substrate (right). Data from 77 listed products.

mineral substrates in general (see Fig. 2 right).

### 3. Materials and methods

#### 3.1. Target building materials

Hydrophobic impregnation in combination with internal insulation is a retrofit measure for external walls of old/historic buildings with architectural or cultural value, for which external insulation is not a feasible solution. The external wall of such buildings is often made of solid masonry (ceramic brick and lime mortar), at least in many Northern, Western and Central European countries. Therefore, the current study looks into ceramic brick (three types) and lime mortar (one

type), described in Table 2.

The Robusta and yellow soft bricks (R brick and Y brick) have been used in research projects at KU Leuven (Leuven, Belgium) and at DTU (Technical University of Denmark, Kgs. Lyngby, Denmark) respectively e.g. (Todorovic and Janssen [41]) (Hansen et al. [7]) and their properties have been thoroughly examined. Samples of a historic brick (H brick) were acquired from a building in Copenhagen constructed in 1944, in order to also impregnate the exposed to weather conditions surface.

In relation to size, the brick samples were divided into three groups: 8x4x4 cm, 1x4x4 cm, and 3 × 8 cm (thickness x diameter) and were cut from regular bricks. Only for the H brick the exposed to weathering surface was kept on the sample. Samples with apparent cracks were

Table 2

Building material used in the current study. Properties of untreated samples.

Name	Description	$A_{cap}^a$ [ $10^{-5}$ kg/m <sup>2</sup> √s]	$w_{cap}^a$ [kg/m <sup>3</sup> ]	$\mu^*$
R brick	Robusta Vandersanden Belgian Brick	60732 (2043)	208 (2.3)	11.3 (1.2)
H brick	Historic Danish Brick from an old building in Copenhagen (1944)	39875 (2288)	249 (3.9)	8.70 (0.9)
Y brick	Yellow soft-molded Danish brick from Helligsø and Vesterled Teglværk	30970 (4584)	276 (19.3)	11.9 (1.4)
L mortar	Carbonated lime mortar	25820 (2041)	227 (6.6)	8.00 (0.4)

<sup>a</sup>  $A_{cap}$  and  $w_{cap}$  derived from water uptake test (each result is an average based on five samples),  $\mu$  from wet cup test [RH 53.2–97.4%] (each result is an average based on four samples). The values in () correspond to the standard deviation. For additional properties of R brick and L mortar see Table B 1 Appendix and for the Y brick see Ref. [18].



excluded in the process as cracks should be repaired before impregnation according to technical data sheets of water repellent agents.

The lime mortar was selected to represent an historic type of mortar. The relative amounts of ingredients for the lime mortar (lime Saint-Astier NHL3.5) was 10 L of water, 12.5 kg of lime, and 50 kg of sand. All ingredients were mixed in large realistic portions and the fresh mortar was placed in wooden molds to form the tested mortar samples. Mortar was kept in the molds for more than 6 months. After this period, the samples were placed in a carbonation chamber (4.7% CO<sub>2</sub> exposure) for 2 weeks in order to represent a carbonated historic mortar [42]. The mortar samples were tested with phenolphthalein in order to check if they were fully carbonated. Because of the small size (8x4x4 cm, 1x4x4 cm and 3 × 8 cm) and the composition (lime) of the mortar samples, in 10 days they became fully carbonated.

### 3.2. Selected water repellent agents

The selected water repellent agents (Table 3) represent the basic variations that can be found on the market of silicon-based water repellent agents according to the characterization shown in Table 1. The selected products include different active ingredients, in liquid or cream form, water or solvent-based, with different concentrations, and recommended for different types of substrate.

The SMK products from Wacker (SILRES BS) are micro-emulsion water-based mixtures of silane/siloxane. SMK 2101 has a high percentage of silane (around 90%) and is recommended for cementitious substrates [28]. SMK 1311 has a high percentage of siloxane (around 90%) and SMK 2100 has a balanced mixture of silane/siloxane (approximately ratio 50/50). SMK products are available with 100% concentration and they can be diluted with tap water (preferably deionized) to produce any concentration [43,44]. The recommended concentration of active ingredient for the SMK products for brick and mortar is between 6 and 10%. In order to investigate the influence of lower and higher than recommended concentrations, 2% and 25% are also tested.

Funcosil Remmers SNL, a solvent-based product and Funcosil Remmers WS, a water-based emulsion product [45,46], are both ready-to-use. Funcosil Remmers FC cream is a water-based silane cream that can be ordered in any possible concentration [47].

### 3.3. Hydrophobization treatment

According to the technical data sheets of the water repellent agents included in the current study, the substrate should be cleaned from dirt, dust and possible efflorescence before the impregnation [28,46,48].

The samples were washed with deionized water to avoid the absorption of extra salts and were carefully cleaned with a brush to remove dirt and dust. Afterwards, the samples were stored for drying in an oven (70 °C) for the absorbed moisture from the intense water exposure to evaporate. After reaching a stable mass (4–5 days), the samples were cooled in order to obtain room T and RH.

For the water uptake testing samples, the impregnation with liquid products followed the test practice of Wacker where samples are dipped



Fig. 3. Impregnation of brick (left) and mortar (right) samples by exposing them to free uptake of water repellent agent (liquid products).

for 5 min in the liquid agent. According to Wacker this represents two to three working operations (personal communication with Hamont, Corne Van, Wacker's representative). In the current study, one surface of each sample was exposed to free agent uptake (contact time) for 5 min (see Fig. 3). For impregnation with cream products the minimum recommended amount, 150–200 ml/m<sup>2</sup>, was applied with a brush [47].

For the vacuum saturation, the mercury intrusion, and the cup test alternatively, the samples were fully hydrophobized, in order to obtain homogeneous specimens. The impregnation with liquid products was conducted via free agent uptake until the agent reaches the top of the sample while for the cream products, a substantial quantity of agent was applied on the top surface of the sample in order for the agent to reach the bottom surface.

Finally, the samples were stored in a climatic chamber (21 °C, 53% RH) for one-month curing, which is longer than the 14 days recommended by Wacker; however the water repellency efficiency depends on the curing time [11].

### 3.4. Experimental set-up

Four main factors that characterize the hydrophobic layer: i) impregnation depth ( $d_p$ ), ii) change in the open porosity ( $\Phi$ ) and the pore volume distribution ( $f_v$ ) (moisture storage), iii) reduction of the water absorption coefficient ( $A_{cap}$ ) (moisture transport), and iv) change of vapour diffusion resistance factor ( $\mu$ ) (moisture transport), were investigated as presented in Table 4.

Each result is an average based on five samples for the vacuum saturation and mercury intrusion test both for untreated and treated samples, as well as for the untreated samples of the capillary water uptake test. However, for all the treated samples of the capillary water uptake test each result is an average based on three samples. For all the latter samples, the water uptake test was repeated. Only for a few samples the water uptake test was repeated for a third time. The same samples were used for measuring the impregnation depth by visual inspection and water uptake test from the non-impregnated side. Only for a few samples the water uptake from the non-impregnated side was repeated for a third time. Between each repetition, the samples were dried in an oven at 70 °C. For cup tests, each result is an average based on four samples for both untreated and treated samples.

Table 3

Water repellent agents used in the current study.

Product	Company	Type	Form	Diluent	Concentration	Substrate
SMK 2101	Wacker	90% silane	Liquid	Water	6, 10, 25** %	Concrete
SMK 1311	Wacker	90% siloxane	Liquid	Water	6, 10, 25** %	Mineral
SMK 2100	Wacker	Silane/siloxane	Liquid	Water	2*, 6, 10, 25** %	Mineral
SNL	Remmers	Siloxane	Liquid	Solvent	7%	Mineral
WS	Remmers	Silane/siloxane	Liquid	Water	10%	Mineral
FC	Remmers	Silane	Cream	Water	10*, 20, 40, 80%	Mineral

Information derived from the technical data sheets of the products.\*Concentration lower than recommended. \*\*Concentration higher than recommended.



**Table 4**

Laboratory experiments. Test plan including measured properties, type of tests, sample size and amount, type of material, and type and composition of water repellent agent.

Material (No. of samples)	Product	Form	Diluent	Concentration	Study the influence of
Impregnation depth ( $d_p$ ) ( $8 \times 4 \times 4$ cm samples)					
R brick (54), L mortar (45), Y brick (6), H brick (12)	Visual inspection & capillary water uptake from the non-impregnated side			Concentration of active ingredient, ratio silane/siloxane, form, diluent	
Open porosity ( $\Phi$ ) by vacuum saturation test ( $1 \times 4 \times 4$ cm samples)					
R brick, L mortar (5)	SMK 2100	Liquid	Untreated	10%	Substrate
R brick L mortar (5)			Water		
Pore volume distribution ( $f_v$ ) by mercury intrusion (dry mass: 1.5–2.5 g samples)					
R brick, L mortar (5)	SMK 2100	Liquid	Untreated	10%	Substrate
R brick, L mortar (5)			Water		
Water absorption coefficient ( $A_{cap}$ ) by capillary water uptake ( $8 \times 4 \times 4$ cm samples)					
R brick, L mortar, Y brick, H brick (5)			Untreated		
R brick, L mortar (9)	SMK 2101	Liquid	Water	6, 10, 25%	Concentration of active ingredient, ratio silane/siloxane, form, diluent
R brick, L mortar (9)	SMK 1311	Liquid	Water	6, 10, 25%	
R brick, L mortar (12)	SMK 2100	Liquid	Water	2, 6, 10, 25%	After treatment water exposure
R brick (3)	SNL	Liquid	Solvent	7%	Duration of water exposure
R brick (3)	WS	Liquid	Water	10%	
R brick, L mortar (12)	FC	Cream	Water	10, 20, 40, 80%	
H brick, Y brick (3)	SMK 2100	Liquid	Water	6%	Substrate
H brick, Y brick (3)	FC	Cream	Water	40%	
H brick (weathered) (3)	SMK 2100	Liquid	Water	6%	Exposure to exterior conditions before impregnation
H brick (weathered) (3)	FC	Cream	Water	40%	
R brick (6), L mortar (3)	SMK 2100	Liquid	Water	6%	Curing and application time
Water vapour diffusion factor ( $\mu$ ) by cup test (8 cm diameter, 3 cm height samples)					
R brick, L mortar (4)	SMK 2100	Liquid	Untreated	10%	Water repellent agent, substrate
R brick, L mortar (4)			Water		
R brick, L mortar, Y brick, H brick (4)	FC	Cream	Untreated	40%	
R brick, L mortar, Y brick, H brick (4)			Water		

The number inside () corresponds to the number of samples tested per material. All surfaces of brick samples were sawn except where indicated (weathered).

Hydrophobic impregnation creates a first, strongly hydrophobized layer as well as a larger volume that is partly hydrophobized [11] (see Fig. 4). The impregnation depth of impregnated samples was initially measured by visual inspection (i.e. measuring the length of the surface that becomes darker after impregnation), right after the impregnation and one month later. In addition, water uptake tests were conducted from the non-impregnated side of the samples to illustrate the redistribution and the extent of spreading of the water repellent agent in the samples. On this study, by “impregnation depth”, we refer to the strong hydrophobized region plus the partly hydrophobized region.

Vacuum saturation test was conducted according to Ref. [49] (ASTM C1699-09, 2009), in order to determine open porosity ( $\Phi$ ), which is proportional to vacuum saturated moisture content  $w_{sat}$ , as described in Ref. [41,50].

Mercury intrusion tests were carried out to determine the pore

volume distribution of hydrophobized brick and mortar according to Ref. [51] as described in Ref. [41].

Water uptake tests were conducted in order to obtain the water absorption coefficient ( $A_{cap}$ ) in accordance with [52] as described in Refs. [50,53]. Since impregnation significantly reduces the capillary water uptake, the duration of the water uptake test of the impregnated samples was 24 h and the measurement time intervals were: 10', 30', 1h, 1h 30', 2h, 3h, 4h, 7h, 9h, 24h. The water absorption coefficient  $A_{cap}$  is the slope of the first stage of the curve in relation to the square root of time and is significantly decreased in a material impregnated with a water repellent agent [8]. However, when the graph of water uptake against the square root of time does not give a straight line but a curve of some form, the absorption coefficient is defined as the measured increase in weight [g] at 24h divided by  $\sqrt{86400}$  [52].

Cup tests were conducted according to Ref. [54], to determine the

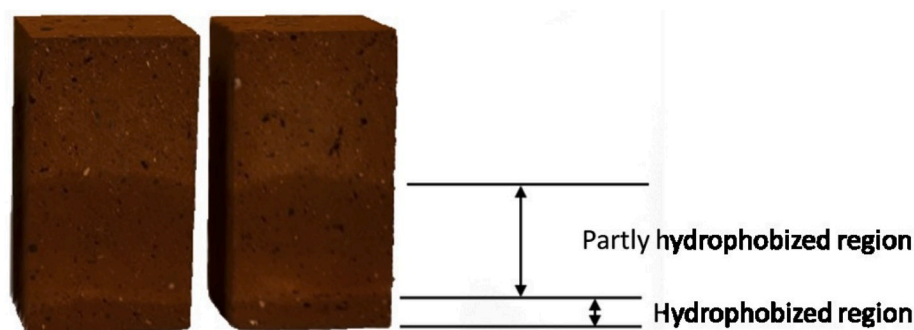


**Fig. 4.** Impregnation depth in H brick right after the impregnation process with a liquid product. Strong hydrophobized layer at bottom (darker surface), partly hydrophobized region above.

water vapour diffusion resistance factor ( $\mu$ ). After pre-conditioning, the samples, enclosed in the lids, were attached to cups containing saturated salt solutions and placed in a climatic chamber. Weighing of the samples was conducted twice per week in four weeks.

## 4. Results

### 4.1. Impregnation depth

A sufficient impregnation depth of the hydrophobic treatment is vital, since a thin hydrophobic layer may pose a risk for water penetration in the case of cracks at the exterior surface. Initially in this study the impregnation depth of impregnated samples was measured by visual inspection right after as well as one month after the impregnation process. The visual inspection indicates impregnation depths (strongly hydrophobized region plus the partly hydrophobized region) of approximately 25 mm on bricks and of 5–10 mm on mortar, right after impregnation with various liquid water repellent agents (for details refer to Table C 1 in Appendix). The redistribution of the agent after one month is visible only in R brick where the impregnation depth is around 30 mm. However, this section aims to illustrate that the redistribution of the agent extends the measured values coming from visual inspection and results in larger impregnation depths.

In order to thoroughly investigate the partly hydrophobized volume, water uptake tests from the impregnated and not-impregnated sides were conducted. Fig. 5 gives an indication of the strength and depth of the partly hydrophobized volume by comparing the water absorption coefficient of samples from the impregnated side and the not impregnated side. The impregnated samples show water repellency even at the not-impregnated side, as the water volume absorbed by the not-impregnated side is significantly reduced compared to the untreated

material. Fig. 5 also illustrates that the redistribution of the agent leads to much larger impregnation depths than the ones measured by visual inspection. After the hydrophobization procedure, the active ingredient spreads further into the material, leading to a major rise in the impregnation depth. All three brick types, when impregnated with liquid products (SMK, SNL and WS), in all tested concentrations, showcase water uptake reductions from the non-impregnated side that are similar to the results for water uptake from the impregnated side (Fig. 5). This leads to the conclusion that the brick samples become almost fully hydrophobized, and therefore, the impregnation depth is greater than the initial measurements via visual inspection. In the case of L mortar the reduction of  $A_{cap}$  from the non-impregnated side is also significant but the samples do not become fully hydrophobized.

Due to the less amount of agent applied with FC cream compared to that of liquid products, this effect is less evident. After 5 min of free liquid agent uptake, R brick absorbs around 5–8 ml of agent, H brick 5–7 ml, Y brick 5–6 ml, L mortar 4–7 ml. The minimum recommended quantity of the FC cream products (150–200 ml/m<sup>2</sup>) corresponds to around 0.5 ml per sample. When five times more cream agent is applied (40% concentration) in R brick and L mortar, the impregnation depth (visual inspection) is 24 and 15 mm respectively and the water absorption coefficient from the not-impregnated side is 235 and 3305 (10<sup>-5</sup> kg/m<sup>2</sup>√s) respectively after one-month of curing.

For SMK 2100 and Remmers FC the water uptake from the impregnated and not-impregnated side was conducted after one month of curing. In the case of SMK 2101, SMK 1311, Remmers SNL and Remmers WS, water uptake from the impregnated side was conducted after one month of curing, while the water uptake test from the not-impregnated side was conducted after five months. With longer curing times and water exposure, the agent can spread deeper, hence yielding an even better performance in R brick impregnated with SMK 2101 and WS in

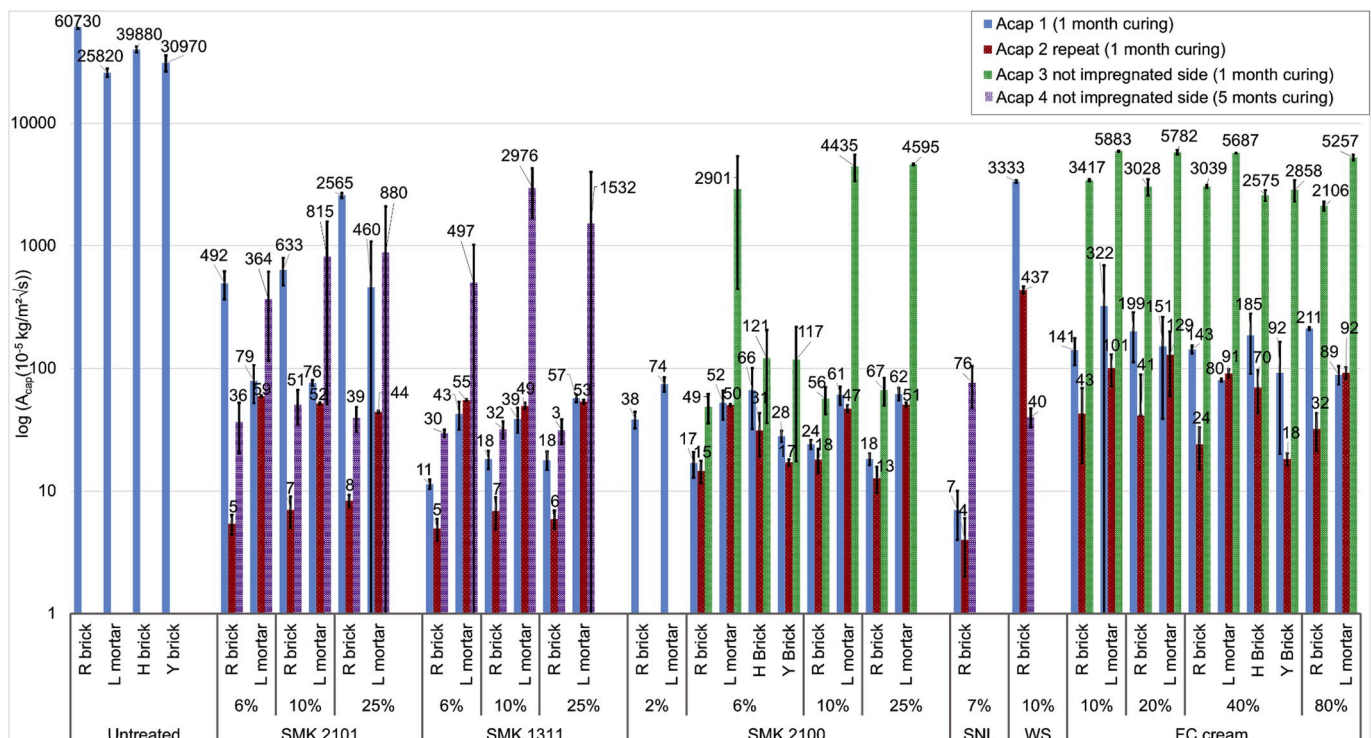


Fig. 5. Water absorption coefficient, initial ( $A_{cap1}$ ) after one month of curing, repeated after water exposure ( $A_{cap2}$ ), from not impregnated side of the sample (height 8 cm) after one month of curing ( $A_{cap3}$ ), from not impregnated side after five months of curing ( $A_{cap4}$ ). R brick, L mortar, H brick and Y brick, untreated and impregnated with different water repellent agents and concentration of active ingredients. Each result is an average based on three samples, error bars correspond to standard deviation, for exact values see Table C 1 Appendix. All the results of  $A_{cap2}$  refer to 1 month of curing except for the SNL where it was measured after 5 months of curing.

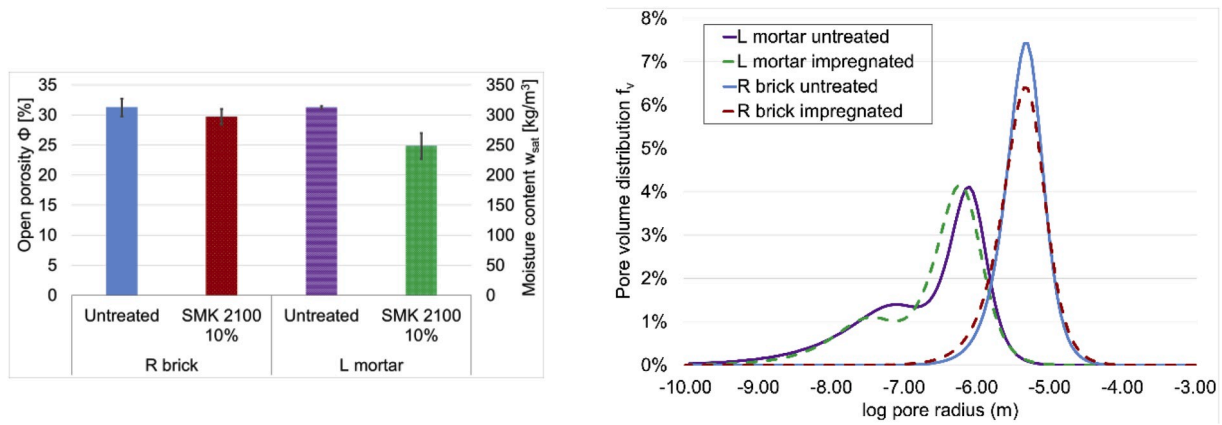


Fig. 6. Open porosity and vacuum saturation moisture content (left) and pore volume distribution (right), R brick and L mortar, untreated and impregnated with SMK 2100 10%. Each result is an average based on five samples, error bars correspond to standard deviation, for exact values see Table B 1 Appendix.

terms of water repellency from the not-impregnated side compared to the impregnated side with one month of curing (see Fig. 5). Moreover, repeating the water uptake test from the not impregnated side for R brick and L mortar treated with FC 40% and for L mortar treated with SMK, results in further reduction of  $A_{cap}$  (see Table C 1 Appendix) building more confidence that the agent spreads deeper with time.

#### 4.2. Moisture storage

Neither open porosity ( $\Phi$ ) nor vacuum saturation moisture content ( $w_{sat}$ ) seems to be significantly influenced by hydrophobic impregnation, both in R brick and L mortar as seen in Fig. 6 (left). The pore volume distribution in Fig. 6 (right) indicates almost the same available pore volume space in the hydrophobized material both in R brick and L mortar, that can be filled after submerging the sample and inducing a hydrostatic overpressure in the vacuum saturation testing (see Fig. 6 (left)). The small reduction of the open porosity especially in the case of L mortar could be due to a limited extent of clogging in the finer pores

[8].

#### 4.3. Moisture transport

##### 4.3.1. Capillary water absorption

A majority of the silicon-based water repellent agents significantly reduce the capillary water absorption of R, H and Y brick and L mortar (Fig. 5). In all cases the water absorption coefficient is negligible compared to the not impregnated samples. Only the WS water-based emulsion product in 10% concentration and the SMK 2101 silane agent in all tested concentrations performed less well in R brick, compared to the rest of the agents in the first water uptake ( $A_{cap1}$ ). However, repeating the water uptake tests ( $A_{cap2}$ ) results in greater reduction of the absorbed water.

Different concentrations, diluents and percentages of silane/siloxane illustrate similar water repellency performance but differ in the time that is needed to reach their optimal performance. Silanes (SMK 2101 and FC cream) and water emulsions (WS) seem to reach an optimal

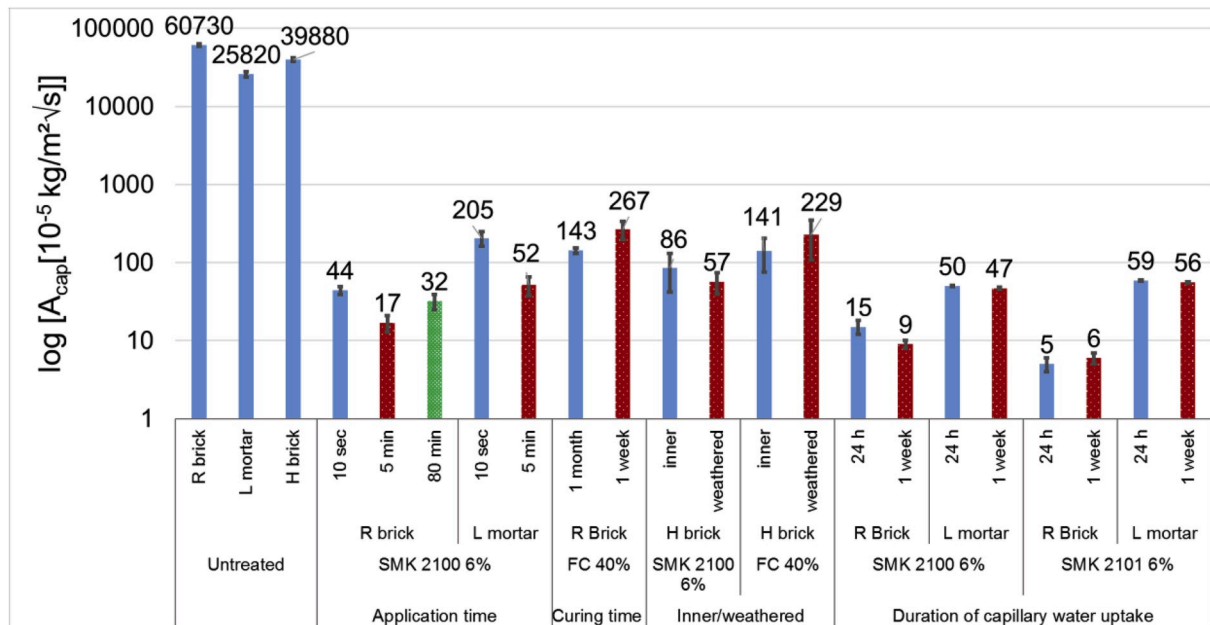


Fig. 7. Capillary water uptake. Influence of application time, curing time, type of surface and duration of water exposure on the water absorption coefficient of R brick, L mortar and H brick impregnated with FC 40% and SMK 2100 6%. Each result is an average based on three samples, error bars correspond to standard deviation. Results for untreated samples are shown as reference.

performance after water exposure. In R brick samples impregnated with SMK 2101 silane 10%, Remmers WS 10% and Remmers cream 40% even after three times of water uptake,  $A_{cap}$  is still slightly reduced (see  $A_{cap3}$  in Table C 1, Appendix).

The different tested substrates do not influence the absorption coefficient reduction, since both bricks and mortar depict similar water repellency performance impregnated with SMK 2100 6% (liquid) and FC 40% (cream). Moreover, low concentrations of 2% for liquid products and 10% for cream products still perform well, but not better than higher concentrations, as it is also described by Soulios et al. [17].

Fig. 7 shows that the absorption coefficient is negligible compared to untreated samples when studying the effect of the application time at impregnation, curing time, type of surface (inner (i.e. sawn) or weathered), or the duration of capillary water uptake.

The application time between the water repellent agent and the material in the process of impregnation did not affect significantly the water repellency of the R brick impregnated with SMK 2100 silane/siloxane 6% (liquid-based) even when extreme time intervals were used (10 s and 80 min). The excess amount of hydrophobic agent absorbed using 80 min contact time is translated to a larger impregnation depth and not to a stronger water repellency, compared to the contact time of 5 min, since the R brick sample becomes fully hydrophobized (8 cm depth) in 80 min. For mortar, the performance in terms of water repellency is slightly worse with a contact time of 10 s, compared to 5 min.

R brick impregnated with FC 40%, performs slightly worse with one-week curing time instead of one month. The performance of hydrophobic impregnation in terms of repelling liquid water is not affected if the agent – instead of an inner (sawn) surface – is applied on a weathered surface of a brick that has been thoroughly cleaned before impregnation. All the tested concentrations and the different percentages of silane/siloxane seem to have almost the same performance after longer exposure to water (continuing the water uptake for 1 week).

#### 4.3.2. Water vapour diffusion

Next to capillary water absorption, another key issue regarding hydrophobization is whether the vapour diffusion resistance factor ( $\mu$ ) of the material is altered after the hydrophobic treatment. The current findings (Fig. 8) support the view that hydrophobic impregnation has a minor effect on the water vapour diffusion resistance factor [5,7,11,13,

21]. There is nevertheless a small increase for all materials tested both with a liquid and a cream water repellent agent. In the case of L mortar at high RH, hydrophobization might eliminate the liquid water islands and the difference between untreated and treated samples is more obvious.

## 5. Discussion

The present study examined the effect of water repellent agents on impregnation depth and on the hygric properties of brick and mortar samples. Silicon-based water repellent agents can create a hydrophobic layer with an increasing impregnation depth over time through the redistribution of the active ingredient, a layer impermeable to liquid water but still permeable to water vapour without major alterations in the pore structure.

Hydrophobic impregnation creates a first, strongly hydrophobized layer as well as a larger volume that is partly hydrophobized [11]. Water uptake tests from the not impregnated side of the 8 cm high samples (see Fig. 5) extend our understanding of a well-defined impregnation depth provided by the technical data sheets of water repellent agents [55], indicating that the active ingredient is spread deeper inside the material and the impregnation depth increases for a period of time after impregnation.

Technical data sheets refer to the strongly hydrophobized region as impregnation depth, because in the partly hydrophobized region liquid water transfer could take place. When only the strongly hydrophobized region is considered, the measured values (after one month) of H brick and Y brick (9.5 and 7.7 mm respectively) impregnated with SMK 2100 fall close to the values provided for the SMK 1311 by Wacker (6–11 mm) for ceramic brick [55]. One more parameter that affects the impregnation depth of liquid products in lab environment is the application time. Longer application time leads to more redistribution in the material, as shown by Besien et al. [12]. Both in R brick and L mortar an application time of 10 s (similar to experiments by Ref. [7,8]), leads to lower impregnation depths than an application time of 5 min both in R brick and L mortar during which larger quantities of hydrophobic agent were absorbed (see Table C 1, Appendix). For on-site applications you flood the wall to saturation wet on wet from top to bottom two to three times with liquid products to ensure a large impregnation depth [46,56]. According to Ref. [6] 10–23 mm impregnation depth is sufficient with a

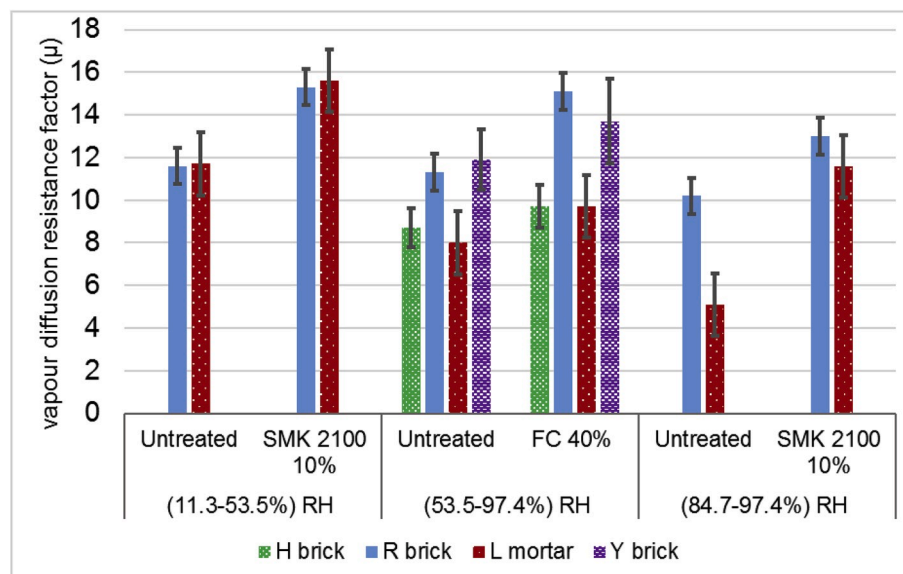


Fig. 8. Water vapour diffusion resistance factor ( $\mu$ ) of R brick, L mortar, H brick and Y brick, untreated and impregnated with SMK 2100 10% and FC 40% in different RH range. Each result is an average based on four samples, error bars correspond to standard deviation, for exact values see Table B 2 and Table B 3 Appendix.



maximum of 40 mm for highly absorbing porous building materials. In cream products it is easier to work with minimum quantities per square meter because the cream is absorbed slowly from the substrate. However, also in cream products the  $A_{cap}$  from the not impregnated side is lower when increasing the application rate from 0.5 ml to 2.5 ml, indicating larger impregnation depth (see  $A_{cap4}$  Table C 1, Appendix).

The different percentages of silane/siloxane and the different percentages of active ingredient don't have a major influence on the impregnation depth, especially after long curing periods and water exposure after treatment. However, the substrate has an impact: the active ingredient penetrates deeper in brick than in mortar, for all tested water repellent agents. Moreover, the standard deviation of  $A_{cap}$  of the three samples for each case of L mortar treated with liquid products (from the non-impregnated side) is significantly higher, indicating a non-uniform impregnation of the samples in the case of L mortar treated with the liquid products.

Another observation is that the different behavior of the hydrophobic layer is not caused by alterations in the pore structure, since there is almost the same available pore volume space in the hydrophobized material (see Fig. 6 (right)) that can be filled after submerging the sample and induce hydrostatic overpressure difference with the vacuum saturation test. The small reduction of the open porosity happens due to a limited extent of clogging in the finer pores [8] and/or the thin polymer chain creation around the perimeter of the pore wall, which is responsible along with the lack of liquid islands, for the small increase of the vapour diffusion resistance factor presented in Fig. 8. However, the small shift towards smaller pores in the pore volume distribution curve of hydrophobized mortar and a more obvious change in the open porosity than brick indicates that the finer the pores the higher the possibility of available pore volume reduction in a hydrophobized material.

The different behavior of the hydrophobic layer is caused by the non-polar film (see section 2.1) that is formed on the pore-walls of the porous building materials. This comparatively thin hydrophobic film ( $0.4\text{--}1.5 \cdot 10^{-9}\text{m}$  for silanes and  $3\text{ to }30 \cdot 10^{-9}\text{m}$  for siloxanes) [30] impedes liquid transfer, which reduces the drying speed [9,17] but allows water vapour diffusion, since it does not completely occupy the pores of mortar ( $5 \cdot 10^{-9}$  to  $5 \cdot 10^{-6}\text{m}$ ) or brick ( $10^{-6}$  to  $10^{-4}\text{m}$ ) (see Fig. 6), thus not fully impeding the drying of the material.

The present study supports previous findings on impregnated bricks, that reported similar reduction in the capillary water uptake with similar water repellent agents [5,8,10,11,16–18]. However, Hansen et al. [7] reported a high variation in terms of water repellency between different water repellent agents tested both in brick and mortar samples. Different conclusions could be caused by differences on duration of the curing period, cleaning of the samples before impregnation [11], as well as the method of impregnation and not in differences in application time (see Fig. 7).

The results reported in this article indicate that the small polymer chain of silane products ( $0.4\text{--}1.5 \cdot 10^{-9}\text{m}$ ) [30], especially in the case of a building material with coarse pores like brick ( $10^{-6}\text{--}10^{-4}\text{m}$ ) (Fig. 6), need more curing time and longer water exposure after treatment to reveal improved performance, due to the time needed for hydrolysis and polycondensation to take place. Given that the silane-containing water

repellent agents, originally recommended for concrete, need more curing time and after-treatment water exposure but can be very effective in both brick and mortar in terms of water repellency and impregnation depth. In a real case scenario, wind-driven rain would represent the after-treatment water exposure, perhaps increasing the impregnation strength and depth due to the washing-off of the emulsifiers, which permits the active ingredient of the water repellent agent to form stronger bonds with the pore walls of the building material. This is the reason why water-based products that contain emulsifiers, demonstrate a significantly increased performance after exposure to water. Products that contain micro-emulsions, increase their performance after water exposure, but tend to reveal their performance faster. Even the solvent-based product (SNL) shows a small reduction in terms of  $A_{cap}$  (Fig. 5) but this is the result of the long curing time between the first and second water uptake tests (five months). However, even without after-treatment exposure to water, the obtained  $A_{cap}$  is already close to zero.

Although the number of samples for the investigation of the effect of curing time in the current study were limited, combining the findings in Figs. 5 and 7, with the findings of Zhao and Meissener [11] support the view that with longer curing time the water repellency performance is increased. Another interesting fact is that for all the liquid water repellent agents tested in mortar samples, the active ingredient is absorbed with a slower rate and it needs longer application time, between the sample and the water repellent agent, than brick to be sufficiently impregnated.

## 6. Conclusions

In this paper the hygric behavior of ceramic bricks and carbonated lime mortar, treated with various water repellent agents, was experimentally studied. The water repellent agents penetrate deep into the materials, successfully blocking capillary effects, while still allowing water vapour diffusion, without notable alterations in the pore structure of the material. Moreover, water exposure after treatment increases the water repellency performance of the hydrophobic layer.

Future studies should include more types of mortar, especially mortars used for brickwork in historic buildings. Moreover, future research would benefit from focusing on durability tests, to study the long-term effect of the water repellency. Also hygrothermal simulations based on experimental data and real experiments in the component level will contribute towards a holistic view of hydrophobization.

## Acknowledgements

The present study is part of the project 'Moisture safe energy renovation of worth preserving external masonry walls', funded by the Danish foundations: The Landowners' Investment Foundation, Denmark The National Building Fund, Denmark and Realdania. This study is also part of RIBuild project that has received funding from Horizon 2020 under grant agreement No 637268. The authors express sincere thanks to Philip X.S. Møller (Introflex-Remmers) and Hamont Corne van (Wacker) for providing the water repellent agents and to Jimmy Van Crieckingen and Bernd Salaets (KU Leuven) for cutting the samples.

## Appendix A. Commercially available water repellent agents

**Table A 1**

Commercially available water repellent agents suitable for mineral substrates identified for this study.

No	Company	Product	Form	Diluent	Conc.	Substrate
<b>Silanes</b>						
1	WACKER	BS CREME C	Cream	water	80%	concrete
2	WACKER	BS 1701	Liquid	undiluted	99%	concrete
3	WACKER	BS 17040	Liquid	water	40%	concrete
4	WACKER	BS 16040	Liquid	water	40%	concrete
5	SIKA	706 Thixo	Cream	water	80%	concrete
6	SIKA	705 L	Liquid	undiluted	99%	concrete
7	SIKA	740 W	Liquid	Water	40%	concrete
8	REMMERS	Funcosil IC	Cream	water	80%	concrete
9	REMMERS	Funcosil FC	Cream	water	40%	masonry
10	DOW	OFS-2306	Liquid	solvent	96%	mineral
11	DOW	IE 6682	Liquid	water	52,5%	mineral
12	MOMENTIVE	Silblock wms	Liquid	water	40%	mineral
13	REYNCHÉMIE	RC SILAN	Liquid	solvent	98%	concrete
14	PEC	ENVIROSEAL 20	Liquid	water	20%	concrete
15	REWAH	ARTISIL B10	Liquid	solvent	10%	concrete
16	REYNCHÉMIE	RC 900	Liquid	solvent	10%	mineral
<b>Silane/Siloxane mixture</b>						
17	WACKER	BS N	Cream	solvent	25%	mineral
18	WACKER	BS 280	Liquid	solvent	100%	mineral
19	WACKER	BS 290	Liquid	solvent	100%	mineral
20	WACKER	BS 39	Liquid	water	25%	mineral
21	WACKER	BS 1001	Liquid	water	50%	mineral
22	WACKER	BS 3003	Liquid	water	60%	mineral
23	WACKER	BS 4004	Liquid	water	50%	mineral
24	WACKER	BS SMK 1311	Liquid	water	100%	mineral
25	WACKER	BS SMK 2100	Liquid	water	100%	mineral
26	WACKER	BS SMK 2101	Liquid	water	100%	concrete
27	DOW	Z-6689	Liquid	solvent	98%	mineral
28	DOW	IE 6683	Liquid	water	40%	mineral
29	DOW	520	Liquid	water	40%	mineral
30	DOW	IE 6694	Liquid	water	60%	mineral
31	Facabelle	Fassapearl S	Liquid	solvent	10%	mineral
32	Facabelle	Technifuge A104	Liquid	solvent	10%	mineral
33	Facabelle	Fassapearl H	Liquid	water	10%	mineral
34	REYNCHÉMIE	RC III	Cream	water	40%	mineral
35	REYNCHÉMIE	RC IV	Cream	water	40%	mineral
36	REYNCHÉMIE	RC 805	Liquid	water	7,5%	mineral
37	SIKA	700 S	Liquid	solvent		mineral
38	SIKA	704 S	Liquid	solvent		concrete
39	SIKA	703 W	Liquid	water		mineral
40	REMMERS	C40	Cream	water	40%	concrete
41	REMMERS	WS	Liquid	water	10%	mineral
42	REWAH	GELIFUGE	Gel	solvent	25%	masonry
43	REWAH	STONEGEL	Gel	water	25%	mineral
44	Soudal	Soudaclear S	Liquid	solvent	8%	mineral
45	Soudal	Soudaclear W	Liquid	water	6,5%	mineral
46	PEC	ENVIROSEAL B	Liquid	water	7%	masonry
47	SCALP	Scalpfuge 35	Liquid	water		masonry
<b>Siloxanes</b>						
48	Facabelle	Fassapearl-Gel	Cream	water	25%	mineral
49	REMMERS	SNL	Liquid	solvent	7%	mineral
50	REYNCHÉMIE	RC IP500	Liquid	solvent	10%	mineral
51	DOW	1 _ 6184	Liquid	water	98%	masonry
52	REMMERS	SL	Liquid	solvent	7%	masonry
53	BLUESTAR	WR 224	Liquid	solvent	69%	mineral
54	BLUESTAR	BP-9400	Liquid	solvent	100%	mineral
55	Facabelle	TECHNISIL hydro	Liquid	water	10%	mineral
56	REYNCHÉMIE	RC SILOX	Liquid	solvent	100%	mineral
57	REYNCHÉMIE	RC 224	Liquid	solvent	10%	mineral
58	WACKER	BS 66	Liquid	solvent	100%	mineral
59	REWAH	REDISIL S	Liquid	solvent	10%	masonry
60	REWAH	RS 8	Liquid	water	8%	masonry
61	BLUESTAR	BP 9710	Liquid	water	44%	mineral
<b>Silicone resins</b>						
62	BLUESTAR	RES 4518	Liquid	solvent	70%	mineral
63	DOW	MR 2404	Liquid	solvent	88,0%	mineral

(continued on next page)

**Table A 1** (continued)

No	Company	Product	Form	Diluent	Conc.	Substrate
64	SCALP	AQUAFUGE 18	Liquid	water		mineral
<b>Organic</b>						
65	REMMERS	OFS	Liquid	water		mineral
66	APP	ThefAPP	Liquid	water	3,1%	mineral
67	APP	APPHD	Liquid	water	1,9%	concrete
68	REYNCHÉMIE	RC 808	Liquid	water	10%	mineral
<b>Silicon &amp; Organic</b>						
69	Facabelle	TECHNISIL Hydro plus	Liquid	water	10%	mineral
70	REWAH	OLEOFUGE F	Liquid	water	10%	mineral
71	Wacker	BS 38	Liquid	solvent	46%	mineral
72	REYNCHÉMIE	RC 806	Liquid	water	10%	mineral
<b>Metal bearing</b>						
73	SCALP	OM 70	Liquid	solvent		mineral
<b>Silicon &amp; Metal bearing</b>						
74	REWAH	ECONOSIL	Liquid	solvent	10%	masonry
75	Facabelle	A101	Liquid	solvent	10%	mineral
76	REWAH	AVT	Liquid	solvent	8%	masonry
<b>Siliconates</b>						
77	PEC	Thoro clear special	Liquid	water	5,5%	limestone

## Appendix B. Hygric properties

**Table B 1**

Vacuum saturation test results. Comparison between untreated and impregnated with SMK 2100 10% R brick and L mortar.

	R brick		L mortar	
	Untreated	Impregnated	Untreated	Impregnated
Bulk density [kg/m <sup>3</sup> ]	1886.1 (35.8)	1900.7 (33.2)	1804.3 (5.7)	1830.2 (11.3)
Moisture content $w_{\text{sat}}$ [kg/m <sup>3</sup> ]	312.4 (14.8)	296.8 (12.9)	312.5 (2.1)	248.2 (21.4)
Open porosity $\Phi$ [%]	31.3 (1.5)	29.7 (1.3)	31.3 (0.2)	24.9 (2.1)
Matrix density [kg/m <sup>3</sup> ]	2745.6 (9.8)	2705.4 (5.8)	2626.2 (2.2)	2437.6 (73.6)

The values in brackets corresponds to the standard deviation of the measurements.

**Table B2**

Cup tests, comparison between untreated and impregnated with SMK 2100 10%, R brick and L mortar.

		R brick	L mortar
Untreated, dry (11.3–53.5%)	$\delta_v$ [ $10^{-11}$ kg/(msPa)]	1.7 (0.1)	1.7 (0.04)
	$\mu$	11.6 (0.5)	11.7 (0.3)
Untreated, wet (84.7–97.4%)	$\delta_v$ [ $10^{-11}$ kg/(msPa)]	1.9 (0.1)	3.9 (0.2)
	$\mu$	10.2 (0.5)	5.1 (0.3)
SMK 2100 10%, dry (11.3–53.5%)	$\delta_v$ [ $10^{-11}$ kg/(msPa)]	1.3 (0.05)	1.3 (0.1)
	$\mu$	15.3 (0.6)	15.6 (1)
SMK 2100 10%, wet (84.7–97.4%)	$\delta_v$ [ $10^{-11}$ kg/(msPa)]	1.5 (0.1)	1.7 (0.01)
	$\mu$	13 (0.6)	11.6 (0.1)

**Table B 3**

Cup tests, comparison of untreated and impregnated with FC 40% R brick, H brick, Y brick and L mortar.

		R brick	H brick	Y brick	L mortar
Untreated	$\delta_v$ [ $10^{-11}$ kg/(msPa)]	1.8 (0.2)	2.3 (0.2)	1.7 (0.2)	2.5 (0.1)
	$\mu_{(53.5-97.4\%)}$	11.3 (1.2)	8.7 (0.9)	11.9 (1.4)	8.0 (0.4)
FC 40%	$\delta_v$ [ $10^{-11}$ kg/(msPa)]	1 (0.8)	2 (0.2)	1 (0.2)	2 (0.1)
	$\mu_{(53.5-97.4\%)}$	15.1 (0.9)	9.7 (1)	13.7 (2)	9.7 (0.7)

## Appendix C. Hygric behavior of hydrophobized building materials

**Table C.1**  
Impregnation depth with visual inspection (dp), agent absorbed and water absorption coefficient ( $A_{cap}$ ) of R brick, H brick, Y brick and L mortar (8x4x4 cm samples).

Agent	Liquid products																	
	SMK 2101						SMK 1311						SMK 2100					
	6%		10%		25%		6%		10%		25%		6%		10%		25%	
Material	R	L	R	L	R	L	R	L	R	L	R	L	R	L	R	L	R	L
brick	brick	mortar	brick	mortar	brick	mortar	brick	mortar	brick	mortar	brick	mortar	brick	mortar	brick	mortar	brick	mortar
$d_p$ (5 min)	26.7 (4.6)	6.8 (0.2)	22.8 (2.1)	8.3 (0.3)	23.3 (1.1)	9.0 (0.9)	23.3 (0.7)	8.4 (0.7)	23.0 (1.2)	8.9 (1.4)	21.4 (0.9)	8.9 (0.5)	26.0 (1.3)	8.6 (1.5)	27.2 (2.9)	17.8 (1.6)	23.2 (1.2)	9.3 (0.6)
$d_p$ (1 month)	28.5 (3.0)	28.4 (3.0)	28.4 (3.0)	28.4 (3.0)	31.2 (1.2)	31.2 (1.2)	26.3 (0.9)	26.3 (0.9)	29.5 (1.1)	29.5 (1.1)	29.5 (2.4)	9.0 (0.5)	30.6 (0.0)	30.6 (0.0)	9.5* (0.5)	7.7* (0.1)	31.5 (1.4)	28.0 (3.0)
Agent absorbed	8.2 (0.8)	5.8 (0.3)	6.7 (1.5)	5.0 (0.0)	7.8 (0.3)	4.5 (0.5)	8.2 (0.3)	6.7 (0.6)	8.8 (0.3)	5.0 (0.0)	6.8 (0.8)	4.3 (0.6)	8.7 (0.6)	7.7 (0.6)	6.5 (0.7)	5.5 (0.5)	9.0 (0.0)	5.3 (0.6)
$A_{cap1}$ [ $10^{-5}$ kg/m <sup>2</sup> √s]	492 (127)	79 (27)	633 (159)	76 (4)	2565 (130)	460 (623)	11 (1)	43 (11)	18 (3)	39 (9)	18 (3)	57 (4)	17 (4)	52 (14)	66 (34)	28 (3)	24 (2)	61 (10)
$A_{cap2}$ [ $10^{-5}$ kg/m <sup>2</sup> √s]	5 (1)	59 (1)	7 (2)	52 (1)	8 (1)	44 (1)	5 (1)	55 (1)	7 (2)	49 (3)	6 (1)	53 (2)	15 (3)	50 (1)	31 (12)	17 (1)	18 (4)	47 (3)
$A_{cap3}$ [ $10^{-5}$ kg/m <sup>2</sup> √s]	6 (0.3)	6 (0.3)	6 (0.3)	6 (0.3)	6 (0.3)	6 (0.3)	6 (0.3)	6 (0.3)	6 (0.3)	6 (0.3)	6 (0.3)	6 (0.3)	6 (0.3)	6 (0.3)	6 (0.3)	6 (0.3)	6 (0.3)	6 (0.3)
$A_{cap4}$ [ $10^{-5}$ kg/m <sup>2</sup> √s]	36 (16)	36.4 (250)	51 (16)	81.5 (764)	39 (9)	880 (1212)	30 (2)	497 (521)	32 (5)	2976 (1304)	31 (7)	1532 (2473)	49 (13)	2901 (2458)	121 (85)	117 (100)	56 (14)	4435 (1085)
$A_{cap5}$ [ $10^{-5}$ kg/m <sup>2</sup> √s]	not imp side (repeat)	not imp side (repeat)	not imp side (repeat)	not imp side (repeat)	not imp side (repeat)	not imp side (repeat)	not imp side (repeat)	not imp side (repeat)	not imp side (repeat)	not imp side (repeat)	not imp side (repeat)	not imp side (repeat)	not imp side (repeat)	not imp side (repeat)	not imp side (repeat)	not imp side (repeat)	not imp side (repeat)	not imp side (repeat)
Conc.	Conc.	Conc.	Conc.	Conc.	Conc.	Conc.	Conc.	Conc.	Conc.	Conc.	Conc.	Conc.	Conc.	Conc.	Conc.	Conc.	Conc.	Conc.
Material	Material	Material	Material	Material	Material	Material	Material	Material	Material	Material	Material	Material	Material	Material	Material	Material	Material	Material
$d_p$ (5 min)	141 (35)	322 (370)	199 (87)	151 (112)	143 (11)	80 (2)	185 (95)	92 (72)	211 (5)	89 (15)	24 (9)	91 (7)	5.5 (2.3)	46.1 (2.5)	2.6 (0.4)	2.4 (0.2)	2.4 (0.2)	2.4 (0.2)
$d_p$ (1 month)	43 (26)	101 (29)	41 (48)	129 (70)	24 (9)	91 (7)	70 (27)	18 (2)	32 (11)	92 (10)	92 (10)	92 (10)	92 (10)	92 (10)	92 (10)	92 (10)	92 (10)	92 (10)
Agent absorbed	0.5	0.5	0.5	0.5	0.5	0.5	0.5	0.5	0.5	0.5	0.5	0.5	0.5	0.5	0.5	0.5	0.5	0.5
$A_{cap1}$ [ $10^{-5}$ kg/m <sup>2</sup> √s]	3417 (68)	5883 (85)	3028 (462)	5782 (234)	3039 (84)	5687 (11)	2575 (253)	2858 (560)	2106 (168)	5257 (281)	235 (94)	3305 (243)	24.0 (2.1)	14.9 (1.1)	9.2 (0.6)	11.8 (1.3)	14.2 (0.3)	7.4 (0.3)
$A_{cap2}$ [ $10^{-5}$ kg/m <sup>2</sup> √s]	not imp side (repeat)	not imp side (repeat)	not imp side (repeat)	not imp side (repeat)	not imp side (repeat)	not imp side (repeat)	not imp side (repeat)	not imp side (repeat)	not imp side (repeat)	not imp side (repeat)	not imp side (repeat)	not imp side (repeat)	not imp side (repeat)	not imp side (repeat)	not imp side (repeat)	not imp side (repeat)	not imp side (repeat)	not imp side (repeat)
$A_{cap3}$ [ $10^{-5}$ kg/m <sup>2</sup> √s]	not imp side (repeat)	not imp side (repeat)	not imp side (repeat)	not imp side (repeat)	not imp side (repeat)	not imp side (repeat)	not imp side (repeat)	not imp side (repeat)	not imp side (repeat)	not imp side (repeat)	not imp side (repeat)	not imp side (repeat)	not imp side (repeat)	not imp side (repeat)	not imp side (repeat)	not imp side (repeat)	not imp side (repeat)	not imp side (repeat)
$A_{cap4}$ [ $10^{-5}$ kg/m <sup>2</sup> √s]	not imp side (repeat)	not imp side (repeat)	not imp side (repeat)	not imp side (repeat)	not imp side (repeat)	not imp side (repeat)	not imp side (repeat)	not imp side (repeat)	not imp side (repeat)	not imp side (repeat)	not imp side (repeat)	not imp side (repeat)	not imp side (repeat)	not imp side (repeat)	not imp side (repeat)	not imp side (repeat)	not imp side (repeat)	not imp side (repeat)
$A_{cap5}$ [ $10^{-5}$ kg/m <sup>2</sup> √s]	not imp side (repeat)	not imp side (repeat)	not imp side (repeat)	not imp side (repeat)	not imp side (repeat)	not imp side (repeat)	not imp side (repeat)	not imp side (repeat)	not imp side (repeat)	not imp side (repeat)	not imp side (repeat)	not imp side (repeat)	not imp side (repeat)	not imp side (repeat)	not imp side (repeat)	not imp side (repeat)	not imp side (repeat)	not imp side (repeat)

The values in brackets corresponds to the standard deviation of the measurements. \* The impregnation depth was higher but this was the only visible darker surface with visual inspection after one month. The impregnation depth corresponds to the strong hydrophobized region plus the partly hydrophobized region.



## Declaration of interests

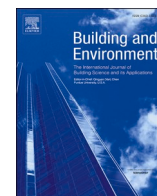
□ The authors declare that they have no known competing financial interests or personal relationships that could have appeared to influence the work reported in this paper.

## References

- [1] EC Adhoc Industrial Advisory Group, Energy Efficient Buildings Public-Private Partnership (PPP): Multi Annual Roadmap and Longer Term Strategy, 2010, <https://doi.org/10.2777/10074>. Brussels.
- [2] M. Jerman, I. Palomar, V. Koci, R. Cerny, Thermal and hygric properties of biomaterials suitable for interior thermal insulation systems in historical and traditional buildings, *Build. Environ.* 154 (2019) 81–88, <https://doi.org/10.1016/j.buildenv.2019.03.020>.
- [3] M. Guizzardi, D. Derome, R. Vonbank, J. Carmeliet, Hygrothermal behavior of a massive wall with interior insulation during wetting, *Build. Environ.* 89 (2015) 59–71, <https://doi.org/10.1016/j.buildenv.2015.01.034>.
- [4] E. Vereecken, Hygrothermal Analysis of Interior Insulation for Renovation Projects, KU Leuven, 2013. <https://doi.org/10.1016/j.buildenv.2015.01.034>.
- [5] J. Engel, P. Heinze, R. Plagge, Adapting hydrophobizing impregnation agents to the object, *Hydrophobe VIIth Int. Conf. Water Repel. Treat. Prot. Surf. Technol. Build. Mater.* 20 (2014) 141–150, <https://doi.org/10.12900/rbm14.20.6-0042>.
- [6] E. Wendler, E. Von Plehwe-Leisen, Water repellent treatment of porous materials. A new edition of the WTA leaflet, in: V. Hydrophobe (Ed.), Fifth Int. Conf. Water Repel. Treat. Build. Mater., 2008, pp. 155–167. [http://www.hydrophobe.org/pdf/bruxelles/V\\_13.pdf](http://www.hydrophobe.org/pdf/bruxelles/V_13.pdf).
- [7] T.K. Hansen, S.P. Bjarlov, R.H. Peuhkuri, K.K. Hansen, Performance of hydrophobized historic solid masonry – experimental approach, *Construct. Build. Mater.* 188 (2018) 695–708, <https://doi.org/10.1016/j.conbuildmat.2018.08.145>.
- [8] J. Carmeliet, G. Hovenaghel, J. Van Schijndel, S. Roels, Moisture phenomena in hydrophobic porous building material Part 1: measurements and physical interpretations/Wechselwirkung hydrophobierter poröser Werkstoffe des Bauwesens mit Feuchtigkeit, Teil 1: messungen und physikalische Interpretationen, *Restor. Build. Monum.* 8 (2002) 165–183, <https://doi.org/10.1515/rbm-2002-5660>.
- [9] K. Sandin, Surface treatment with water repellent agents, in: *Hydrophobe I*, 1995, pp. 1–9. Delft, <http://hydrophobe.org/pdf/delft/1.18.pdf>.
- [10] H. Kober, Water thinnable silicone impregnating agents for masonry protection, in: *Hydrophobe I Delft*, 1995, pp. 1–13. <http://www.hydrophobe.org/pdf/delft/1.3.pdf>.
- [11] J. Zhao, F. Meissener, Experimental investigation of moisture properties of historic building material with hydrophobizing treatment, *Energy Procedia* 132 (2017) 261–266, <https://doi.org/10.1016/j.egypro.2017.09.716>.
- [12] T. Van Besien, S. Roels, J. Carmeliet, A laboratory study of the efficiency of a hydrophobic treatment of cracked porous building materials, in: 2nd Int. Conf. Build. Phys., 2003, pp. 1–7. <https://www.irbnet.de/daten/iconda/CIB2372.pdf>.
- [13] K. Fukui, C. Iba, S. Hokoi, Moisture behavior inside building materials treated with silane water repellent, *Energy Procedia* 132 (2017) 735–740, <https://doi.org/10.1016/j.egypro.2017.10.018>.
- [14] H. Janssen, B. Blocken, S. Roels, J. Carmeliet, Wind-driven rain as a boundary condition for HAM simulations: analysis of simplified modelling approaches, *Build. Environ.* 42 (2007) 1555–1567, <https://doi.org/10.1016/j.buildenv.2006.10.001>.
- [15] A. Erkal, D. D'Ayala, L. Sequeira, Assessment of wind-driven rain impact, related surface erosion and surface strength reduction of historic building materials, *Build. Environ.* 57 (2012) 336–348, <https://doi.org/10.1016/j.buildenv.2012.05.004>.
- [16] J. Sadauskienė, J. Ramanaukas, V. Stankevicius, Effect of hydrophobic materials on water impermeability and drying of finish brick masonry, *Issn Mater. Sci.*, 2003, 1392–1320, [https://www.researchgate.net/profile/Jolanta\\_Sadauskienė/publication/237779777\\_Effect\\_of\\_Hydrophobic\\_Materials\\_on\\_Water\\_Impervability\\_and\\_Drying\\_of\\_Finish\\_Brick\\_Masonry/links/53fb1c580cf27c365cf06ef8.pdf](https://www.researchgate.net/profile/Jolanta_Sadauskienė/publication/237779777_Effect_of_Hydrophobic_Materials_on_Water_Impervability_and_Drying_of_Finish_Brick_Masonry/links/53fb1c580cf27c365cf06ef8.pdf).
- [17] V. Soulios, E.J. de Place Hansen, H. Janssen, Hygric properties of hydrophobized building materials, in: MATEC Web Conf, 2019, pp. 1–6, <https://doi.org/10.1051/mateconf/201928202048>. Prague.
- [18] T. Kvist Hansen, S.P. Bjarlov, R. Peuhkuri, Moisture transport properties of brick – comparison of exposed, impregnated and rendered brick, in: Proc. Int. RILEM Conf. - Mater. Syst. Struct. Civ. Eng. Segm. Moisture Mater. Struct., 2016, pp. 351–360, in: [http://orbit.dtu.dk/ws/files/128040737/Pages\\_from\\_Moisture\\_conf\\_proceedings\\_3.pdf](http://orbit.dtu.dk/ws/files/128040737/Pages_from_Moisture_conf_proceedings_3.pdf).
- [19] A.G. Momentive, Silblock Wms Technical Data Sheet, 1–4, 2011. [https://www.momentive.com/docs/default-source/productdocuments/silblock-wms/silblock-wms-mb-indd.pdf?sfvrsn=d50e61c\\_14](https://www.momentive.com/docs/default-source/productdocuments/silblock-wms/silblock-wms-mb-indd.pdf?sfvrsn=d50e61c_14).
- [20] H. De Clercq, E. De Witte, Effectiveness of commercial silicon based water repellents applied under different conditions, *Restor. Build. Monum.* an Int. J. = Bauinstandsetz. Und Baudenkmalpf. Eine Int. Zeitschrift. 8 (2002) 149–164, <https://doi.org/10.1515/rbm-2002-5659>.
- [21] A.E. Charola, Water-repellent treatments for building stones: a practical overview, *APT Bull. J. Preserv. Technol.* 26 (1995) 10–17, <https://doi.org/10.2307/1504480>.
- [22] M. Roos, F. König, S. Stadtmüller, B. Weyershausen, Evolution of silicone based water repellents for modern building protection, 5th Int. Conf. Water Repel. Treat. Build. Mater. 16 (2008) 3–16. [http://www.hydrophobe.org/pdf/bruxelles/V\\_01.pdf](http://www.hydrophobe.org/pdf/bruxelles/V_01.pdf).
- [23] E.B. Møller, C. Rode, Hygrothermal Performance and Soiling of Exterior Building Surfaces, Technical University of Denmark, 2004. <https://orbit.dtu.dk/files/5285541/byg-r068.pdf>.
- [24] B. Lubelli, R.P.J. van Hees, Evaluation of the effect of nano-coatings with water repellent properties on the absorption and drying behaviour of brick, in: *Hydrophobe VI Proc. 6th Int. Conf. Water Repel. Treat. Build. Mater.*, 2011, pp. 125–135. [http://www.hydrophobe.org/pdf/rome/VI\\_12.pdf](http://www.hydrophobe.org/pdf/rome/VI_12.pdf).
- [25] J. MacMullen, Z. Zhang, E. Rirsch, H.N. Dhakal, N. Bennett, Brick and mortar treatment by cream emulsion for improved water repellence and thermal insulation, *Energy Build.* 43 (2011) 1560–1565, <https://doi.org/10.1016/j.enbuild.2011.02.014>.
- [26] M. Stefanidou, A. Kerozu, Testing the effectiveness of protective coatings on traditional bricks, *Construct. Build. Mater.* 111 (2016) 482–487, <https://doi.org/10.1016/j.conbuildmat.2016.02.114>.
- [27] K. Ren, D. Kagi, Evaluation of an oil and water repellent on masonry substrates. *Hydrophobe VIII, Hongkong*, 2017, pp. 44–52. <http://www.hydrophobe.org/pdf/hongkong/A-1-3.pdf>.
- [28] A.G. Wacker Chemie, Silres® Bs Smk 2101, Technical Data Sheet, 2014, pp. 3–4. [https://www.brenntag.com/media/documents/bsi/product\\_data\\_sheets/material\\_science/wacker\\_silicone\\_resins/silres\\_bs\\_smk\\_2101\\_pds.pdf](https://www.brenntag.com/media/documents/bsi/product_data_sheets/material_science/wacker_silicone_resins/silres_bs_smk_2101_pds.pdf).
- [29] A. Syed, M. Donadio, Silane Sealers/Hydrophobic Impregnation - the European Perspective, 2013, pp. 1–6. [https://cdn.ymaws.com/www.icri.org/resource/resmgr/crb/2013septoct/CRBSepOct13\\_Syed-Donadio.pdf](https://cdn.ymaws.com/www.icri.org/resource/resmgr/crb/2013septoct/CRBSepOct13_Syed-Donadio.pdf).
- [30] A.G. Sika Services, Refurbishment Sika Technology and Concepts for Hydrophobic Impregnations, 2017, pp. 1–20.
- [31] H. Mayer, Masonry protection with silanes, siloxanes and silicone resins, *Surf. Coating. Int.* 81 (1998) 89–93, <https://doi.org/10.1007/BF02692337>.
- [32] T. Szymura, D. Barnat-hunek, Protection of stone building structures against corrosion caused by moisture, 2013, pp. 65–76. <http://br.wszia.edu.pl/zeszyty/pdfs/br32.07szymura.pdf>.
- [33] A.G. Wacker Chemie, Silres® Bs 38, Technical Data Sheet, 2011, pp. 1–2. [https://www.brenntag.com/media/documents/bsi/product\\_data\\_sheets/material\\_science/wacker\\_silicone\\_resins/silres\\_bs\\_38\\_pds.pdf](https://www.brenntag.com/media/documents/bsi/product_data_sheets/material_science/wacker_silicone_resins/silres_bs_38_pds.pdf).
- [34] Technichem S.A., Technisil Hydro Plus, W.T.C.B., (2005) 1–2.
- [35] N.V. Rewah, F. Oleofuge, Technical Data Sheet 1–3, 2018. <http://www.rewah.com/images/products/166/technicalsheet.pdf?refresh=1572963183>.
- [36] E. De Witte, H. De Clercq, R. De Bruyn, A. Pien, Systematic testing of water repellent agents, *Restor. Build. Monum.* 2 (1996) 133–144, <https://doi.org/10.1515/rbm-1996-5093>.
- [37] A.E. Charola, Water repellents and other “protective” Treatments : a critical review, in: *Hydrophobe III. 3rd Int. Conf. Surf. Technolgy with Water Repel. Agents. Aedif. Publ.*, 2001, pp. 3–20. [http://www.hydrophobe.org/pdf/hannover/III\\_01.pdf](http://www.hydrophobe.org/pdf/hannover/III_01.pdf).
- [38] N.V. Rewah, ARTISIL B10, Technical Data Sheet, 2016, pp. 1–2. <http://www.rewah.com/images/products/12/technicalsheet.pdf>.
- [39] D. Corning, Dow Corning® Z-6689 Water Repellent, Safety Data Sheet, 2017, pp. 1–4. <https://www.dow.com/en-us/pdp.dowzil-z-6689-water-repellent.04023290z.html>.
- [40] Hilde De Clercq, RC 805 ECO REYNCHÉMIE NV, Test Report, 2004, pp. 1–10. <http://www.reynchemie.com/Content/Bestanden/20123-RC805ECO-KIK-nl.pdf>.
- [41] J. Todorović, H. Janssen, The impact of salt pore clogging on the hygric properties of bricks, *Construct. Build. Mater.* 164 (2018) 850–863, <https://doi.org/10.1016/j.conbuildmat.2017.12.210>.
- [42] Ö. Cizer, K. Van Balen, J. Elsen, D. Van Gemert, Real-time investigation of reaction rate and mineral phase modifications of lime carbonation, *Construct. Build. Mater.* 35 (2012) 741–751, <https://doi.org/10.1016/j.conbuildmat.2012.04.036>.
- [43] A.G. Wacker Chemie, Silres® Bs Smk 1311, Technical Data Sheet, 2014, pp. 1–3. <http://www.vardhmanpolymers.com/wp-content/uploads/2019/01/1311.pdf>.
- [44] A.G. Wacker Chemie, Silres® Bs Smk 2100, Technical Data Sheet, 2014, pp. 1–2.
- [45] A.G. Remmers, S.N.L. Funcosil, Technical Data Sheet, 2016, pp. 1–3. [http://www.stonewarestudios.com/PDF/DampControl/Funcosil\\_SNL.pdf](http://www.stonewarestudios.com/PDF/DampControl/Funcosil_SNL.pdf).
- [46] A.G. Remmers, W.S. Funcosil, Technical Data Sheet, 2016, pp. 1–2. [http://www.bg.remmers.com/fileadmin/dam/produkte/tm/TM1\\_0614\\_EN.pdf](http://www.bg.remmers.com/fileadmin/dam/produkte/tm/TM1_0614_EN.pdf).
- [47] A.G. Remmers, F.C. Funcosil, Technical Data Sheet, 2016, pp. 1–3. [https://www.introflex.dk/images/pdf/DK\\_0711\\_-08\\_13.pdf](https://www.introflex.dk/images/pdf/DK_0711_-08_13.pdf).
- [48] N.V. Rewah, N.E.W. Gelifuge, Technical Data Sheet, 2016, pp. 1–3. <http://www.rewah.com/images/products/121/technicalsheet.pdf>.
- [49] ASTM C1699-09, Standard Test Method for Moisture Retention Curves of Porous Building Materials Using Pressure Plates, 2015, <https://doi.org/10.1520/C1699-09R15>.
- [50] C. Feng, H. Janssen, Y. Feng, Q. Meng, Hygric properties of porous building materials: analysis of measurement repeatability and reproducibility, *Build. Environ.* Times 85 (2015) 160–172, <https://doi.org/10.1016/j.buildenv.2014.11.036>.
- [51] ASTM D4404-18, Standard Test Method for Determination of Pore Volume and Pore Volume Distribution of Soil and Rock by Mercury Intrusion Porosimetry, 2018, <https://doi.org/10.1520/D4404-18>.

- [52] ISO 15148 : 2002, Hygrothermal Performance of Building Materials and Products Determination of Water Absorption Coefficient by Partial Immersion, English Version of DIN EN ISO 15148, 2003, pp. 1–14.
- [53] C. Feng, H. Janssen, Hygric properties of porous building materials (III): impact factors and data processing methods of the capillary absorption test, *Build. Environ.* 134 (2018) 21–34, <https://doi.org/10.1016/j.buildenv.2018.02.038>.
- [54] ISO 12572, Hygrothermal Performance of Building Materials and Products -transmission Properties -Cup Method, 2016, pp. 1–5. <https://www.sis.se/api/document/preview/920749/>.
- [55] A.G. Wacker Chemie, Hydrophobic Impregnation with Silres BS, 2017, pp. 1–22.
- [56] A.G. Sika Services, Sikagard ® -700 S Technical Data Sheet, 2016, pp. 1–3.





## Durability of the hydrophobic treatment on brick and mortar

Vasilis Soulios<sup>a,\*</sup>, Ernst Jan de Place Hansen<sup>a</sup>, Ruut Peuhkuri<sup>a</sup>, Eva Møller<sup>b</sup>, Afshin Ghanbari-Siahkali<sup>c</sup>

<sup>a</sup> Department of the Built Environment, Aalborg University, Denmark

<sup>b</sup> DTU Civil Engineering, Technical University of Denmark, Kgs. Lyngby, Denmark

<sup>c</sup> Danish Technological Institute, Gregersensvej, Taastrup, Denmark

### A B S T R A C T

Hydrophobization lessens the water absorption by facade materials and is thus presumed to reduce moisture problems in internally insulated facades. However, to do this it should retain the water repellency performance throughout aging. The aim of this study is to evaluate the impact of aging on the durability of the hydrophobic treatment on bricks and mortars. The resulting absorption coefficient, after 635 repeating artificial aging cycles of alternating UV radiation (102 min) and water exposure (18 min) reveals that the hydrophobic layer maintains its water repellency performance both in brick and mortar. The samples were treated with two different water repellent agents in different concentrations and tested for capillary water uptake. Additionally, the findings show that cycles of weathering could contribute positively to further reduction of the absorption coefficient of hydrophobized brick and mortar samples. Subsequently, Karsten tube tests on samples from artificial aging illustrate the same water repellency performance as mock-up walls exposed to ambient conditions, six years after being hydrophobized. Contact angle measurements before and after artificial aging reveal that the beading effect declines through aging. However, the beading effect seems to be just a surface effect affected by UV-light. Moreover, after aging, hydrophobized brick and mortar samples, tested by visual inspection, maintain their appearance while untreated samples show signs of efflorescence. In total, these findings indicate that the water uptake of hydrophobized brick or mortar remains very low after aging including water spraying and UV light.

### 1. Introduction

Denmark is targeting to be independent of fossil fuels by the year 2050 [1]. In the EU, existing buildings represent 99% of the building stock [2], which accounts for about 40% of the total energy consumption [3]. 10%–40% of these buildings [4] are historical, high energy-consuming buildings [3,5–7]. The household's energy consumption within EU-27 is dominated by space heating in a percentage of 67% [8]. Often such buildings have worth preserving solid facades, making internal insulation the only feasible technique for thermal insulation [9]. Internal insulation itself can reduce the heat losses of a wall by 76% in the case of mineral wool plus vapor barrier and 63% in the case of CaSi, in a climate like Copenhagen [10]. However, internal insulation may lead to moisture-related problems [4,5,11–14]. The main source of the problems derives from the accumulated moisture load from wind-driven rain [15,16], and internal insulation negatively affects the drying potential of the masonry wall [12,17–19]. Studies comparing the overall hygrothermal performance of internally insulated solid masonry walls, tend to suggest vapor open and capillary active internal insulation systems to counterbalance the reduced inward drying [5,20]. However, applying water repellent agent in the internally insulated wall

practically eliminates the absorption of the wind-driven rain [21–24].

Moisture transfer in building materials plays a vital role in the durability and thereby sustainability of built structures [12,25,26]. Absorption of moisture is the main mechanism for the deterioration of porous building materials and the starting point for many moisture-related damages in the building structure potentially affecting the durability. Moreover, absorption of moisture increases the thermal conductivity of building components resulting in increased heat losses [10,21]. So, water absorption that remains at low levels over time enhances the durability of the porous building materials and consequently the durability of the whole structure. Hydrophobization is proven to significantly reduce the absorption coefficient of both brick and mortar and at the same time to allow water vapor diffusion, thus not fully impeding the drying of the material [21,22]. But there is very little experience in the literature about the durability of the hydrophobic treatment of brick masonry and brick and mortar samples, especially regarding the possible changes of the absorption coefficient of hydrophobized brick and mortar. Some studies however, have used Karsten tube tests to measure water uptake on hydrophobized aged masonry [27, 28] and on aged brick and natural stone samples [29]. White efflorescence is widely known as an aesthetic problem of brick masonry, where

\* Corresponding author.

E-mail addresses: [vsou@build.aau.dk](mailto:vsou@build.aau.dk), [v.soulios@ihu.edu.gr](mailto:v.soulios@ihu.edu.gr) (V. Soulios).

<https://doi.org/10.1016/j.buildenv.2021.107994>

Received 19 March 2021; Received in revised form 20 May 2021; Accepted 21 May 2021

Available online 26 May 2021

0360-1323/© 2021 The Authors. Published by Elsevier Ltd. This is an open access article under the CC BY license (<http://creativecommons.org/licenses/by/4.0/>).

water transport plays an essential role [30,31]. Concrete impregnated with a water repellent agent in cream form illustrates resistance against salt formation [32] but there are no similar studies for brick and mortar. Each of these factors highlights the need to investigate the durability of hydrophobized masonry and prior to that, the durability of masonry components, i.e. hydrophobized brick and mortar samples, expressed by the absorption coefficient, as well as the appearance of the hydrophobized materials after aging. Moreover, even though contact angle measurement is not a precise indicator to assess the water repellency performance [33], comparing the contact angle in hydrophobized materials before and after artificial aging could provide information on the influence of the aging on the beading effect.

By providing an artificial aging test with hydrophobized brick and mortar samples this paper aims to meet this need. It begins by describing the building materials and water repellent agents used for this study as well as describing the methodology for artificial aging and the experiments conducted to investigate water absorption, beading effect, and discoloration through aging. This is followed by a section presenting how the absorption coefficient of the hydrophobized materials develops after several rounds of repeating cycles of artificial aging. A supplementary section, using Karsten tube tests, compares the water uptake of the samples used in the artificial aging with mock-up walls constructed with the same building materials. A subsequent section presents results from contact angle measurements on hydrophobized samples before and after artificial aging. It also considers the discoloration of untreated samples after artificial aging. Finally, the paper discusses the results, contrasting them with previous work.

## 2. Materials and methods

### 2.1. Target building materials

The building materials used in the current study were selected to represent building materials to be found in a typical Danish building from before 1950 (see Table 1); soft-molded brick and air-lime mortar. Further, cement mortar was included, as it is common practice in Denmark to perform repointing of mortar joints before impregnation, normally with cement mortar.

The yellow soft-molded brick from Helligsø Teglvaerk in Denmark imitates a historic Danish brick and its properties have been thoroughly analyzed [10,21,22,34–37]. Further, historic brick samples were obtained from an old building in Denmark constructed in 1944 in order to test a brick that was exposed to actual weathering before hydrophobization. Material properties of the historic brick could be found in Refs. [10,21].

Most of the old masonry buildings in Denmark have been constructed with air lime mortar. The air lime mortar used in this study was supplied as ready-mix from Wewers and mixed with tap water to form fresh mortar which was placed in molds for casting. In order to imitate the mortar being placed towards bricks as in a brick masonry, wound cleaning swabs were placed at both sides of the molds (top and bottom) and the samples were placed in a climatic chamber (65% RH, 20 °C) for one month [38]. For the air lime mortar samples to represent a historic type of air lime mortar that has been part of brick masonry for many years [39], the samples were placed in a carbonation chamber (1% CO<sub>2</sub> exposure) for three months. The air lime mortar samples were tested with phenolphthalein and they were fully carbonated.

The type of cement mortar supplied from Wewers is the one that is usually used to repoint mortar joints in Denmark and has not been carbonated in order to represent a fresh cement mortar used to re-point the mortar joints before impregnation.

The size of the tested samples was 2 × 5 × 15 cm to fit the Atlas weather-ometer (see section 2.4 Experimental set-up).

### 2.2. Selected water repellent agents

The selected water repellent agents (Table 2) are ready-to-use, in cream form, as cream products are widely used nowadays due to their easy application and long contact time that requires just a single treatment [21]. Further, liquid and cream-based products are shown to have the same effect in terms of water repellency on brick and mortar samples [21]. Funcosil Remmers FC cream is a water-based silane cream, recommended for mineral substrates, that can be ordered in any possible concentration [40], but commonly used in Denmark with a 40% concentration. The Wacker BS cream C is a water-based silane cream in 80% concentration that is recommended for concrete [41].

**Table 1**  
Building materials used in the current study.

Name	Description
Y brick	Yellow soft-molded Danish brick from Helligsø Teglvaerk
H brick	Historic Danish Brick from an old building in Copenhagen (1944)
AL mortar	Carbonated air lime mortar with aggregates of 0–4 mm grain size (7.7%) (Wewers)
C mortar	Cement mortar with aggregates of 0–4 mm grain size (Wewers)

**Table 2**  
Water repellent agents used in the current study.

Product	Company	Type	Form	Diluent	Concentration	Substrate
FC	Remmers	Silane	Cream	Water	40%	Mineral
BS	Wacker	Silane	Cream	Water	80%	Concrete

Information derived from the technical data sheets of the products. Both water repellent agents are mainly silane but they contain small percentage of siloxane.

**Table 3**

Laboratory experiments. Test plan including measured properties, type of tests, sample size and amount, type of material, and water repellent agent.

Material (No. of samples for each type)	Treatment	0 cycles	165 cycles	335 cycles	482 cycles	635 cycles
<b>Water absorption coefficient (<math>A_{cap}</math>) by capillary water uptake (<math>2 \times 5 \times 15</math> cm samples)</b>						
Y brick, H brick, AL mortar, C mortar (3)	Untreated	X				X
Y brick, H brick, AL mortar, C mortar (3)	FC 40%	X	X	X	X	X
Y brick, H brick, AL mortar, C mortar (3)	BS 80%	X	X	X	X	X
<b>Water absorption by Karsten tube (<math>2 \times 5 \times 15</math> cm samples)</b>						
Y brick, H brick, AL mortar, C mortar (3)	Untreated					X
Y brick, H brick, AL mortar, C mortar (3)	FC 40%					X
Y brick, H brick, AL mortar, C mortar (3)	BS 80%					X
<b>Water absorption by Karsten tube (<math>1 \times 2</math> m walls)</b>						
Y brick and AL mortar mock-up walls (3)	Untreated					
	FC 40%					
	BS 80%					
<b>Contact angle (<math>\gamma</math>) by dropsnake method (<math>2 \times 5 \times 15</math> cm samples)</b>						
Y brick, H brick, AL mortar, C mortar (3)	Untreated					
Y brick, H brick, AL mortar, C mortar (3)	FC 40%	X				X
Y brick, H brick, AL mortar, C mortar (3)	BS 80%	X				X
<b>Discoloration by visual inspection (<math>2 \times 5 \times 15</math> cm samples)</b>						
Y brick, H brick, AL mortar, C mortar (3)	Untreated	X				X
Y brick, H brick, AL mortar, C mortar (3)	FC 40%	X				X
Y brick, H brick, AL mortar, C mortar (3)	BS 80%	X				X

### 2.3. Hydrophobic treatment

Samples of all types were cleaned with a brush to remove dirt and dust and washed with deionized water to prevent absorption of extra salts. Then, they were stored in an oven at 55 °C, so that moisture from the intense water exposure could evaporate. When reached a stable weight (after 4–5 days), the samples were cooled down to room temperature. For impregnation with cream products the minimum recommended amount, 150–200 ml/m<sup>2</sup>, was applied with a brush [40]. Only one face (5 × 15 cm) was treated with a water repellent agent. The opposite face was left untreated, while the four smaller faces were waterproofed with epoxy resin. Finally, the samples were stored at room temperature and relative humidity for one month of curing.

### 2.4. Experimental set-up

The durability of the hydrophobic layer was characterized by the ability to repel liquid water and the ability to keep the substrate clean from dirt and possible efflorescence. Table 3 describes how the study has been conducted.

To evaluate the durability of the hydrophobic surface treatment on brick and mortar, artificial aging was conducted, according to ISO 4892–2 [42], with Atlas Ci 4000 weather-ometer, at the Danish Technological Institute, Taastrup (Fig. 1). ISO 4892 [42] is targeted at the durability of plastics but its key features (UV radiation and water spray) are in line with [29], also performing artificial weathering of hydrophobized porous building materials in Atlas weather ometer. The samples were placed in plastic holders that cover the edges (from the 75 cm<sup>2</sup> of the samples' face surface, only 57.8 cm<sup>2</sup> are exposed to water spray and UV radiation). The plastic holders were placed on a carousel, inside a climatic chamber. The samples were exposed to sprayed water and UV radiation only from the interior of the carousel. The water repellency performance is evaluated by the water absorption coefficient ( $A_{cap}$ ) of the samples, obtained via water uptake tests in accordance with [43], as described in Refs. [44,45]. The samples were placed in a plastic container with deionized water that covered less than one cm of the sample, over plastic net support, for 1-D free capillary water uptake. The mass of the sample was determined with a balance reading 0.001 g and the samples were wiped with wet paper before each measurement. Since impregnation decreases the rate of capillary water uptake, the water uptake tests for the impregnated samples lasted for 24 h and the time intervals for the measurements were: 10', 30', 1h, 1h 30', 2h, 3h, 4h, 7h, 9h, and 24h. When displaying water uptake in kg/m<sup>2</sup> towards  $\sqrt{\text{seconds}}$

does not produce a straight line but a curve of some form,  $A_{cap}$  is defined as the increase in weight ( $\Delta m$ ) in kg/m<sup>2</sup> at 24h divided by  $\sqrt{86400}$  [43].

$$A_{cap} = \frac{\Delta m}{\sqrt{86400}} \quad (1)$$

For the untreated samples, the water absorption coefficient was measured before and after artificial aging. For the treated samples, capillary water uptake tests were carried out one month after the application of the water repellent agent, during artificial aging (every two weeks), and after artificial aging. Before each measurement, the samples were dried in an oven at 55 °C and then cooled down at room temperature. Each result is an average based on three samples. The whole procedure of artificial aging consisted of 635 cycles and the water absorption coefficient measurements were carried out after 165, 335, 482, and 635 cycles. One cycle consisted of:

102 min: Lamp Xenon
Irradiance level: 0.5 W/m <sup>2</sup> at 340 nm (UV)
Back panel temperature: 63 °C
Chamber temperature: 38 °C
Relative humidity: 50%
Specimen water spray: off
Back water spray: off
18 min: Specimen water spray (deionized): 0.2 L/min, pressure: 138–344 kPa (20–30 psi)
The rest of the weathering test conditions remained the same

The 635 cycles used in the present study were selected to represent similar exposure hours to UV radiation and water spray as in De Witte [29]. There is no official equivalence of the artificial cycles to actual years.

As a first approach to translate the artificial weathering cycles to actual years, vertical Karsten tube tests were conducted on the samples after 635 cycles. The results were compared with horizontal Karsten tube tests, conducted on bricks and mortar joints (covering also a small area of brick) of mock-up walls constructed with Yellow brick and air lime mortar at the Technical University of Denmark and impregnated with FC 40% in February 2015 [37], about 6 years before the artificial aging test.

Both vertical and horizontal Karsten tube tests consist of a 30 mm diameter dome (3 cm<sup>2</sup> test area) attached to a glass tube of 10 cm head of water (15 ml volume), a pressure roughly corresponding to double the wind pressure of a hurricane. The Karsten tube is pasted onto the substrate to be tested using plasticine as a sealing material. The drop in the



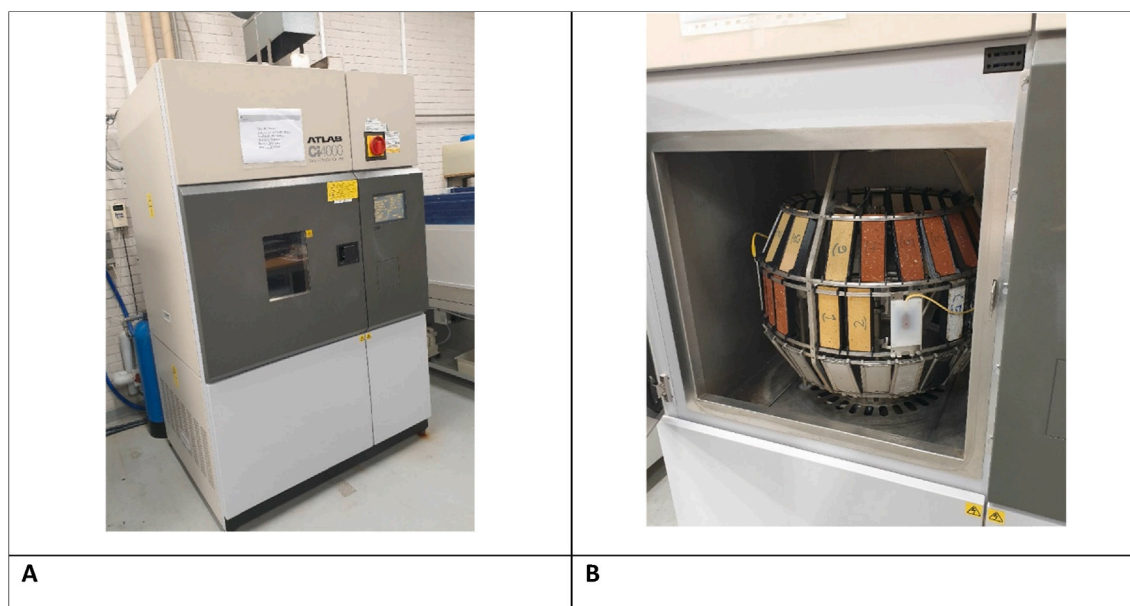


Fig. 1. Test setup for artificial aging. A) Atlas Ci4000 weather-ometer and B) test specimens on carousel sample holder inside the chamber.

water level is recorded every minute for 11 min and the water absorption in ml/min is calculated by taking the average of the last 10 measurements. The first minute is not taken into account, to avoid surface wetting to be included in the results. In order to maintain steady water pressure, the water in the tube is kept during the test by adding more water every time 1 ml of water is absorbed [46].

Contact angle measurements took place, as an indicator for the beading effect before and after artificial aging. The measurements were performed on 3  $\mu$ l (microliter) water droplets placed on the treated surface of the materials via pipette. The shape of the droplets was

recorded by a CCD camera and the resulting images were analyzed by DropSnake [47,48], a plugin for ImageJ software, similarly to Ref. [49]. The contact angles were measured immediately after the droplet fell on the surface.

The substrates of both untreated and treated samples were inspected visually for potential discoloration after the artificial aging.

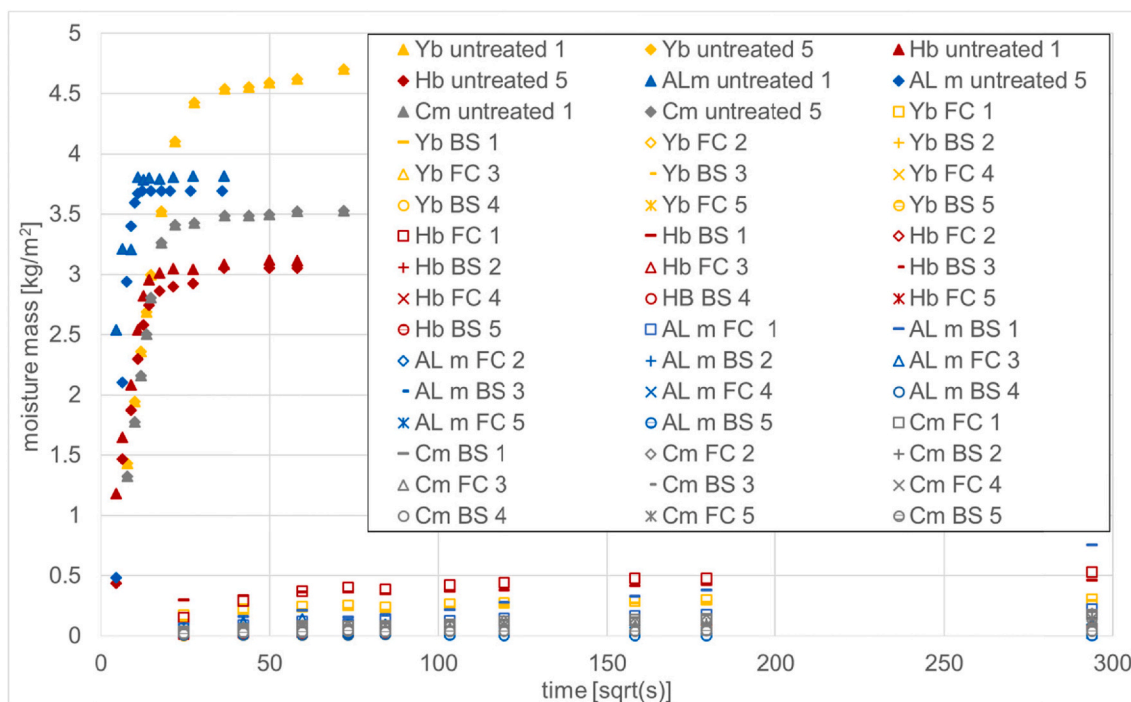
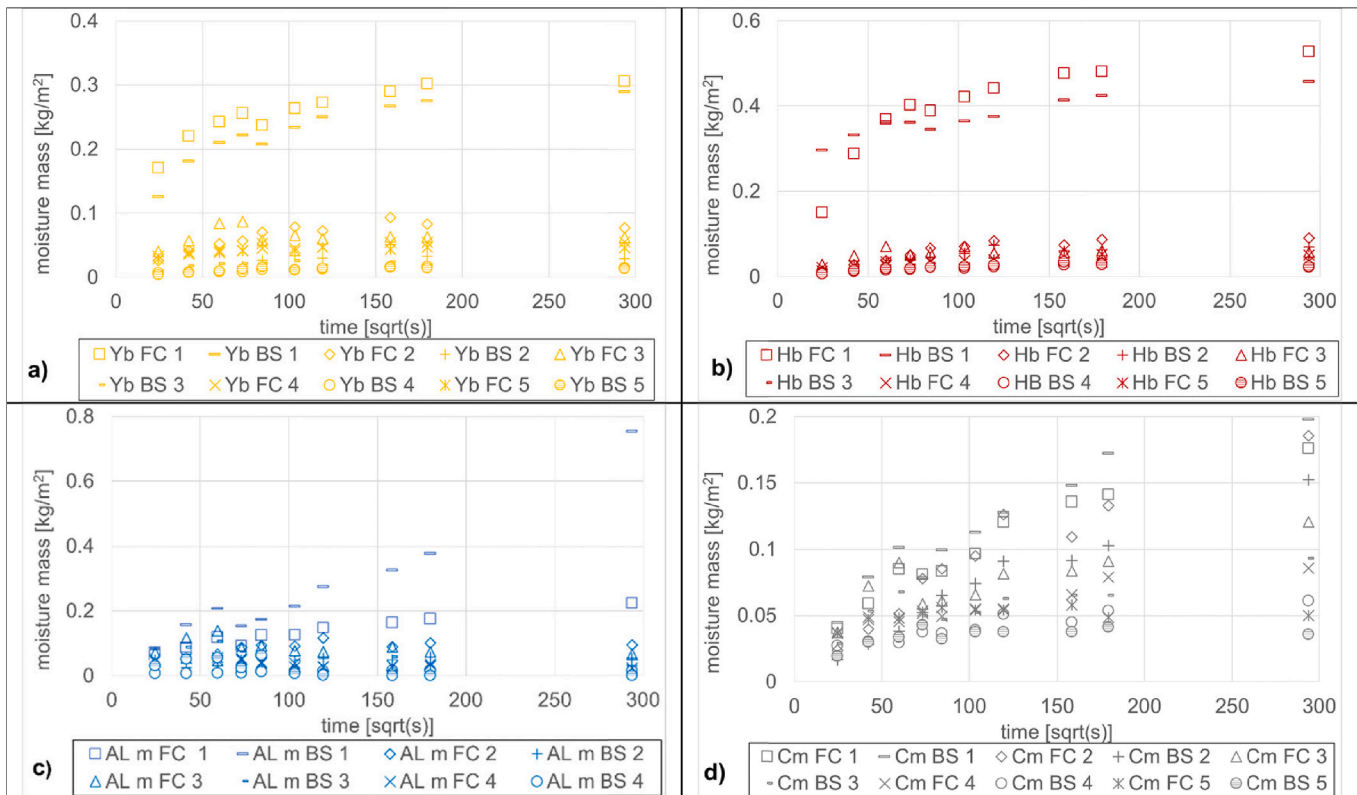
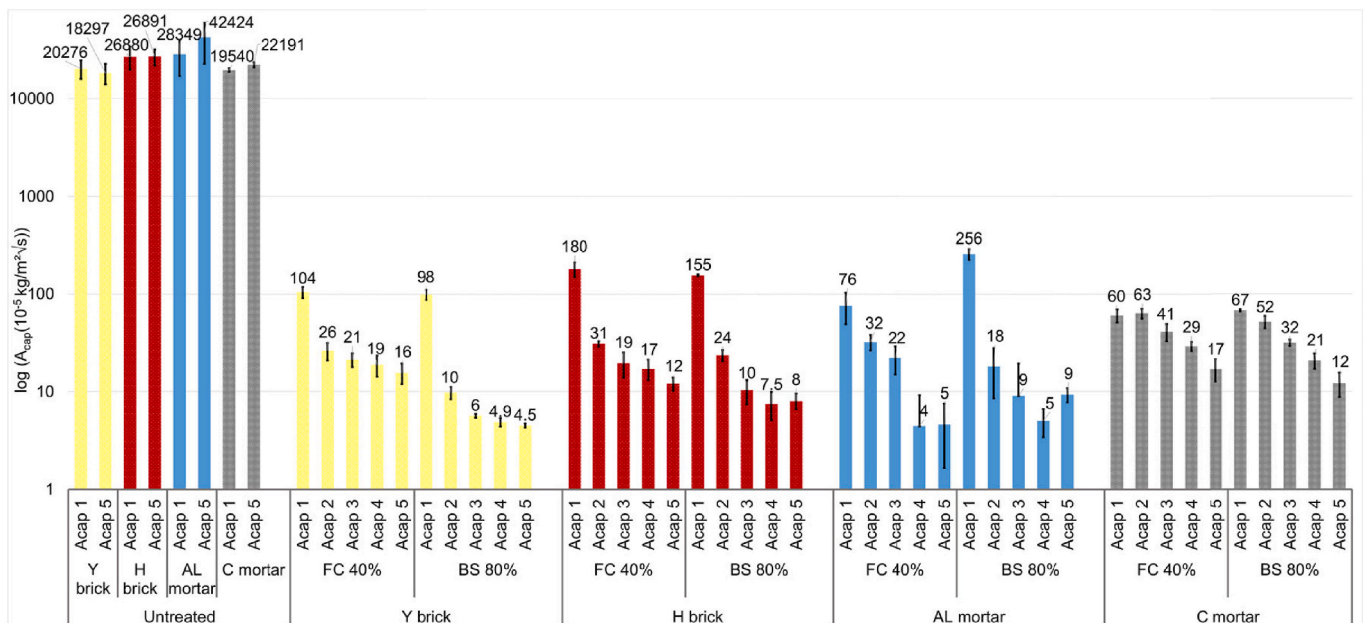


Fig. 2. Capillary water uptake of Y brick, H brick, C mortar, AL mortar, untreated and impregnated with Remmers FC cream 40% and Wacker BS cream C 80%. 1: 1st water uptake before artificial aging, 2: 2nd water uptake after 165 cycles of artificial aging, 3: 3rd water uptake test after 335 cycles of artificial aging, 4: 4th water uptake after 482 cycles of artificial aging, 5: 5th water uptake after 635 cycles of artificial aging. Each point of each curve is the average value of the respective measurements of three different samples.



**Fig. 3.** Capillary water uptake of a) Y brick, b) H brick, c) AL mortar, d) C mortar, impregnated with Remmers FC cream 40% and Wacker BS cream C 80%:1: 1st water uptake before artificial aging, 2: 2nd water uptake after 165 cycles of artificial aging, 3: 3rd water uptake test after 335 cycles of artificial aging, 4: 4th water uptake after 482 cycles of artificial aging, 5: 5th water uptake after 635 cycles of artificial aging. Each point of each curve is the average value of the respective measurements of three different samples.



**Fig. 4.** Water absorption coefficient by capillary water uptake test of Y brick, H brick, AL mortar, C mortar, untreated and impregnated with Remmers FC cream 40% and Wacker BS cream C 80%. Acap 1: absorption coefficient before artificial aging, Acap 2: after 165 cycles of artificial aging, Acap 3: after 335 cycles of artificial aging, Acap 4: after 482 cycles of artificial aging, Acap 5: after 635 cycles of artificial aging. Each result is an average based on three samples, error bars correspond to standard deviation.



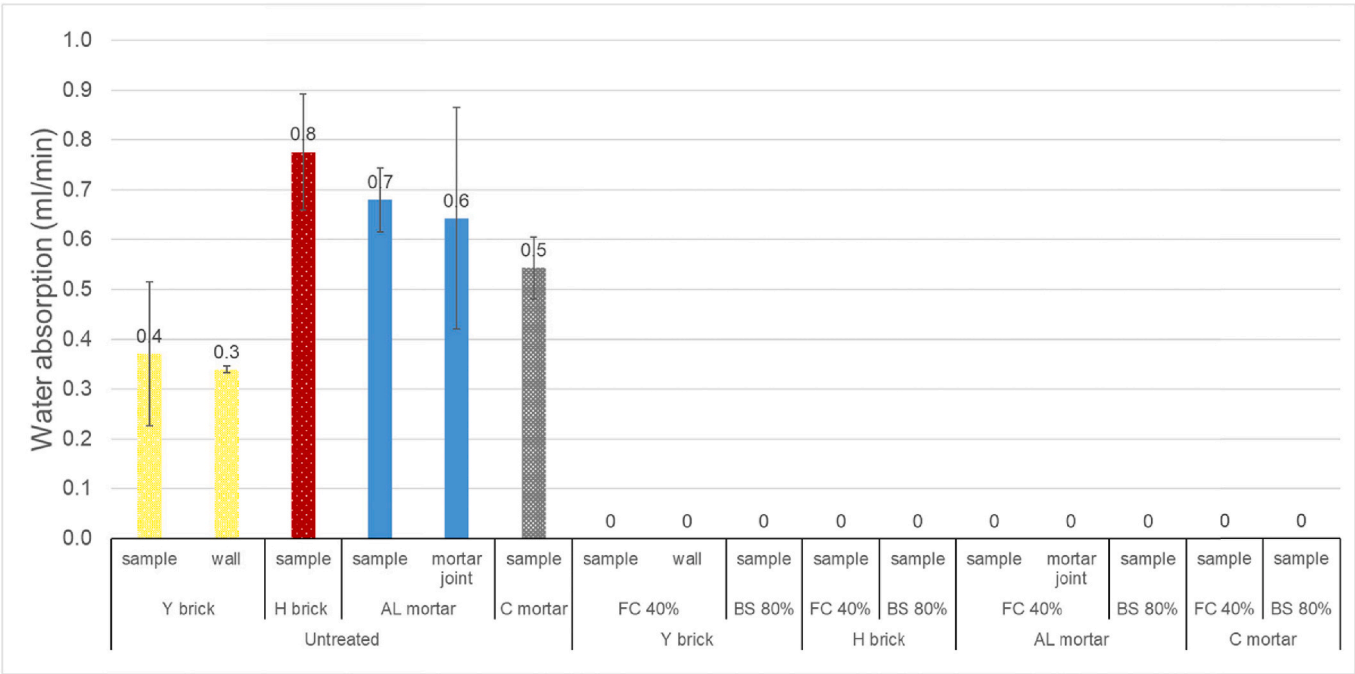


**Fig. 5.** Water absorption by Karsten tube test, Y brick, H brick, AL mortar, C mortar, and mock-up wall, untreated and impregnated with Remmers FC cream 40% and Wacker BS cream C 80%. “Sample” refers to samples from artificial aging, “wall” and “mortar joint” refer to mock-up wall measurements on brick and mortar joints respectively. Each result is an average based on three measurements, error bars correspond to standard deviation.

**3. Results**

**3.1. Capillary water uptake test before/after artificial aging**

Fig. 2 illustrate the capillary water uptake curves both of untreated and treated samples during the artificial weathering while Fig. 3 shows

only the treated samples. The water uptake curves of all the treated samples were significantly reduced compared to untreated. The moisture mass difference against sqrt(s) did not give a straight line, but could follow a curve of some form (Fig. 3).

Fig. 4 focuses on the water absorption coefficient of the different samples during the testing period. The untreated samples did not show

**Table 4**  
Water droplets in hydrophobized surfaces before and after artificial aging.

	FC 40%		BS 80%	
	Before aging	After aging	Before aging	After aging
Y Brick				
H Brick				
C Mortar				
AL mortar				

In the case of mortar samples treated with FC 40%, after aging, it was not possible to take a picture of the droplets, since they were not forming sufficient spherical droplets.

**Table 5**

Contact angle measurements before and after artificial aging.

	Y brick		H brick		C mortar		AL mortar	
	FC 40%	BS 80%	FC 40%	BS 80%	FC 40%	BS 80%	FC 40%	BS 80%
Before aging ( $\gamma^\circ$ )	130 (8)	128 (4)	124 (3)	123 (1)	130 (5)	125 (7)	132 (9)	130 (9)
After aging ( $\gamma^\circ$ )	104 (4)	111 (3)	91 (15)	121 (4)		111 (6)		109 (9)

In the case of mortar samples treated with FC 40%, after aging, it was not possible to measure the contact angle of the droplets, since it was significantly reduced. Each result is an average based on three samples. The values in () correspond to the standard deviation.

significant changes in the water uptake after 635 cycles of aging. All treated samples showed reduced water uptake after treatment, and the water uptake was further reduced during the aging period.

The absorption coefficient on the first test before aging was reduced approximately by a factor of 200 due to hydrophobization (e.g Y brick treated with FC 40%,  $A_{cap1}$ :  $0.00104 \text{ kg/m}^2\text{s}^{1/2}$  from untreated  $A_{cap}$ :  $0.2 \text{ kg/m}^2\text{s}^{1/2}$ ) and was further reduced by a factor of more than 1000 ( $A_{cap5}$ :  $0.00016 \text{ kg/m}^2\text{s}^{1/2}$ ) after aging for all the tested materials, compared to untreated. Consequently, the ability of the hydrophobization to reduce water uptake is not diminished by the performed artificial aging. The absorption coefficient seems to be positively influenced by artificial aging since it is further reduced during the process of repeated cycles.

### 3.2. Karsten tube measurements

The Karsten tube test, as an additional indicator, supported the observation that hydrophobization blocked liquid water transport even after aging in brick and mortar since the water penetrated neither samples nor brick and mortar joints of the mock-up wall hydrophobized six years ago (see Fig. 5). Also, the water absorption of untreated brick and mortar samples was similar to untreated bricks and mortar joints of the mock-up walls, as seen in Fig. 5.

### 3.3. Contact angle measurements

Contact angle measurements provide additional information for the surface behavior of the hydrophobized building materials. The level of contact angle was similar between brick and mortars but for all the materials there was a tendency of reduced contact angle after artificial aging. In the case of C mortar and AL mortar impregnated with FC 40% the contact angle after aging was significantly reduced, making the capture of the droplet image challenging (see Table 4 and Table 5).

### 3.4. Discoloration of untreated samples after aging

The exterior appearance of the treated substrates remains clear after artificial aging while the untreated samples reveal a discoloration (white stains) as shown in Table 6. The discoloration on the untreated mortar samples may not appear clearly on the pictures but it was noticeable by the naked eye.

## 4. Discussion

The present study examined the effect of accelerated weathering on untreated and hydrophobized brick and mortar samples. The results show that silicon-based water repellent agents in cream form can create a durable hydrophobic layer that maintains both its water repellency performance and its appearance through artificial aging (exposure to UV radiation and water spray) but loses its beading effect.

The absorption coefficient of the untreated samples was not significantly affected by artificial aging. For the hydrophobized samples, the absorption coefficient was negligible compared to that of the untreated, revealing more than 99% reduction for all the tested materials before, during, and after artificial aging. However, by carefully observing Fig. 4, the after-treatment water exposure and longer curing time appeared to

improve the water repellency performance of hydrophobized samples, as absorption coefficient ( $A_{cap}$ ) was further reduced, in all the tested materials, especially between first and second capillary water uptake, as also reported in Ref. [21].

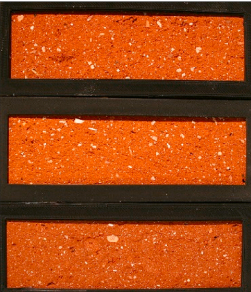
Two different types of brick, one type of air lime mortar and one type of cement mortar, all representing materials present in historic Danish buildings, illustrated the same behavior in terms of water repellency during aging resulting in very low absorption coefficients. Although air lime does not contain hydroxylated surfaces, the active ingredient was able to form irreversible bonds with the pore walls of the air lime mortar, since mortar also contains sand that has hydroxylated surfaces and thus kept the very low absorption coefficient after accelerated weathering similar to hydraulic lime mortar [21] and cement mortar (Fig. 4).

The mock-up walls were built with the same types of brick and mortar that were used as the samples that underwent artificial aging. Moreover, they were impregnated six years earlier (Feb 2015) with a water repellent agent included in the artificial aging tests (FC 40%). Both the Y brick and AL mortar samples and the Y brick and AL mortar joints illustrated zero penetration of water when tested with Karsten tube (Fig. 5). This is an indication that the artificial aging cycles corresponded to at least 6 years in real life, with the limitation that the artificial cycles do not include frost cycles.

Karsten tube tests show that the hydrophobic layer of a lime plaster facade impregnated with liquid water repellent agents can stay durable and repel liquid water even after 50 years [27]. In line with these findings, van Hees [28] reported that the effectiveness of the hydrophobic treatment, with liquid products, can last even more than 30 years after testing with Karsten tube over 60 case studies in three different countries (Netherlands, Belgium, Italy), but the effectiveness of the treatment is quite variable even within one wall. Cream-based water repellent agents became commercially available in the early 2000s [21], after [40] was published but no studies on the durability of cream-based products on brick and mortar have been reported in the literature. Fig. 5 illustrates that treatment of masonry with cream-based water repellent agents also stayed durable and repelled liquid water in a mock-up wall impregnated six years ago. The results depicted in Figs. 4 and 5 are in agreement with a test of hydrophobized brick and natural stone samples in Atlas weather-ometer [29]; their performance did not decrease with aging, although it might decrease when concentrations of water repellent agents lower than recommended were used. According to tests including freeze-thaw cycles, which neither the current paper nor [29] include, impregnated concrete maintained its effectiveness in terms of water repellency, tested with capillary water uptake, after aging [50]. However, observations regarding concrete are not necessarily valid for mortar or especially brick, since they are quite different building materials.

Capillary water uptake and Karsten tube tests illustrated that hydrophobization blocked the liquid water absorption of brick and mortar and showed the effectiveness and durability of hydrophobization after artificial aging with water spray and UV-light. The water repellent agents used in this study contain emulsifiers that allow the active ingredient to be mixed with water as a ready-to-use mixture. After the application of the water repellent agent, hydrolysis and poly condensation take place, requiring the presence of water. With these processes, the alkoxy groups (-OH) of the active ingredient molecules create irreversible bonds with the pore walls of the building material and the alkyl

**Table 6**  
Substrate appearance of Y brick, H brick, C mortar, AL mortar after 635 cycles of artificial aging.

	Untreated	FC 40%	BS 80%
Y brick			
H brick			
C mortar			
AL mortar			

Each case is represented from 3 samples placed in the sample holder as it was located during the artificial weathering experiment except the AL mortar where the untreated and the treated with BS 80% is represented by two samples.

groups (-R) provide the hydrophobic properties to the compound. Wind driven rain will then “wash off” the emulsifiers and the active ingredient forms new bonds with the pore walls of the building material making the hydrophobic layer stronger, reducing the  $A_{cap}$  further and inducing redistribution of the active ingredient deeper inside the material. Complementary to that, water coming from rain, or as a by-product of condensation reaction, acts as a reactant in the first part of polymerization (hydrolysis) [51]. Over time, this effect becomes less noticeable, since there is less active ingredient to form new bonds with the pore walls of the building material [21].

However, the four tested substrates showed a tendency of contact angle reduction after artificial aging that caused a declined beading effect (droplet formation on the facade during rain events). The contact angle reduction was more obvious to the cream with a lower concentration (40%) (Tables 4 and 5). The sample holders covered the edges of

the samples (4.5 mm thickness). In this area, which was not exposed to UV radiation, the contact angle was not reduced after artificial aging in any sample. Since the whole surface of the samples was exposed five times to water uptake for 24 h, there was an indication that the exposure to UV radiation and not the exposure to water was responsible for the reduction of the beading effect after aging.

UV radiation, due to its high energy, can cause the formation of free radicals (i.e. molecules with an excess of electrons), which can cause degradation on polymeric surfaces [52]. The hydrophobic effect can be broken down by UV radiation, as manifested by the gradual decrease of the contact angle on the substrate (reduced beading effect). In concrete, UV light has been reported to break the Si–O–Si bonds between hydrophobic molecules and the substrate [50]. However, this only occurs in the outermost layer of the substrate, since UV light cannot penetrate deeper in the material [53]. UV radiation was not critical in terms of



water absorption performance, because the Si–O–Si bonds remained intact in the subsurface [50] of brick and mortar, and liquid water did not penetrate into the materials (see Figs. 4 and 5). After aging, the exterior surface of the substrate may lose its hydrophobicity, although the inner layers of the building material keep their hydrophobic properties. Complementary to the current study, spectroscopic and microscopic techniques could be performed in order to investigate further the influence of UV radiation to the hydrophobic treatment.

The beading effect is not necessarily an indicator of good hydrophobic treatment and is not always desirable for the building owner, who wants to maintain the exact appearance and visual behavior of the facade (personal communication with Corne van Hamont, Wacker's representative). However, the beading effect could last longer by applying a higher percentage of siloxane [21] and higher concentrations of the active ingredient (see Table 5).

Artificial aging revealed that hydrophobization acts positively in retaining the exterior appearance of the samples since contrary to treated samples, all the untreated samples revealed white stains (efflorescence) after artificial aging (see Table 4). The migration of salts to the exterior surface is due to salts present inside the materials since the samples were sprayed with deionized water during the artificial aging. Efflorescence should be avoided as it is an aesthetic problem that harms the prestige of the building [30].

Mortar joints are regarded as the weak point of a masonry facade [28], however, they are not easy to characterize with a Karsten tube test. During Karsten tube tests on the mock-up wall (Fig. 5) it was challenging to adjust the glass tube on the mortar joints without having leakages. Especially, in buildings with concave mortar joints, it would be very difficult to test the water uptake with the Karsten tube test. Karsten tube is an accurate method for testing water uptake on bricks but it is more difficult to give accurate results on mortar joints [54]. Additional in-situ measurement equipment, not available for this study, covers wider wall areas [55]. However, the impregnation depth is reported to be lower in mortar samples and mortar joints than in bricks [21,28], and the possibility of cracks after treatment is higher in mortar joints, as well as in the interface between bricks and mortar joints. Moreover, brick absorbs the water repellent agent much faster than mortar [21]. During the application process of the cream products, a percentage of the cream placed in the mortar joints would be absorbed by the brick, leaving less active ingredient for the mortar joints. Furthermore, since the beading effect is reduced due to UV radiation exposure, the water is being absorbed into the first mm of the substrate and during winter this water may freeze, expanding its volume and induce spalling. If this continues to occur and mortar joints start to crumble, cracks may reach untreated areas after years. This could also happen to brick although less possible as the impregnation depth is larger [21]. These observations indicate that mortar joints should be studied further.

The impregnation depth could be increased by applying a higher amount of water repellent agent than recommended and by increasing the concentration of the active ingredient [21]. However, longer curing time and after-treatment water exposure are needed to reveal an improved performance cf. Fig. 4 and [21]. For that reason, the hydrophobic performance of a hydrophobized wall is expected to improve with longer curing time and rain exposure in a period of months after the treatment. Moreover, the water repellency performance should be tested occasionally since re-treatment of substrates is possible [50].

It has been found that the storage properties and the vapor permeability of brick and mortar samples do not significantly change after hydrophobization, although the drying rate of the hydrophobized material is significantly lowered due to the reduced liquid transfer [21,22,56]. The impregnation depth is higher in brick than in mortar and the redistribution of the active ingredient creates a first strong hydrophobic layer and a second area that is partially hydrophobized. The active ingredient continues to spread for many months after treatment increasing the partially hydrophobized area, positively influenced by the after-treatment water exposure [21]. As long as impregnation depth

increases, the drying speed of the masonry decreases. For how long the active ingredient could spread inside the material and whether after-treatment water exposure continues to influence the impregnation depth should be addressed in future work.

Material properties are very important in determining the input parameters of hygrothermal simulations, which can be very helpful in the decision-making process to renovate and design a building [57–61]. Hydrophobization is proven to significantly reduce the absorption coefficient of both brick and mortar [21,22,62]. Moreover, hygrothermal simulations using experimental results to imitate the hydrophobic layer illustrate that hydrophobization is the missing element for a moisture-safe energy renovation of internally insulated masonry walls, regardless of the insulation system [10]. But for the hygrothermal simulations to be proven true, the hydrophobic layer should be durable through aging; the absorption coefficient of both brick and mortar should stay at low levels. The fact that absorption coefficient remained at very low levels after artificial aging both in brick and mortar (Fig. 4), in combination with no water-penetration both in the artificially aged samples and the six-year-old hydrophobized mock-up walls (Fig. 5), builds more confidence in the results of the hygrothermal simulations [10]. These results indicate that an internally insulated hydrophobized wall could provide a moisture safe construction. However, high moisture loads from the interior of the building could still be a risk for the wall even when hydrophobization eliminated the wind-driven rain load.

There were two main limitations in this study: firstly, in a wall of a building, there is the interaction between brick and mortar during the contraction/expansion of the materials, or other factors that may induce cracks after treatment, a scenario that is not taken into consideration when performing durability tests on brick and mortar separately. The second limitation is that during the artificial aging the temperature remains constant at 38 °C inside the cabinet and the samples were not exposed to low temperatures in order to investigate the risk of frost damage which may give too optimistic outcome in this study. Moreover, the retrofit of internal insulation increases the frost damage risk [63], thus making the risk of frost damage a very important aspect to be tested.

The current findings have important implications for practitioners and policymakers since the hygrothermal benefits of the combined effect of hydrophobization and internal insulation [10,18,64] can be obtained only if hydrophobization maintains its water repellency performance through aging which needs further studies involving exposure to frost to be fully revealed.

## 5. Conclusions and perspectives

In this paper, the durability of the hydrophobic layer in brick and mortar samples was experimentally studied. The water repellent agents were proven to successfully block capillary effects while avoiding efflorescence at the treated substrate during the process of artificial aging. Karsten tube tests revealed zero water penetration both on hydrophobized samples from artificial aging and on hydrophobized mock-up walls. Moreover, UV radiation was found responsible for the declined beading effect while the after-treatment water exposure seems to influence the water repellency of the treated samples in a positive way since the absorption coefficient is further reduced throughout the procedure of accelerated aging, for all the tested building materials.

Future studies could reveal the frost damage risk in hydrophobized samples compared to untreated. Moreover, future research would benefit from focusing on Karsten tube tests in buildings hydrophobized years ago. Further investigation should include more types of building materials like natural stone and concrete. The results of the current paper and [10] could be used as input in a life cycle cost assessment of hydrophobization in combination with internal insulation which could contribute to a holistic view of hydrophobization.

## Declaration of competing interest

The authors declare that they have no known competing financial interests or personal relationships that could have appeared to influence the work reported in this paper.

## Acknowledgements

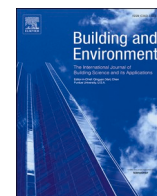
The present study is the third journal paper after [10,21] in a series of papers reviewing hydrophobization treatment at BUILD, the Department of the Built Environment, Aalborg University Copenhagen. The study is part of the project 'Moisture safe energy renovation of worth preserving external masonry walls' funded by the Danish foundations: The Landowners' Investment Foundation, The National Building Fund, and Realdania. The authors express sincere thanks to Leif Christiansen (Wewers) for providing the mortars, to Thomas Lenart Svensson (Danish Technological Institute) for cutting the brick samples, to Bravo Miguel (Syntix) for designing and manufacturing with 3D printing the molds for the samples and to Lasse Borgstrøm Eriksen (BUILD) for transporting the samples. We would also like to offer our thanks to Philip Møller (previously Introfex-Remmers), Corne van Hamont (Wacker), and Susanna Stubb-Eliasson (Wacker) for providing water repellent agents.

## References

- [1] M. Morelli, M. Harrestrup, S. Svendsen, Method for a component-based economic optimisation in design of whole building renovation versus demolishing and rebuilding, *Energy Pol.* 65 (2014) 305–314, <https://doi.org/10.1016/j.enpol.2013.09.068>.
- [2] M. Morelli, M.A. Lacasse, A systematic methodology for design of retrofit actions with longevity, *J. Build. Phys.* 42 (2019) 585–604, <https://doi.org/10.1177/1744259118780133>.
- [3] C.A. Balaras, A.G. Gaglia, E. Georgopoulou, S. Mirasgedis, Y. Sarafidis, D.P. Lalas, European residential buildings and empirical assessment of the Hellenic building stock, energy consumption, emissions and potential energy savings, *Build. Environ.* 42 (2007) 1298–1314, <https://doi.org/10.1016/j.buildenv.2005.11.001>.
- [4] M. Jerman, I. Palomar, V. Koci, R. Cerný, Thermal and hygric properties of biomaterials suitable for interior thermal insulation systems in historical and traditional buildings, *Build. Environ.* 154 (2019) 81–88, <https://doi.org/10.1016/j.buildenv.2019.03.020>.
- [5] E. Vereecken, S. Roels, Wooden beam ends in combination with interior insulation: an experimental study on the impact of convective moisture transport, *Build. Environ.* 148 (2019) 524–534, <https://doi.org/10.1016/j.buildenv.2018.10.060>.
- [6] H. Tommerup, S. Svendsen, Energy savings in Danish residential building stock, *Energy Build.* 38 (2006) 618–626, <https://doi.org/10.1016/j.enbuild.2005.08.017>.
- [7] T. Odgaard, S.P. Bjarlov, C. Rode, Interior insulation – experimental investigation of hygrothermal conditions and damage evaluation of solid masonry façades in a listed building, *Build. Environ.* 129 (2018) 1–14, <https://doi.org/10.1016/j.buildenv.2017.11.015>.
- [8] M. Morelli, E.B. Møller, Energy savings and risk of mold growth in apartments renovated with internal insulation, *Sci. Technol. Built Environ.* 25 (2019) 1199–1211, <https://doi.org/10.1080/23744731.2019.1629241>.
- [9] M. Guizzardi, D. Derome, R. Vonbank, J. Carmeliet, Hygrothermal behavior of a massive wall with interior insulation during wetting, *Build. Environ.* 89 (2015) 59–71, <https://doi.org/10.1016/j.buildenv.2015.01.034>.
- [10] V. Soulios, E.J. de Place Hansen, R. Peuhkuri, Hygrothermal performance of hydrophobized and internally insulated masonry walls - simulating the impact of hydrophobization based on experimental results, *Build. Environ.* 187 (2021) 107410, <https://doi.org/10.1016/j.buildenv.2020.107410>.
- [11] E. Vereecken, S. Roels, A comparison of the hygric performance of interior insulation systems: a hot box-cold box experiment, *Energy Build.* 80 (2014) 37–44, <https://doi.org/10.1016/j.enbuild.2014.04.033>.
- [12] E. Vereecken, L. Van Gelder, H. Janssen, S. Roels, Interior insulation for wall retrofitting - a probabilistic analysis of energy savings and hygrothermal risks, *Energy Build.* 89 (2015) 231–244, <https://doi.org/10.1016/j.enbuild.2014.12.031>.
- [13] X. Zhou, D. Derome, J. Carmeliet, Hygrothermal modeling and evaluation of freeze-thaw damage risk of masonry walls retrofitted with internal insulation, *Build. Environ.* 125 (2017) 285–298, <https://doi.org/10.1016/j.buildenv.2017.08.001>.
- [14] M. Morelli, S. Svendsen, Investigation of interior post-insulated masonry walls with wooden beam ends, *J. Build. Phys.* 36 (2013) 265–273, <https://doi.org/10.1177/1744259112447928>.
- [15] H. Janssen, B. Blocken, S. Roels, J. Carmeliet, Wind-driven rain as a boundary condition for HAM simulations: analysis of simplified modelling approaches, *Build. Environ.* 42 (2007) 1555–1567, <https://doi.org/10.1016/j.buildenv.2006.10.001>.
- [16] A. Nielsen, E.B. Møller, T.V. Rasmussen, E.J. de Place Hansen, Use of sensitivity analysis to evaluate hygrothermal conditions in solid brick walls with interior insulation, in: 5th Int. Build. Phys. Conf., 2012, pp. 377–384, [http://vbn.aau.dk/ws/files/72605823/Use\\_of\\_sensitivity\\_analysis\\_to\\_evaluate\\_hygrothermal\\_conditions\\_in\\_solid\\_brick\\_walls\\_with\\_interior\\_insulation.pdf](http://vbn.aau.dk/ws/files/72605823/Use_of_sensitivity_analysis_to_evaluate_hygrothermal_conditions_in_solid_brick_walls_with_interior_insulation.pdf).
- [17] E. Vereecken, S. Roels, Wooden beam ends in combination with interior insulation: an experimental study on the impact of convective moisture transport, *Build. Environ.* 148 (2019) 524–534, <https://doi.org/10.1016/j.buildenv.2018.10.060>.
- [18] V. Soulios, E.J. de Place Hansen, R. Peuhkuri, Hygrothermal simulation assessment of internal insulation systems for retrofitting a historic Danish building, *MATEC Web Conf* 282 (2019), 02049, <https://doi.org/10.1051/mateconf/201928202049>.
- [19] V. Metavitsiadis, V. Soulios, H. Janssen, S. Roels, Wall hydrophobization and internal insulation: the impact of impregnation strength and depth on moisture levels and moisture damages, in: *Hydrophobe III*, 2017, pp. 69–76, <http://www.hydrophobe.org/pdf/hongkong/C-1-1.pdf>. (Accessed 26 April 2020).
- [20] Z. Pavlík, M. Jirícková, J. Pavlík, R. Cerný, Interior thermal insulation system based on hydrophilic mineral wool, *J. Therm. Envelope Build. Sci.* 29 (2005) 21–35, <https://doi.org/10.1177/1744259105051795>.
- [21] V. Soulios, E.J. de Place Hansen, C. Feng, H. Janssen, Hygric behavior of hydrophobized brick and mortar samples, *Build. Environ.* 176 (2020) 106843, <https://doi.org/10.1016/j.buildenv.2020.106843>.
- [22] V. Soulios, E.J. de Place Hansen, H. Janssen, Hygric properties of hydrophobized building materials, *MATEC Web Conf* 282 (2019), 02048, <https://doi.org/10.1051/mateconf/201928202048>.
- [23] J. Engel, P. Heinze, R. Plagge, Adapting hydrophobizing impregnation agents to the object, *Hydrophobe VII* 7th Int. Conf. Water Repel. Treat. Prot. Surf. Technol. Build. Mater. 20 (2014) 141–150, <https://doi.org/10.12900/rbm14.20.6-0042>.
- [24] J. Carmeliet, G. Houvenaghel, J. Van Schijndel, S. Roels, Moisture phenomena in hydrophobic porous building material Part 1: measurements and physical interpretations/Wechselwirkung hydrophobierter poröser Werkstoffe des Bauwesens mit Feuchtigkeit, Teil 1: messungen und physikalische Interpretationen, *Restor. Build. Monum.* 8 (2002) 165–183, <https://doi.org/10.1515/rbm-2002-5660>.
- [25] E. Vereecken, S. Roels, H. Janssen, Inverse hygric property determination based on dynamic measurements and swarm-intelligence optimisers, *Build. Environ.* 131 (2018) 184–196, <https://doi.org/10.1016/j.buildenv.2017.12.030>.
- [26] J. Langmans, R. Klein, S. Roels, Hygrothermal risks of using exterior air barrier systems for highly insulated light weight walls: a laboratory investigation, *Build. Environ.* 56 (2012) 192–202, <https://doi.org/10.1016/j.buildenv.2012.03.007>.
- [27] A.G. Wacker Chemie, *Hydrophobic Impregnation with Silres BS*, 2014, pp. 1–22.
- [28] R.P.J. van Hees, The performance of surface treatments for the conservation of historic brick masonry, *Compat. Mater. Prot. Eur. Cult. Herit* 2 (1998) 279–287.
- [29] E. de Witte, H. De Clercq, R. De Bruyn, A. Pien, Systematic testing of water repellent agents, *Restor. Build. Monum.* 2 (1996) 133–144, <https://doi.org/10.1515/rbm-1996-5093>.
- [30] H. Brocken, T.G. Nijland, White efflorescence on brick masonry and concrete masonry blocks, with special emphasis on sulfate efflorescence on concrete blocks, *Construct. Build. Mater.* 18 (2004) 315–323, <https://doi.org/10.1016/j.conbuildmat.2004.02.004>.
- [31] J. Chwast, J. Todorović, H. Janssen, J. Elsen, Gypsum efflorescence on clay brick masonry: field survey and literature study, *Construct. Build. Mater.* 85 (2015) 57–64, <https://doi.org/10.1016/j.conbuildmat.2015.02.094>.
- [32] B.O. Brandt, T. Van, B. Grell, K.K. Hansen, S.B. Hansen, *Imprægneringsmidlers Indvirkning På Betons Holdbarhed: Del 2: Undersøgelse Af Effekten Af Imprægnering På Kloridindtrængning I Beton Udsat for Varierende Kloridbelastning*, 2018.
- [33] E.B. Møller, C. Rode, Hygrothermal performance and soiling of exterior building surfaces, Technical University of Denmark, 2004. <https://orbit.dtu.dk/files/5285541/byg-r068.pdf>.
- [34] T.K. Hansen, S.P. Bjarlov, R.H. Peuhkuri, K.K. Hansen, Performance of hydrophobized historic solid masonry – experimental approach, *Construct. Build. Mater.* 188 (2018) 695–708, <https://doi.org/10.1016/j.conbuildmat.2018.08.145>.
- [35] T. Odgaard, S.P. Bjarlov, C. Rode, Influence of hydrophobation and deliberate thermal bridge on hygrothermal conditions of internally insulated historic solid masonry walls with built-in wood, *Energy Build.* 173 (2018) 530–546, <https://doi.org/10.1016/j.enbuild.2018.05.053>.
- [36] N.F. Jensen, T.R. Odgaard, S.P. Bjarlov, B. Andersen, C. Rode, E.B. Møller, Hygrothermal assessment of diffusion open insulation systems for interior retrofitting of solid masonry walls, *Build. Environ.* 182 (2020) 107011, <https://doi.org/10.1016/j.buildenv.2020.107011>.
- [37] N. Feldt Jensen, S.P. Bjarlov, C. Rode, E.B. Møller, Hygrothermal assessment of four insulation systems for interior retrofitting of solid masonry walls through calibrated numerical simulations, *Build. Environ.* 180 (2020) 107031, <https://doi.org/10.1016/j.buildenv.2020.107031>.
- [38] R. Stenholt-Jacobsen, M.T. Houen, T.L. Christiansen, *Air Lime Mortars. Slaking Methods, Workability & Strength Development*, Technical University of Denmark, 2019.
- [39] Ö. Cizer, K. Van Balen, J. Elsen, D. Van Gemert, Real-time investigation of reaction rate and mineral phase modifications of lime carbonation, *Construct. Build. Mater.* 35 (2012) 741–751, <https://doi.org/10.1016/j.conbuildmat.2012.04.036>.
- [40] A.G. Remmers, F.C. Funcosil, Technical data sheet, 1–3, [https://www.introflex.dk/images/pdf/DK\\_0711\\_-\\_08\\_13.pdf](https://www.introflex.dk/images/pdf/DK_0711_-_08_13.pdf), 2016.
- [41] Wacker Chemie AG, Silres® bs creme c, Technical data sheet, 4–7, <https://www.wacker.com/h/en-us/medias/SILRES-BS-CREME-C-en-2020.07.01.pdf>, 2020.

- [42] Iso 4892-2:2013, Plastics — Methods of Exposure to Laboratory Light Sources — Part 2: Xenon-Arc Lamps, 2013, p. 13.
- [43] Iso 15148 : 2002, Hygrothermal Performance of Building Materials and Products Determination of Water Absorption Coefficient by Partial Immersion, English Version of DIN EN ISO 15148, 2003, pp. 1–14.
- [44] C. Feng, H. Janssen, Y. Feng, Q. Meng, Hygric properties of porous building materials: analysis of measurement repeatability and reproducibility, *Build. Environ.* 85 (2015) 160–172, <https://doi.org/10.1016/j.buildenv.2014.11.036>.
- [45] C. Feng, H. Janssen, Hygric properties of porous building materials (III): impact factors and data processing methods of the capillary absorption test, *Build. Environ.* 134 (2018) 21–34, <https://doi.org/10.1016/j.buildenv.2018.02.038>.
- [46] TQC, Karsten tube penetration test II7500, manual, 1–4, <https://mk0tqcsheendm9hfmd0.kinstacdn.com/wp-content/uploads/2016/05/karsten-tube-penetration-test-ii7500-m44.pdf>, 2020.
- [47] A.F. Stalder, T. Melchior, M. Müller, D. Sage, T. Blu, M. Unser, Low-bond axisymmetric drop shape analysis for surface tension and contact angle measurements of sessile drops, *Colloids Surfaces A Physicochem. Eng. Asp.* 364 (2010) 72–81, <https://doi.org/10.1016/j.colsurfa.2010.04.040>.
- [48] A.F. Stalder, G. Kulik, D. Sage, L. Barbieri, P. Hoffmann, A snake-based approach to accurate determination of both contact points and contact angles, *Colloids Surfaces A Physicochem. Eng. Asp.* 286 (2006) 92–103, <https://doi.org/10.1016/j.colsurfa.2006.03.008>.
- [49] M. Rahimi, P. Fojan, L. Gurevich, A. Afshari, Effects of aluminium surface morphology and chemical modification on wettability, *Appl. Surf. Sci.* 296 (2014) 124–132, <https://doi.org/10.1016/j.apsusc.2014.01.059>.
- [50] L. Courard, V. Lucquiaud, O. Gérard, M. Handy, F. Michel, Evaluation of the durability of hydrophobic treatments on concrete architectural heritage, in: *Hydrophobe VII*, 2014, pp. 29–38. [http://www.hydrophobe.org/pdf/lisboa/VII\\_03.pdf](http://www.hydrophobe.org/pdf/lisboa/VII_03.pdf).
- [51] A.E. Charola, Water-repellent treatments for building stones: a practical overview, *APT Bull. J. Preserv. Technol.* 26 (1995) 10–17, <https://doi.org/10.2307/1504480>.
- [52] R. Asmatulu, G.A. Mahmud, C. Hille, H.E. Misak, Effects of UV degradation on surface hydrophobicity, crack, and thickness of MWCNT-based nanocomposite coatings, *Prog. Org. Coating* 72 (2011) 553–561, <https://doi.org/10.1016/j.porgcoat.2011.06.015>.
- [53] I.J. De Vries, Hydrophobic treatment, *Construct. Build. Mater.* 11 (1997) 259–265. <https://pdf.sciencedirectassets.com/271475/1-s2.0-S0950061800X00207/1-s2.0-S0950061897000469/main.pdf?X-Amz-Security-Token=IQoJb3JpZ2luX2VjEBQACXVzLWVhc3QtMSJHMEUcIARwT9f9%2B%2F4uPdWTTbOmg1eV6XRFxUtnG8%2FzFyEcre0AiEAg7sLvd7Qk7XT7eGJ2ow1dtVV%2B0TguOBEf45L>.
- [54] P. Freudenberg, Monitoring data basis of European case studies for sound performance evaluation of internal insulation systems under different realistic boundary conditions RIBuild D3.2. [https://static1.squarespace.com/static/5e8c2889b5462512e400d1e2/t/5e9db87943530a16d2f414eb/1587394701972/RIBuild\\_D3.2\\_v1.0.pdf](https://static1.squarespace.com/static/5e8c2889b5462512e400d1e2/t/5e9db87943530a16d2f414eb/1587394701972/RIBuild_D3.2_v1.0.pdf), 2019.
- [55] E.B. Møller, Report on the material properties RIBuild D2.1. [https://static1.squarespace.com/static/5e8c2889b5462512e400d1e2/t/5e9db81f43530a16d2f3fecf/1587394609561/RIBuild\\_D2.1\\_v1.0.pdf](https://static1.squarespace.com/static/5e8c2889b5462512e400d1e2/t/5e9db81f43530a16d2f3fecf/1587394609561/RIBuild_D2.1_v1.0.pdf), 2018.
- [56] C. Feng, H. Janssen, Impact of water repellent agent concentration on the effect of hydrophobization on building materials, *J. Build. Eng.* 39 (2021) 102284, <https://doi.org/10.1016/j.jobbe.2021.102284>.
- [57] C. Feng, A.S. Guimarães, N. Ramos, L. Sun, D. Gawin, P. Konca, C. Hall, J. Zhao, H. Hirsch, J. Grunewald, M. Fredriksson, K.K. Hansen, Z. Pavlík, A. Hamilton, H. Janssen, Hygric properties of porous building materials (VI): a round robin campaign, *Build. Environ.* 185 (2020), <https://doi.org/10.1016/j.buildenv.2020.107242>.
- [58] X. Zhou, J. Carmeliet, D. Derome, Influence of envelope properties on interior insulation solutions for masonry walls, *Build. Environ.* 135 (2018) 246–256, <https://doi.org/10.1016/j.buildenv.2018.02.047>.
- [59] C. Feng, S. Roels, H. Janssen, Towards a more representative assessment of frost damage to porous building materials, *Build. Environ.* 164 (2019) 106343, <https://doi.org/10.1016/j.buildenv.2019.106343>.
- [60] L. Shi, H. Zhang, Z. Li, X. Man, Y. Wu, C. Zheng, J. Liu, Analysis of moisture buffering effect of straw-based board in civil defence shelters by field measurements and numerical simulations, *Build. Environ.* 143 (2018) 366–377, <https://doi.org/10.1016/j.buildenv.2018.07.018>.
- [61] L. Havinga, H. Schellen, Applying internal insulation in post-war prefabricated housing: understanding and mitigating the hygrothermal risks, *Build. Environ.* 144 (2018) 631–647, <https://doi.org/10.1016/j.buildenv.2018.08.035>.
- [62] Y.D. Aktas, H. Zhu, D. D'Ayala, C. Weeks, Impact of surface waterproofing on the performance of brick masonry through the moisture exposure life-cycle, *Build. Environ.* 197 (2021) 107844, <https://doi.org/10.1016/j.buildenv.2021.107844>.
- [63] P. Johansson, L. Lång, C.-M. Capener, E.B. Møller, E. Quagliarini, M. D'orazio, A. Gianangeli, H. Janssen, C. Feng, J. Langmans, N.F. Jensen, E.J. de Place Hansen, R. Peuhkuri, T.K. Hansen, Threshold values for failure, linked to types of building structures and failure modes RIBuild, AAU, 2019. [https://www.ribuild.eu/sites/default/files/media/RIBuild\\_D2.2\\_v1.0\\_1.pdf](https://www.ribuild.eu/sites/default/files/media/RIBuild_D2.2_v1.0_1.pdf).
- [64] E.J. de Place Hansen, T.K. Hansen, V. Soulios, Deep renovation of an old single-family house including application of a water repellent agent – a case story, in: *IOP Conf. Ser. Earth Environ. Sci.*, 2021, pp. 1–9. [https://vbn.aau.dk/files/411162525/427\\_EJdePlaceHansen\\_Deep\\_renovation\\_of\\_an\\_old\\_single\\_family\\_house.pdf](https://vbn.aau.dk/files/411162525/427_EJdePlaceHansen_Deep_renovation_of_an_old_single_family_house.pdf).





# Hygrothermal performance of hydrophobized and internally insulated masonry walls - Simulating the impact of hydrophobization based on experimental results

Vasilis Soulios<sup>\*</sup>, Ernst Jan de Place Hansen, Ruut Peuhkuri

Department of the Built Environment, Aalborg University, Denmark

## ABSTRACT

Buildings are accountable for around 40% of the European energy consumption. Installing thermal insulation is an effective approach to improve the energy efficiency of the building envelope. Internal insulation is often the only renovation option in the case of historic buildings with worth-preserving masonry façades. However, it can lead to several moisture problems related to the rain load, such as mould growth, wood rot and frost damage. Hydrophobizing the façade reduces water absorption by the materials, while decreasing their drying rate, threatening the desired outcome. The paper evaluates the impact of hydrophobization when combined with internal insulation. To understand the hygrothermal effect of hydrophobization on internally insulated walls, it is important to examine how the hydrophobic layer of the masonry can be accurately modeled and how the hygrothermal response of the wall configuration changes after treatment. A significant increase in the thermal conductivity of capillary saturated samples compared to dry samples was experimentally measured. The hydrophobic model is able to predict the hygrothermal behavior of the hydrophobized brick, using experimental results from water uptake and drying tests as reference, as well as in the component level, using as reference relative humidity and temperature measurements in a mock-up wall. The current results indicate that hydrophobization contributes positively towards a moisture-safe construction with reduced heat losses when applied before or in parallel with internal insulation. These findings confirm that hydrophobization can successfully be combined either with a capillary-active or a water-vapor-tight internal insulation system, providing a moisture-safe energy renovation of building enclosures.

## 1. Introduction

In the EU Member states, the building stock accounts for about 40% of the total energy consumption [1], and 10–40% of the building stock in each country consists of historic buildings (constructed before 1950) [2]. Denmark among other countries is targeting towards the sustainable energy-independent city of tomorrow where the maintenance of cultural heritage is of primary importance, requiring a renovation of the building enclosure. Historic buildings are responsible for a sizable fraction of the energy consumption by the built environment, as they typically lack thermal insulation. Approximately 33% of total heat loss in poorly insulated buildings is contributed to external walls [3]. Often such buildings have worth preserving facades making internal insulation the only feasible technique [4].

However, internal insulation significantly modifies the hygrothermal performance of the façade, yielding in moisture-related problems like frost damage, wooden beam decay, interstitial condensation, and mould growth [5,6]. In cold periods of the year, the temperature of the original structure becoming lower due to applying internal insulation makes the construction more vulnerable to moisture loads from inside. Preventing

access of humid indoor air in the interface between the original wall and the internal insulation is one of the key challenges in ensuring moisture safe solutions. However, the moisture load from outside, and especially absorption of the wind-driven rain, add to the harmful impacts of moisture on internally insulated walls [7,8]. Hydrophobization of the exterior surface may have a potential to be the unique missing element for a sustainable moisture-safe energy renovation of historic buildings since it minimizes the water absorption by the façade materials [9–11].

To be able to design and assess the effect of hydrophobization on the hygrothermal behavior of internally insulated facades, the hydrophobic layer of the façade must be modeled in a realistic way. A few attempts have been made to include the effect of hydrophobization in numerical hygrothermal simulation models: by modeling the simulation of the hydrophobic layer as a water-tight surface with an additional surface diffusion resistance of 0.2 m [12], by reducing the absorption of wind-driven rain to 1% [13] or by neglecting the wind-driven rain [14, 15]. Further, it is indicated that small cracks (up to 1 mm) created before impregnation, do not affect hydrophobization if thoroughly impregnated [12]. All three studies conclude that hydrophobization improves the hygrothermal performance of both uninsulated and internally

<sup>\*</sup> Corresponding author.

E-mail address: [vsou@build.aau.dk](mailto:vsou@build.aau.dk) (V. Soulios).

<https://doi.org/10.1016/j.buildenv.2020.107410>

Received 6 September 2020; Received in revised form 23 October 2020; Accepted 25 October 2020

Available online 28 October 2020

0360-1323/© 2020 Elsevier Ltd. All rights reserved.



insulated walls.

However, these attempts to model the hydrophobized layer may be too simple as the hydrophobic impregnation significantly alternates the behavior of a porous building material [9,11,16–20], hence creating a “new” material with different properties. One previous attempt to simulate the hydrophobic layer as a new separate wall element has been made [21,22], but the modified material properties were based on limited experimental results or speculations.

The current study presents an improved attempt to model the hydrophobic layer based on experimental results measuring the hygric properties (presented in [9]) and thermal properties (presented in the current article) of brick. These are used as input parameters to the model and the attempt is to transfer the effect of hydrophobization from the material level to the component level through hygrothermal simulations in Delphin software [23].

The difference in thermal conductivity between dry and wet brick and mortar samples is found to be much larger [3] than presented in the thermal conductivity function in Delphin software [23]. Thus, an experimental work to determine the thermal conductivity of dry and capillary saturated brick and mortar samples is presented in order to update the Delphin thermal conductivity function.

Although the temperature and relative humidity in different points of the wall assembly of internally insulated buildings [24–27] have been monitored, the combined effect of hydrophobization with internal insulation has been measured only with mock-up walls [19,28,29]. The impact of combining hydrophobization with internal insulation in real inhabited buildings and the long term performance of such buildings through hygrothermal simulations should be further investigated. The average moisture content in the masonry, the risk of mould growth in the interface between masonry and internal insulation, and the additional potential energy savings of hydrophobization by keeping the wall dry would be important topics.

The main aim of this paper is to evaluate the hygrothermal performance when combining hydrophobization with internal insulation and to accurately model the behavior of the hydrophobic layer (labelled ‘hydrophobic model’). Serving the above-mentioned aim, the paper describes the input for the hydrophobic model and presents difference in thermal conductivity between dry and capillary saturated building materials. Further, it is validated whether the hydrophobic model captures the basic behavior of wetting and drying by duplicating in Delphin, the capillary absorption test and the drying test that have been conducted in the laboratory. Moreover, the hydrophobic model is validated with a mock-up wall through the comparison of relative humidity (RH) and temperature (T) in the interface between masonry and internal insulation. Subsequently, the effect of hydrophobization, when combined with internal insulation, is investigated, quantified by calculating the average moisture content in the masonry, the mould growth in the interface between masonry and internal insulation, the accumulated heat loss and the additional energy savings due to hydrophobization. Moreover, a parametric analysis is carried out taking into account orientation, climate, masonry and insulation thickness, hydrophobization before/after internal insulation, weak impregnation, and potential risk of wood degradation. Finally, the paper presents the measurements of RH in the interface between masonry and internal insulation of an inhabited Danish dwelling where the water repellent agents applied two years after internal insulation.

## 2. Methods

### 2.1. Hydrophobic model

#### 2.1.1. Hygric properties

The complete characterization of the hygric properties of a building material requires the definition of the moisture retention curve and the moisture permeability curve. However, extracting the curves to a full extent with the existing experimental procedures is impeded, since

liquid transport is significantly reduced as a result of hydrophobization [9–11,16–18,22,30,31]. Therefore for this study, values for hygric properties are derived from laboratory tests performed at hydrophobized samples [9]. This adjustment scales the moisture retention and permeability curves accordingly as well as the vapor permeability curve.

**2.1.1.1. Storage properties.** A previous experimental study [9] does not indicate a significant change in the moisture storage properties after hydrophobization, especially in materials with coarse pores, such as brick. In the current model, the open porosity and by extension, the moisture retention curve, are left untouched.

**2.1.1.2. Transport properties.** The transport properties change significantly in terms of reduced absorption coefficient ( $A_{cap}$ ), whereas the vapor diffusion resistance factor ( $\mu$ -value) remains almost the same both in brick and mortar [9]. Therefore, to represent a hydrophobized brick via a model that can be used for hygrothermal simulations, the absorption coefficient is reduced and this scales down the moisture permeability curve, but the moisture retention curve remains untouched. In addition, the vapor diffusion resistance factor is slightly modified to represent the small increase of  $\mu$ -value in the hydrophobic layer and this scales down accordingly the vapor permeability curve (see Table 1).

#### 2.1.2. Thermal properties

The thermal conductivity of dry and saturated brick samples was measured to illustrate the potential energy savings as a result of hydrophobization. Three different types of brick and one type of mortar were tested in a heat flow meter in dry condition and in capillary saturated condition in accordance with [32]. For measurement in dry condition, the samples were stored in an oven (70 °C) until they reach a stable mass, while for measurement in capillary saturated state, the samples were soaked in the water for 24 h. Although only the thermal conductivity of Y brick (presented in Section 2.2) is used in this study, two additional brick types: Robusta Vandersanden Belgian Brick (R brick) and Historic Danish Brick from an old building in Copenhagen (1944) (H brick) and one carbonated lime mortar type: Lime Saint-Astier NHL3.5 (L mortar), described in [9], were tested as well, to build more confidence concerning the relative difference in thermal conductivity between dry and capillary saturated building materials.

#### 2.1.3. Thickness of the hydrophobic layer

When simulating the hydrophobic layer, the impregnation depth is used as thickness. An impregnation depth of 11.4 mm was reported in Y brick impregnated with Funcosil Remmers cream 40% (FC 40%) [19], while [9] indicates that the active ingredient is spread even deeper inside the material after longer curing time and water exposure. Nonetheless, the minimum impregnation depth reported in [9] (2.4 mm) is used as base case. The effect of a deeper impregnation depth (40 mm) is also presented in section 2.5 parametric analysis.

## 2.2. Brick properties

The Yellow soft-molded Danish brick (Y brick) from Helligsø and

**Table 1**

Y brick properties in untreated (Untd) and hydrophobized condition (FC 40%).

Material property	Untd	FC 40%
Saturation moisture content ( $W_{sat}$ ) [ $m^3/m^3$ ]	0.290	0.290
Capillary absorption coefficient ( $A_{cap}$ ) [ $kg/m^2s^{0.5}$ ]	0.32	0.0009
Vapor resistance factor ( $\mu$ ) [-]	11.9	13.7
Dry thermal conductivity ( $\lambda_{dry}$ ) [W/mK]	0.63	0.63
Thermal conductivity at capillary saturation ( $\lambda_{wet}$ ) [W/(m K)]	1.47	1.47
Bulk density ( $\rho$ ) [ $kg/m^3$ ]	1643	1643
Thermal capacity ( $C_p$ ) [J/(kg K)]	942	942

Vesterled Teglværk (see Table 1) was used for hygrothermal simulations in Delphin as well as for capillary water uptake tests, and drying tests. Furthermore, the solid masonry mock-up walls used for the validation of the hydrophobic layer at the component level were constructed with the same brick (section 2.3.2). It was selected due to the available Delphin material file of the untreated brick, prepared by TU Dresden, and experimental results of Y brick impregnated with Funcosil Remmers FC cream 40% (FC 40%), a water-based silane cream [9]. These specific hygric properties are used as input for the hygrothermal simulations.

### 2.3. Experimental validation of the hydrophobic model

#### 2.3.1. Material level

After defining the methodology of simulating the hydrophobic layer based on experimental results in section 2.1, the current section validates whether the hydrophobic layer is able to capture the wetting and drying behavior at the material level.

Water uptake tests, conducted in accordance with [33,34], and drying tests were initially performed on untreated samples of Y brick and brick samples hydrophobized with FC 40% in the laboratory [9,10]. These tests are of high importance in relation to hydrophobization, since they indicate the rate of wetting and drying of the hydrophobized material compared to the untreated material. The drying test showcase the rate of drying of an untreated saturated bottom layer of one cm and an impregnated dry top layer of one cm (sample size 1x4x4 cm), while the bottom and lateral sides are sealed. The water uptake and drying tests were duplicated in a simulating environment (Delphin), aiming at achieving comparable results using the hydrophobized brick model. The drying conditions at the top surface of the top layer, both for the experimental and simulation curves are 21 °C and 53% RH.

#### 2.3.2. Component level

The hydrophobic model is also validated at the component level using a SW oriented, hydrophobized (FC 40%) mock-up wall, constructed with Y brick and air lime mortar (7.7% lime adjusted mortar, grain size 0–4 mm) to represent a Danish historic multi-story building from the period 1850–1930, internally insulated with a polyurethane foam with calcium silicate channels (iQ-therm). The wall (1 × 2 m) was built in a container segment at the Technical University of Denmark (DTU), on a test site in Kongens Lyngby, Denmark (55.79 °N, 12.53 °E) presented in [28]. The masonry wall was constructed in September 2014, and six months later iQ-therm was installed at the interior surface while it was hydrophobized externally (March 2015). Moreover, between December 2014 and April 2015 forced drying was performed by heating the indoor climate to 40–50 °C, resulting in an indoor relative humidity of 10–30%. Relative humidity and temperature sensors were used to measure the indoor and outdoor conditions of the container and the conditions in the interface between masonry and internal insulation.

A 1D-model was constructed in Delphin to emulate the container mock-up wall as described in Fig. 1 and Table 2. The Delphin files of Y

brick and air lime mortar were developed at TU Dresden based on laboratory measurements of material properties. The Delphin file of the insulation system (iQ-therm), the adhesive mortar (iQ fix), and the plaster render (iQ top) are from the Delphin material database [35]. The hydrophobized brick was modeled as a separate material with 2.4 mm thickness, as described in sections 2.2 and 2.1.

The climatic data were collected from the DTU weather station [36]. The initial moisture content in the masonry and in the air lime mortar layers corresponded to values close to 100% RH, as the initial relative humidity measurements started from this value.

For the validation, the measurement data from the sensors (RH, T) placed in the interface between masonry and internal insulation, were compared with the corresponding output from the Delphin simulations.

### 2.4. Simulation input

Three different wall configurations were studied by simulating the effect of hydrophobization (Fig. 2). The reference case is an uninsulated 350 mm masonry wall. Two insulated configurations use either a vapor-open capillary active internal insulation (calcium silicate (CaSi)) or a vapor-tight internal insulation system (mineral wool with vapor barrier), both with a thickness of 100 mm. As interior finishing, the reference wall has 10 mm of plaster and acrylic paint. The plaster layer was kept in the configurations with an insulation system, i.e. placed in the interface between masonry and internal insulation. As interior finishing, the CaSi configuration has 12.5 mm of gypsum board and a vapor open paint, while the mineral wool configuration has a vapor barrier, 12.5 mm of gypsum board, and acrylic paint. Table 3 describes the properties of materials that were included in the simulation.

Since all simulations are one-dimensional, some aspects of the construction, like mortar joints and wooden beams, were neglected. The masonry wall was thus presumed to be composed of one (untreated walls) or two (treated walls) layers of isotropic brick materials.

The climatic data were based on the Climate for Culture project [37] which contains estimations for future climate. The duration of the simulations was five years, starting January 1, 2020 (12:00 a.m.). Copenhagen was chosen as location and an south-west (SW) oriented facade was simulated as being worst-case scenario in Denmark with regard to wind-driven rain [38].

In the simulations, default values of exterior and interior boundary conditions were used. The exterior boundary conditions in Delphin simulations consist of convective heat exchange (exchange coefficient 25 W/m<sup>2</sup>K) and long- and short-wave radiation for the thermal part, and of convective vapor exchange (exchange coefficient 2\*10<sup>-6</sup> s/m) and wind-driven rain for the hygric part. The interior boundary conditions consist of convective heat exchange (exchange coefficient 8 W/m<sup>2</sup>K) and long-wave radiation and convective vapor exchange (exchange coefficient 3\*10<sup>-8</sup> s/m) for heat and moisture respectively, with constant indoor conditions (20 °C and 50 % RH). The simulations cover a simulation interval of five years, as it takes some time for the moisture

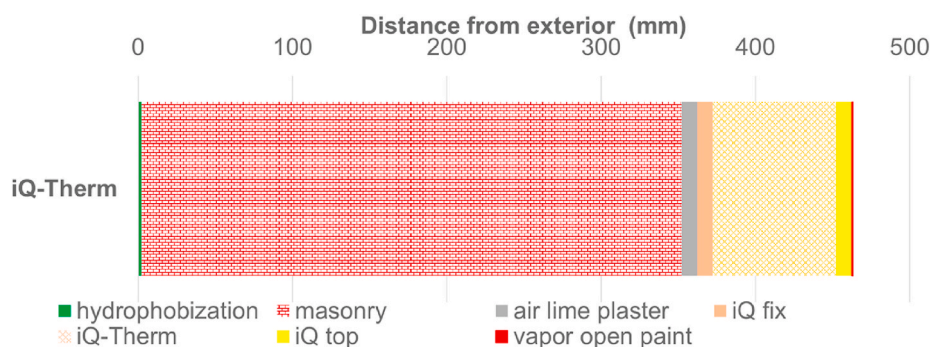
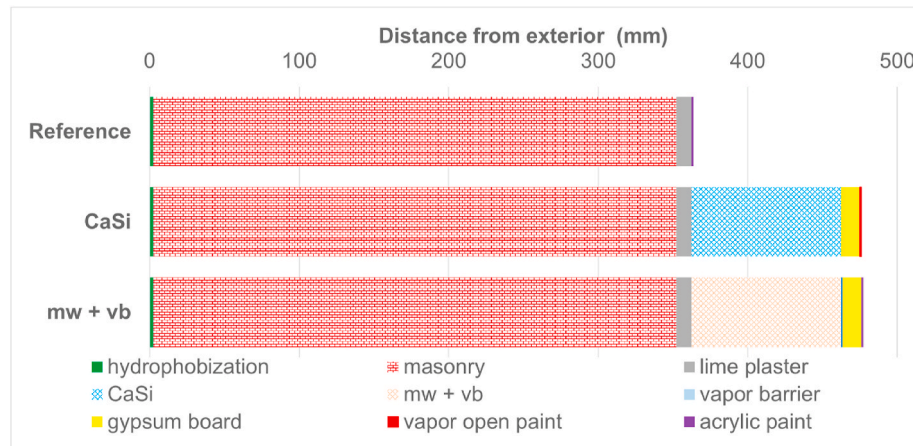


Fig. 1. Configuration of the container mock-up wall. Hydrophobization: 2.4 mm impregnation depth, masonry (Y brick): 350 mm, air lime mortar: 10 mm, iQ fix, and iQ top: 10 mm, iQ-therm: 80 mm, vapor open paint sd = 0.01 m. sd: equivalent air layer thickness ( $\mu \cdot$  material thickness).

**Table 2**

Material properties of wall elements with iQ-therm used for hygrothermal simulation. Density ( $\rho$ ), specific heat capacity ( $c_p$ ), thermal conductivity ( $\lambda$ ), moisture content at saturated condition ( $w_{sat}$ ), capillary moisture content ( $w_{cap}$ ), capillary water uptake coefficient ( $A_{cap}$ ) and water vapor diffusion factor ( $\mu$ ).

	$\rho$ [kg/m <sup>3</sup> ]	$c_p$ [J/(kg K)]	$\lambda$ [W/(m K)]	$w_{sat}$ [m <sup>3</sup> /m <sup>3</sup> ]	$w_{cap}$ [m <sup>3</sup> /m <sup>3</sup> ]	$A_{cap}$ [kg/(m <sup>2</sup> √s)]	$\mu$ [-]
Hydrophobization	1643	942	0.6	0.290	0.275	0.0009	13.7
Masonry (Y brick)	1643	942	0.6	0.290	0.275	0.32	11.9
Air lime plaster	1243	998	0.44	0.428	0.253	0.39	22.4
iQ fix	1313	863	0.496	0.277	0.2	0.005	18.7
iQ-Therm	49	1400	0.037	0.090	0.070	0.013	27
iQ top	1269	1453	0.478	0.327	0.210	0.222	13.9



**Fig. 2.** Wall configuration without (reference) and with internal insulation. Hydrophobization: 2.4 mm impregnation depth, masonry (Y brick): 350 mm, lime mortar: 10 mm, insulation system: 100 mm, gypsum board: 12.5 mm, vapor open paint sd = 0.01 m, vapor barrier (vb) sd = 70 m (mineral wool (mw) system) and acrylic paint sd = 0.18 m. sd: equivalent air layer thickness ( $\mu \cdot$  material thickness).

**Table 3**

Material properties of wall elements with CaSi or mineral wool used for hygrothermal simulation. Density ( $\rho$ ), specific heat capacity ( $c_p$ ), thermal conductivity ( $\lambda$ ), moisture content at saturated condition ( $w_{sat}$ ), capillary moisture content ( $w_{cap}$ ), capillary water uptake coefficient ( $A_{cap}$ ) and water vapor diffusion factor ( $\mu$ ).

	$\rho$ [kg/m <sup>3</sup> ]	$c_p$ [J/(kg K)]	$\lambda$ [W/(m K)]	$w_{sat}$ [m <sup>3</sup> /m <sup>3</sup> ]	$w_{cap}$ [m <sup>3</sup> /m <sup>3</sup> ]	$A_{cap}$ [kg/(m <sup>2</sup> √s)]	$\mu$ [-]
Hydrophobization	1643	942	0.6	0.290	0.275	0.0009	13.7
Masonry	1643	942	0.6	0.290	0.275	0.32	11.9
Lime plaster	1800	850	0.820	0.285	0.253	0.127	12
CaSi	351	902	0.067	0.850	0.807	1.330	9.2
Mineral wool	134	840	0.040	0.900	0.900	0.000	1
Gypsum board	850	850	0.200	0.551	0.400	0.277	10

conditions to come to a sufficiently steady response.

The primary goal of impregnating an internally insulated masonry wall at the exterior surface is the elimination or reduction of potential moisture damage. Thus, initially, the average moisture content in the masonry and mould growth at the interface between masonry and internal insulation was examined. The mould growth risk was calculated with the VTT-mould growth model [39] – being an integrated part of the Delphin simulation software – requiring values of temperature and relative humidity. The mould growth was set to have almost no decline in relation to time in order to represent the worst-case scenario and medium resistance. A side effect of hydrophobization is the energy savings achieved by keeping the wall dry. For that reason, the accumulated heat loss during the simulation period (5 years) was calculated as well as the additional energy savings induced by hydrophobization by estimating the percentage change of accumulated heat loss between treated and untreated.

## 2.5. Parametric analysis

A parametric analysis involving orientation (North, East, West, South, Southwest), climate (Copenhagen, Munich, and Milan), masonry thickness (350, 590, 710 mm) insulation thickness (60, 100, 300 mm), insulation system (CaSi, mw + vb, iQ-Therm, XPS Multipor, Kingspan), impregnation depth (2.4 and 40 mm) and strength ( $A_{cap}$  0.0009 and 0.033 [kg/m<sup>2</sup>√s]), hydrophobization before/after internal insulation represented by initial moisture content in the wall, as well as degradation of wooden beams, was conducted. The results are found in Appendix and are discussed in parallel with the base case simulations in Sections 3 and 4. To simulate the effect of hydrophobization in an already internally insulated wall, the average moisture content of the insulated wall during five years of simulation is used as the initial moisture content in the masonry at the time of becoming hydrophobized. The internally insulated hydrophobized wall is simulated for



**Fig. 3.** Location of the case building. Left: Map of Denmark, and indication of the location of the test house on the northern coast of Zealand. Right: northern façade after renovation.

another five years.

The risk of wood decay is quantified via the VTT wood decay model, which is incorporated in Delphin. The VTT wood decay model requires the conditions (temperature, relative humidity) that the wood would be subjected to during a course of time [40]. Given that the wooden beams are not part of the current one-dimensional simulations, they are approximated with the conditions at a distance of 110 mm from the exterior part of the masonry wall, which is the expected location for the edge of the wooden beam in a typical 350 mm (1½ brick) Danish wall. The risk of wood decay is also calculated in the interface between masonry and internal insulation.

## 2.6. Case study building

The case study building is located by the sea, on the coast of northern Zealand in Denmark (see Fig. 3). It's a solid masonry building constructed in 1875 with three brick layers (37 cm) on east and west facades and two brick layers on north and south facades. During 2016, the house underwent an extensive renovation, including internal insulation with 80 mm of iQ-Therm. The exterior surfaces of the building were sand-blasted during renovation and plastered with a thin layer of bank sand mortar.

In September 2018, FC cream 40% was applied with a paint roller in the specified amounts of 0.15–0.20 l/m<sup>2</sup>. The relative humidity was monitored at the interface between masonry and internal insulation; West and South facades each had one sensor installed, North and East facades each had two sensors, one placed 50 cm above the floor, and one 50 cm below the ceiling. The built-in sensors are climaSpot sensors with accuracy ±1.8% for 10–90% RH and ±4% for 0–10% and 90–100%. The relative humidity and temperature conditions have been monitored every half hour since the summer of 2016, still measuring (June 2020). The data are stored on a server provided by fugtlog.dk, and can be downloaded from a distance.

## 3. Results

### 3.1. Experimental measurements of thermal conductivity

For the tested brick and mortar types, the differences in thermal conductivity between dry and capillary saturated material are of a comparable size (Fig. 4) and for Y brick the difference is larger than given in the Delphin material file. Although Y brick is the only of the tested materials for which a Delphin material file exists, it is representative for Delphin material files concerning the relationship between thermal conductivity and moisture content (m<sup>3</sup>/m<sup>3</sup>). Therefore, compared to experimental results, thermal conductivity in wet conditions seems to be underestimated in Delphin and this can underestimate

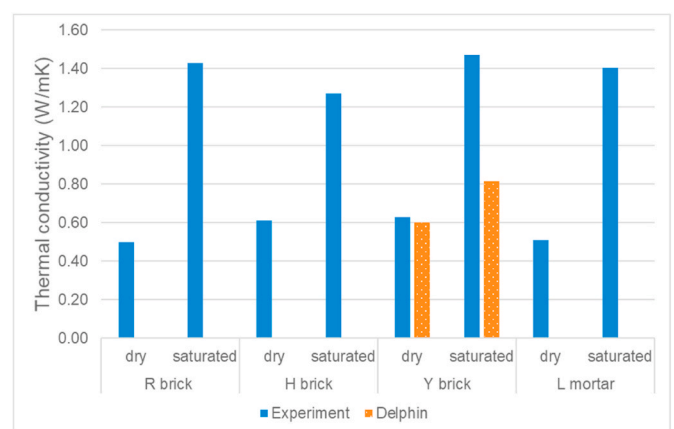


**Fig. 4.** Thermal conductivity in dry and capillary saturated building materials: Robusta Vandersanden Belgian Brick (R brick), Historic Danish Brick from an old building in Copenhagen (1944) (H brick), Yellow soft-molded Danish brick from Helligsø and Vesterled Teglværk (Y brick), Carbonated lime mortar (L mortar), all described in [9]. (For interpretation of the references to colour in this figure legend, the reader is referred to the Web version of this article.)

the percentage of energy savings that a dry wall provides after hydrophobic treatment. For this study, the heat function in the Delphin material file is therefore modified to represent the measured thermal conductivity values derived from the heat flow meter.

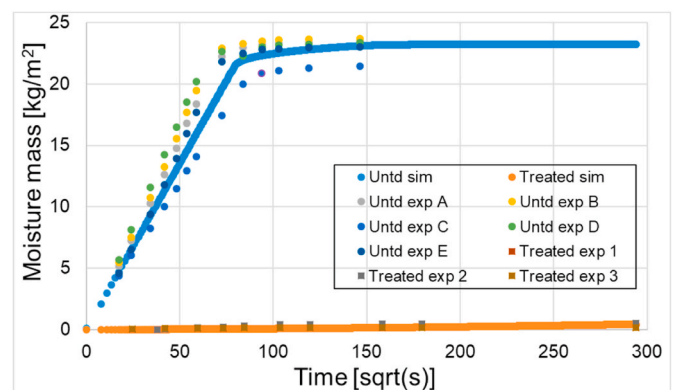


**Fig. 5.** Water uptake of Y brick. Comparison of experimental (exp) and simulation (sim) results. Untreated (Untd) and impregnated (Treated) with FC 40%.



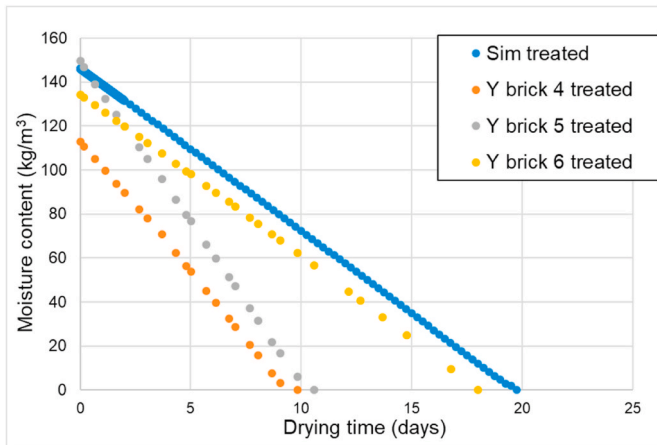


Fig. 6. Drying test of Y brick impregnated with FC 40%. Comparison of experimental (Y brick) and simulation (Sim) results.

### 3.2. Experimental validation of the hydrophobic model

#### 3.2.1. Material level

The hydrophobic model seems to capture the basic characteristics of water repellency, as illustrated in Fig. 5 comparing capillary absorption curves derived from experimental and simulation results of untreated and impregnated Y brick.

The simulation results for the drying test (Fig. 6) however are on the safe side, as the measured drying time is lower than the simulated. The difference is explained by i) the amount of agent applied on the samples used in the drying tests being different from the amount in the water uptake tests (on which the model is based), and ii) loss of water due to imperfect sealing and time needed for preparation (attaching and sealing the samples).

The samples used in the drying test were fully impregnated to represent one cm of hydrophobic layer. To ensure that they became fully

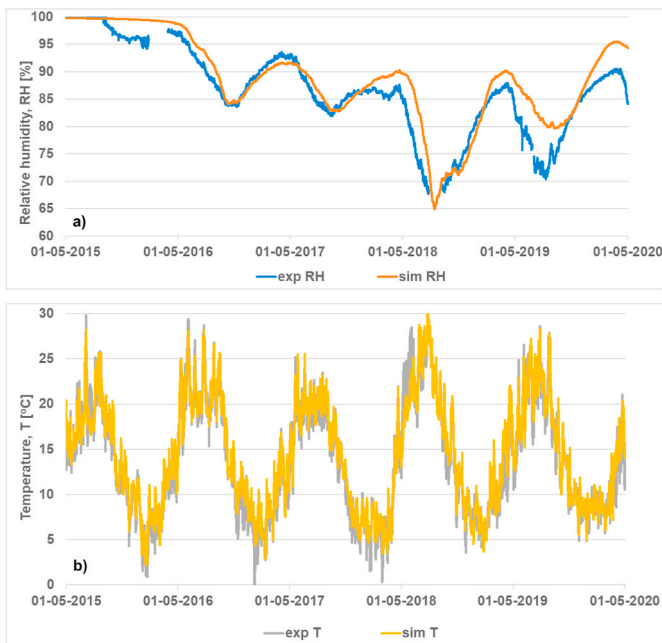


Fig. 7. Relative humidity (a) and temperature (b) in the interface between hydrophobized (FC 40%) masonry and internal insulation (IQ-therm). Comparison of experimental (exp) results from [28] and simulation (sim) results using [9] as input for Delphin. The water repellent agent was applied at the same time with the internal insulation.

impregnated, higher than recommended amounts of water repellent agent was used. This means that the hydrophobic layer needs more curing time and exposure to water to reveal an improved performance, in terms of a reduced  $A_{cap}$  [9]. For the same curing time, samples impregnated with less agent (samples for water uptake) would have a lower  $A_{cap}$ . Since liquid transfer has an impact on the drying tests, the capillary saturated samples used in the experimental drying test, dry faster than the hydrophobized brick model, by having higher  $A_{cap}$ .

#### 3.2.2. Component level

Fig. 7 compares the experimental and simulation results in the interface between masonry and internal insulation, regarding the variation in relative humidity and temperature with respect to time (5 years). The results show that there is a high level of agreement between the measured and predicted values. Moreover, it appears that the model is able to predict the peaks and bottoms of both temperature and relative humidity.

### 3.3. Simulation study

#### 3.3.1. Average moisture content in masonry

After having verified the hydrophobic model, it was used to simulate different scenarios. The first analysis examined whether hydrophobization reduces the average moisture content in the masonry layer of a wall. Fig. 8 depicts the average moisture content in brick masonry in a five year period in the uninsulated case, and when insulated with CaSi or mineral wool with a vapor barrier, either with or without hydrophobization. In the hydrophobized cases, both hydrophobization and internal insulation are present when the simulation starts. As expected, adding internal insulation increases the average moisture content in the masonry wall. By ensuring a strong hydrophobic layer (low  $A_{cap}$ ) the masonry wall becomes almost dry (less than  $6 \text{ kg/m}^3$ ), regardless of the wall configuration.

Fig. 9 shows the effect of applying a water repellent agent in parallel with or five years after internal insulation. In the second case, the accumulated moisture from the first simulation period, where the internally insulated wall was exposed to wind-driven rain, needs time to dry out, depending mainly on the insulation system and the impregnation depth of the treatment. A vapor-tight internal insulation system (mw + vb) and higher impregnation depth of the treatment results in longer drying periods.

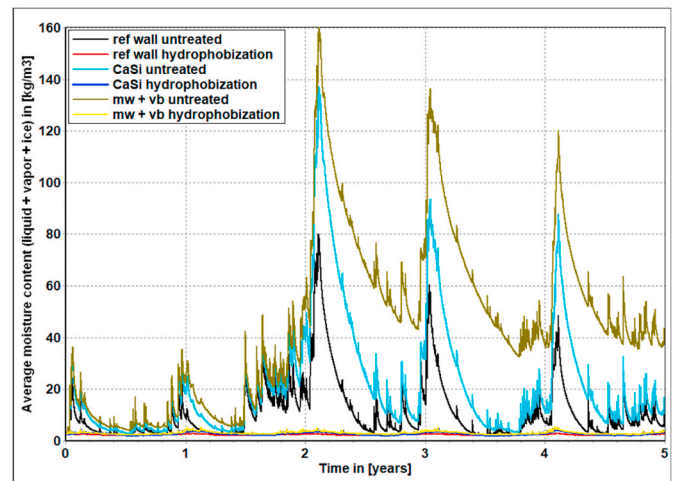
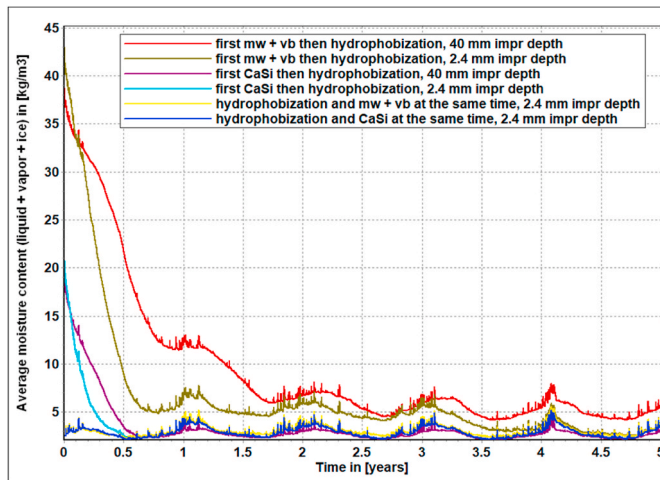


Fig. 8. Average moisture content in the masonry in SW-oriented wall configurations, including a reference wall (ref wall), a wall internally insulated with calcium silicate (CaSi), and a wall internally insulated with mineral wool and a vapor barrier (mw + vb). In all three cases with or without hydrophobization. Impregnation depth 2.4 mm. Simulation based on climate data for Copenhagen 2020–2024.



**Fig. 9.** Average moisture content in the masonry in SW-oriented wall configurations, in the case of applying a water repellent agent at the same time as internal insulation (as in Fig. 8) or five years after. Yellow and blue curves are the same as in Fig. 8, while olive and turquoise curves are the continuation of curves in Fig. 8. Impregnation depth 2.4 mm or 40 mm. The configurations include a wall internally insulated with calcium silicate (CaSi) and a wall internally insulated with mineral wool and a vapor barrier (mw + vb). Simulation based on climate data for Copenhagen 2020–2024. (For interpretation of the references to colour in this figure legend, the reader is referred to the Web version of this article.)

### 3.3.2. Mould growth in the interface between masonry and internal insulation

After showing that hydrophobization is able to reduce the average moisture content markedly, the next question is whether it is possible by hydrophobizing the masonry to reduce the risk of mould growth in the interface between masonry and internal insulation, compared to not

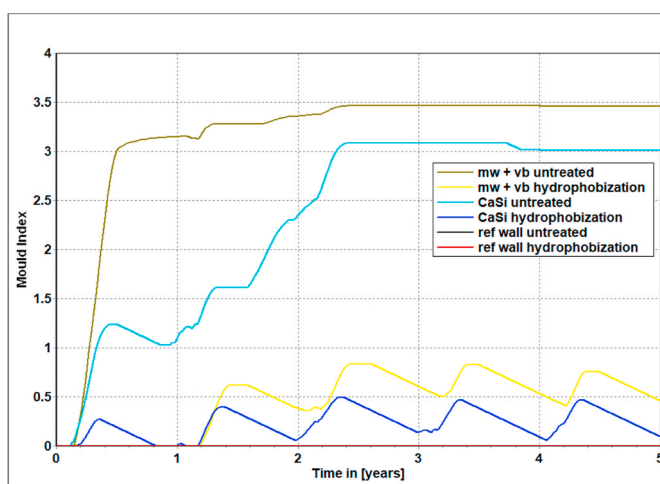


**Fig. 10.** Mould growth expressed as mould index in the interface between masonry and internal insulation in SW-oriented wall configurations, including a reference wall (ref wall), a wall internally insulated with calcium silicate (CaSi) and a wall internally insulated with mineral wool and a vapor barrier (mw + vb). In all three cases with or without hydrophobization (applied at the same time as internal insulation). Impregnation depth 2.4 mm. Simulation based on climate data for Copenhagen 2020–2024.

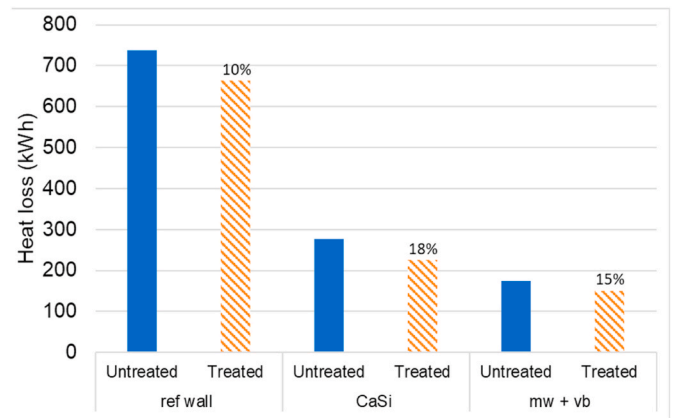


**Fig. 11.** Accumulated heat loss in SW-oriented wall configurations, including a reference wall (ref wall), a wall internally insulated with calcium silicate (CaSi), and a wall internally insulated with mineral wool and a vapor barrier (mw + vb). In all three cases without (untreated) with (treated) hydrophobization, applied at the same time as internal insulation. Impregnation depth 2.4 mm. Simulation based on climate data for Copenhagen 2020–2024. The percentages indicate the additional energy savings due to hydrophobization.

hydrophobized cases, a well-known problem in Denmark [41]. Fig. 10 verifies this. The parametric analysis, focusing on different wall orientations, climates, insulation systems, masonry, and insulation thicknesses, follows the same trend: hydrophobization reduces or eliminates the increase in mould growth risk that is caused by applying internal insulation (see Appendix).

### 3.3.3. Moisture safe energy savings

Hydrophobizing a wall as part of energy renovation is mainly done to reduce the driving rain load, however, hydrophobization in itself might contribute to energy savings (in terms of reduction in heat loss) by reducing the moisture content thereby lowering the thermal conductivity of the masonry. The accumulated heat loss after five years shows that hydrophobization of a SW-oriented façade located in Copenhagen produces energy savings as a single approach and produces additional energy savings when combined with internal insulation (Fig. 11). Additional energy savings are also present with other wall orientations in Copenhagen or if the wall is placed in Munich or Milan, however to a lesser extent (see Appendix for different orientations and climates). Further, additional energy savings increase with increasing insulation thickness, with any type of insulation. The effect is more obvious in capillary active systems where energy savings increases from 18% to 32% by replacing 100 mm of CaSi-insulation with 300 mm (see Appendix for different insulation thickness). Moreover, hydrophobization exhibits 50% additional energy savings when it is combined with Kingspan, much higher than CaSi (18%) and mineral wool (15%) (see Appendix for different insulation systems). Interestingly, a weak hydrophobic layer ( $A_{cap} 0,033 \text{ kg}/(\text{m}^2 \sqrt{\text{s}})$ ) results in energy loss instead of energy savings (see Appendix, ‘Weak impregnation’).

### 3.4. Case study building

Fig. 12 illustrates four years of monitoring of relative humidity at the interface between masonry and internal insulation in the case building. Hydrophobization lessens RH peaks but further time is needed for RH to reach lower levels due to the build-in moisture that stems from applying internal insulation two years before hydrophobization. The west façade still experiences 100% RH but RH is expected to drop like in the rest of the orientations.

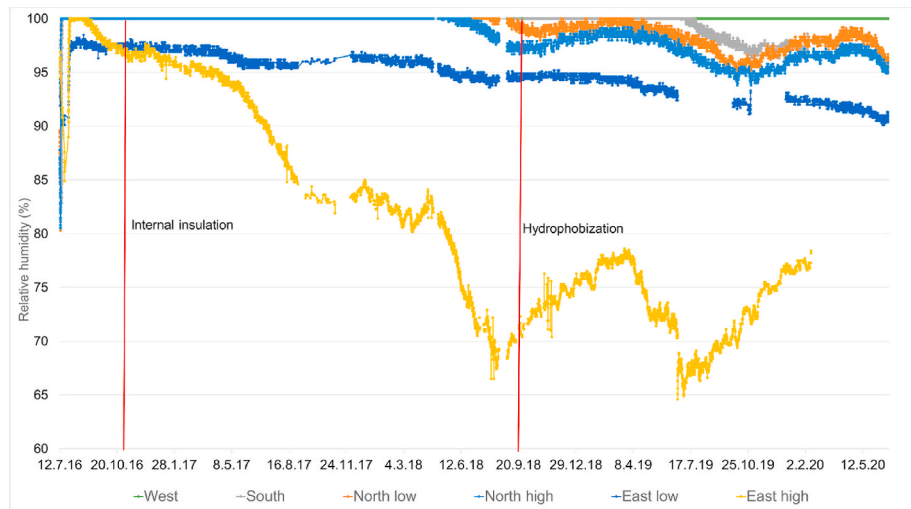


**Fig. 12.** Relative humidity during a four year period (2016–2020) in the interface between masonry and internal insulation (iQ-Therm) in case building. West (green), South (grey), North (orange and light blue), and East (blue and yellow) oriented wall configurations. (For interpretation of the references to colour in this figure legend, the reader is referred to the Web version of this article.)

#### 4. Discussion

The present study examined the effect of hydrophobization combined with internal insulation. A hydrophobized brick model has been evaluated through hygrothermal simulations and has been deemed able to predict the hygrothermal behavior both at the material level (wetting and drying) (Figs. 5 and 6) and at the component level (relative humidity and temperature in the interface between masonry and internal insulation) (Fig. 7). Numerical simulations show that hydrophobization eliminates the moisture-related problems in solid external brick masonry walls, induced by internal insulation (Figs. 8 and 10). Furthermore, a noteworthy rise in thermal conductivity between dry and saturated brick samples (Fig. 4), results in energy savings of hydrophobization as a single approach and additional energy savings when combined with internal insulation (Fig. 11). The case study building in

combination with numerical simulations illustrate that in the case where internal insulation is not part of the construction, hydrophobization should be done before or at the same time as internal insulation, otherwise, the hygrothermal response of the wall could be worse the first years but in the long-run, hydrophobization will be still beneficial (Figs. 9 and 12).

The results of this study provide support for the view that hydrophobization improves the hygrothermal performance of both uninsulated and internally insulated walls [12–14]. Although the method of excluding wind driven rain [14,15] (see Appendix, ‘Exclude wind driven rain method’) captures the wetting behavior when the capillary water absorption coefficient ( $A_{cap}$ ) of the impregnated material is close to zero, it does not capture the drying behavior (Fig. 13). Similarly, the method of reducing the absorption of wind-driven rain to 1% [13] does not capture the drying behavior when initial moisture content exists in the wall (Fig. 13).

The level of relative humidity in the interface between masonry and internal insulation has been thoroughly analyzed in the literature [5,24, 28] due to its critical nature for mould formation and interstitial condensation and the fact that it is easy to install a sensor in that location, during the renovation of a building. Relative humidity in the interface between masonry and internal insulation has three main sources of moisture: wind-driven rain transported by liquid transfer, outdoor RH, and indoor RH transported via diffusion and air leakages. Hydrophobization blocks liquid transfer but allows vapor transport [9]. The drying speed of the moisture present in the newly hydrophobized masonry wall depends on whether the hydrophobic agent is applied before or after the internal insulation is installed, although other factors also play a role, such as the hygric properties of the building materials and the climate at the location. Applying a water repellent agent at the same time as installing internal insulation can help in eliminating build-in moisture due to wind-driven rain fast enough to avoid moisture problems at a later stage (see Fig. 7). By hydrophobizing the wall after the internal insulation, longer time is needed for the build-in moisture load to be eliminated. However, hydrophobization is again beneficial in the long run (see Figs. 9 and 12).

Due to the fact that hydrophobization allows vapor transport, RH in the interface between masonry and internal insulation in a North European climate follows the seasonal wetting (winter period, high levels of outdoor RH) and drying (summer period, lower levels of RH outdoor). However, hydrophobization gradually decreases the RH peaks in the winter period due to the elimination of one of the three moisture loads

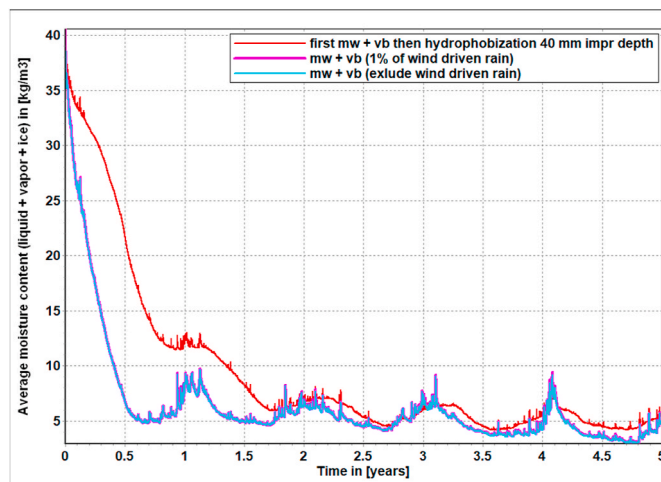


**Fig. 13.** Average moisture content in the masonry in SW-oriented wall configurations, including the method of the current article (red curve), the method of keeping 1% of wind-driven rain provided by [13] (magenta curve) and the method of excluding driving rain provided by [14,15] (turquoise curve). In all three cases, the initial moisture content represents the moisture content at hydrophobization, taking place five years after implementing internal insulation. Simulation based on climate data for Copenhagen 2020–2024. (For interpretation of the references to colour in this figure legend, the reader is referred to the Web version of this article.)

(wind-driven rain) (Figs. 7 and 12). However, in the case of a very high outdoor RH during winter or/and high internal moisture load, RH in the interface between masonry and internal insulation can reach high values even when hydrophobization has played its role in eliminating the wind-driven rain load. Given these considerations, the mould growth and interstitial condensation risk are high in cases where the levels of RH in the interface between masonry and internal insulation remain elevated (close to 100% RH) for many years after hydrophobization, during the whole year. However, the mock-up wall (Fig. 7) and five of the six sensors in the case building (Fig. 12) illustrate that after hydrophobization, the RH levels gradually decrease, following the seasonal wetting and drying. One sensor in the west façade shows 100% RH two years after hydrophobization, indicating that two years of monitoring is not enough time to draw final conclusions.

All the different internal insulation systems included in this study, vapor-tight (XPS, mw + vb, Kingspan), vapor-open (CaSi, Multisor) and vapor-tight with capillary open channels (iQ-Therm) cause the average moisture content in brick masonry wall to increase compared to the situation prior to internal insulation, but after hydrophobization the average moisture content becomes almost zero. This observation is independent of orientation and climate (see Appendix, Table A1).

Increasing the insulation thickness increases the average moisture content in the masonry but the combination of hydrophobization and internal insulation results in a moisture safe masonry wall configuration. However, a weak impregnation ( $A_{cap}$  0,033 kg/(m<sup>2</sup>√s)) results in increased moisture levels in the (un)insulated wall configurations compared to a strong impregnation ( $A_{cap}$  0,0009 kg/(m<sup>2</sup>√s)). This is due to water being able to penetrate the masonry in the case of a weak impregnation (i.e.  $A_{cap}$  0,033 kg/(m<sup>2</sup>√s)), combined with a significantly reduced drying rate, yielding in trapped moisture inside the wall. A weak impregnation (low level of water repellency) might exacerbate the hygrothermal behavior of the external wall. However, the weak impregnation ( $A_{cap}$  0,033 kg/(m<sup>2</sup>√s)) derives from a water repellent agent (water-based liquid emulsion) that improves the water repellency performance with longer curing time and water exposure, so in the long term, the  $A_{cap}$  will decrease and there will be no negative effect on the hydrothermal performance of the wall [9]. A permanent weak impregnation could arise from not cleaning the facade before impregnation [9, 18].

The most crucial properties needed to capture the hygrothermal behavior of a hydrophobized building material is the capillary water absorption coefficient and the thermal conductivity. The default thermal conductivity function used in Delphin underestimates the additional energy savings due to hydrophobization; by using the corrected thermal conductivity function of brick, energy savings in the base case scenario are 10% for the reference wall instead of 4.3% with the existing thermal conductivity function from Delphin, 18.1% instead of 15.7% for CaSi and 14.8% instead of 12% for 'mw + vb' (see Default thermal conductivity change between dry and saturated brick, Appendix, Table A1). One limitation of this study is that it does not experimentally measure the difference of thermal conductivity between dry and saturated insulation materials, and that could be larger than the one presented in Delphin library (as for brick and mortar). This affects especially the cases of capillary active insulation systems, like CaSi, which can have much higher thermal conductivity after becoming wet.

The presented work in this paper illustrates that the elimination of the rain load induces additional energy savings by keeping the whole structure dry and as a consequence, the thermal conductivity of the materials at a low (dry) level. This is also the reason why hydrophobization performs better in terms of energy savings, in climates with

high rain loads like Copenhagen (14.8% energy savings) or Munich (10.8% energy savings) than in climates with low rain loads such as Milan (1.3% energy savings) (see Different climates in Appendix, Table A1).

The results also showed that hydrophobization completely eliminates the risk of wooden beam decay in the three wall configurations, both 110 mm from the exterior part of the wall and in the interface between masonry and internal insulation (see wooden beam degradation in Table A2 Appendix). Since the conditions applied to the model correspond to those in the brick and not in the wooden beam ends, the predictions of wood degradation cannot be considered reliable and are useful only as indications regarding the possible risk of wood decay and to compare the different wall configurations.

Ever since water repellent agents were introduced as a way to treat building surfaces, one of the main hesitations has been how to deal with cracks, as they may allow water to enter the existing masonry and cause freeze-thaw damage, because of water films at the backside of the water repellent layer [42]. This may be due to the transfer of indoor air by convection through cracks to the cold masonry, where it condenses. It might also be due to rain leakage at penetrations especially at windows, small cracks that form after treatment, or large cracks present before treatment. The current and previous [9] studies indicate that vapor transport through the hydrophobic layer is still possible, making the problem of cracks less critical, but the liquid transport is still impeded.

A major limitation of the present study is the assumption that larger cracks have been repaired before treatment and small possible cracks after treatment do not go deeper than the impregnation depth. Further, that workmanship is sufficient, especially in the areas around windows and doors. The water repellency performance and the impregnation depth on the Y brick reported in this study as well as other bricks and mortars reported in [9] may be sufficient. But for buildings with other types of materials and especially monumental buildings with historical value it is recommended to extract samples of building materials from the masonry wall, before applying the water repellent treatment to the whole building and test the water repellency and the impregnation depth after treatment, as failures resulting from the use of hydrophobization have been also reported [42–44].

Due to a low exposure to wind-driven rain, hydrophobization appears unnecessary at north-oriented facades. However, they experience the lowest temperature and after internally insulating the façade the temperature of the masonry further declines. In that sense, hydrophobization is recommended as a way to reduce the possible risk of frost damage. Furthermore, the very low mould growth index in the interface between masonry and internal insulation in all the simulated cases after hydrophobization is an indication of a lower risk of interstitial condensation.

## 5. Conclusions

In this paper, the hygrothermal performance of internally insulated hydrophobized walls was studied. The developed hydrophobic model captures the main impacts of water repellent treatments. Hydrophobization decreases the moisture level and the possibility of moisture-related damage in exposed facades, successfully blocking the wind-driven rain, while it produces energy savings on its own and additional energy savings when combined with internal insulation. The presented results support the idea of hydrophobization being a missing element for a sustainable and moisture safe energy renovation of historic buildings. Moreover, the results indicate that in order for hydrophobization to be more beneficial for the wall configuration, it should be



applied before or at the same time as internal insulation to avoid moisture being trapped during the first period after installation. However, in the case where internal insulation is already part of the construction, hydrophobization can still be recommended, since it yields much better hygrothermal performance in the long run compared to the untreated internal insulated case.

Future studies should include experiments in the component level with real buildings and the hydrophobic model should be further validated by comparing the results of numerical simulations with in-situ measurements in real buildings. Moreover, 2D and probably 3D simulations, including possible cracks after treatment, would help in building more confidence about the performance of the hydrophobic treatment. Furthermore, future research would benefit from focusing on durability tests, to study the long-term effect of the water repellency. Also, life cycle cost assessment of hydrophobization in combination with internal insulation as well as the payback period and a financial analysis will contribute towards a holistic view of hydrophobization.

### Declaration of competing interest

The authors declare that they have no known competing financial interests or personal relationships that could have appeared to influence

the work reported in this paper.

### Acknowledgements

The present study is the second journal article after Ref. [9] in a series of articles reviewing hydrophobization treatment at the Department of the Built Environment, Aalborg University Copenhagen. The study is part of the project 'Moisture safe energy renovation of worth preserving external masonry walls' funded by the Danish foundations: The Landowners' Investment Foundation, Denmark, The National Building Fund, Denmark, and Realdania, Denmark. The experimental part at the material level took place at the KU Leuven Building Physics department. The first author and his supervisors express their gratitude to Professor Hans Janssen who hosted the first author during his stay. Also, Dr. Wouter Van De Walle is acknowledged for his supervision on the use of the thermal conductivity meter. We are grateful to Professor Eva B. Møller and her Ph.D. student Nickolaj Feldt Jensen from DTU Denmark, for granting us access to their experimental data of mock-up walls that were used in the validation of the hydrophobic model in the component level. We would like to offer our thanks to Dr. Tessa Kvist Hansen who contributed to the collection of the monitoring data of the case study building.

### Appendix

**Table A1**

Hygrothermal simulation results. Average moisture content ( $\text{kg/m}^3$ ), mould growth in the masonry - internal insulation interface (index), heat loss (kWh), and energy savings due to hydrophobization (%) for different simulated wall configurations. Msy thick: Masonry thickness, Insul: Insulation, Ins thick: Insulation thickness, dp: Impregnation depth, Acap: Absorption coefficient,  $\mu$ : vapor diffusion resistance factor, Clim: Climate, Orien: Orientation, mw + vb: mineral wool plus vapor barrier, CPH: Copenhagen, MUC: Munich, MXP: Milan.

Wall configuration								Numerical Results			
Msy thick mm	Insul	Ins thick mm	dp mm	Acap $\text{kg/m}^2\sqrt{s}$	$\mu$	Clim	Orien	Moisture content $\text{kg/m}^3$ (min-max)	Mould growth index	Heat Loss KWh	Energy savings %
<b>Base case scenario</b>											
350	-			0.32	11.9	CPH	SW	11.1 (2–80.1)	0	737	10.0
350			2.4	0.0009	13.4	CPH	SW	2.3 (2–3.2)	0	663	
350	CaSi	100		0.32	11.9	CPH	SW	22.1 (2.5–137.1)	3	276	18.1
350		100	2.4	0.0009	13.4	CPH	SW	2.9 (2.1–5.3)	0.5	226	
350	mw + vb	100		0.32	11.9	CPH	SW	45.5 (2.5–160.3)	3.5	175	14.8
350		100	2.4	0.0009	13.4	CPH	SW	3.1 (2.3–5.6)	1	149	
<b>Different orientations</b>											
350	-			0.32	11.9	CPH	N	2.8 (2–22.1)	0	691	1.2
350			2.4	0.0009	13.4	CPH	N	2.4 (2–3.1)	0	683	
350	CaSi	100		0.32	11.9	CPH	N	4 (2.2–24.2)	1.2	237	2.1
350		100	2.4	0.0009	13.4	CPH	N	2.9 (2.2–4.9)	0.5	232	
350	mw + vb	100		0.32	11.9	CPH	N	5.2 (2.5–25.7)	3	156	1.7
350		100	2.4	0.0009	13.4	CPH	N	3.1 (2.3–5.5)	0.9	153	
350	-			0.32	11.9	CPH	E	5 (1.9–41.7)	0	669	4.3
350			2.4	0.0009	13.4	CPH	E	2.3 (1.9–3.1)	0	640	
350	CaSi	100		0.32	11.9	CPH	E	7.5 (2.2–46.3)	2	233	6.4
350		100	2.4	0.0009	13.4	CPH	E	2.8 (2–5.1)	0.3	218	
350	mw + vb	100		0.32	11.9	CPH	E	10.2 (2.5–52.6)	3.2	155	7.1
350		100	2.4	0.0009	13.4	CPH	E	2.9 (2.2–5.5)	0.6	144	
350	-			0.32	11.9	CPH	S	9.4 (2–61.3)	0	710	9.0
350			2.4	0.0009	13.4	CPH	S	2.3 (1.9–3.1)	0	646	
350	CaSi	100		0.32	11.9	CPH	S	17.6 (2.3–107.5)	3.0	260	15.5
350		100	2.4	0.0009	13.4	CPH	S	2.8 (2.1–5.2)	0.4	218	
350	mw + vb	100		0.32	11.9	CPH	S	30 (2.5–129)	3.5	169	13.7
350		100	2.4	0.0009	13.4	CPH	S	3 (2.2–5)	0.6	146	
350	-			0.32	11.9	CPH	W	6.1 (2–51.6)	0	723	6.4
350			2.4	0.0009	13.4	CPH	W	2.4 (2–3)	0	677	
350	CaSi	100		0.32	11.9	CPH	W	11.3 (2.5–69.4)	2.6	258	10.5
350		100	2.4	0.0009	13.4	CPH	W	2.9 (2.1–5)	0.5	230	
350	mw + vb	100		0.32	11.9	CPH	W	17.1 (2.5–77.7)	3.4	170	10.3
350		100	2.4	0.0009	13.4	CPH	W	3.1 (2.3–5.7)	1	153	
<b>Different climates</b>											
350	-			0.32	11.9	MUC	SW	6.2 (2.3–34.9)	0	717	7.3
350			2.4	0.0009	13.4	MUC	SW	2.2 (1.9–2.5)	0	664	

(continued on next page)

Table A1 (continued)

Wall configuration							Numerical Results			
350	CaSi	100		0.32	11.9	MUC SW	8.6 (2.4–38.5)	2.1	251	9.9
350		100	2.4	0.0009	13.4	MUC SW	2.5 (1.9–3.5)	0.2	226	
350	mw + vb	100		0.32	11.9	MUC SW	11.4 (2.4–42.2)	3.4	167	10.2
350		100	2.4	0.0009	13.4	MUC SW	2.4 (2–3.3)	0	150	
350	-			0.32	11.9	MXP SW	2 (1.6–10.5)	0	208	1.2
350			2.4	0.0009	13.4	MXP SW	1.9 (1.6–2.5)	0	205	
350	CaSi	100		0.32	11.9	MXP SW	2.1 (1.5–10.3)	0	71	1.3
350		100	2.4	0.0009	13.4	MXP SW	2 (1.4–2.5)	0	70	
350	mw + vb	100		0.32	11.9	MXP SW	2.1 (1.7–10.5)	0	47	1.3
350		100	2.4	0.0009	13.4	MXP SW	2 (1.4–2.5)	0	46	
Different masonry thickness										
590	-			0.32	11.9	CPH SW	13.1 (2.5–67)	0	491	11.5
590			2.4	0.0009	13.4	CPH SW	2.4 (2–3.2)	0	435	
590	CaSi	100		0.32	11.9	CPH SW	25.8 (2.5–91.5)	2.5	229	17.0
590		100	2.4	0.0009	13.4	CPH SW	2.8 (2.2–4.2)	0.16	190	
590	mw + vb	100		0.32	11.9	CPH SW	37.1 (2.5–101.1)	3.4	155	13.7
590		100	2.4	0.0009	13.4	CPH SW	2.9 (2.4–4.5)	0	134	
710	-			0.32	11.9	CPH SW	14.4 (2.5–61.7)	0	422	12.1
710			2.4	0.0009	13.4	CPH SW	2.4 (2.1–3.2)	0	371	
710	CaSi	100		0.32	11.9	CPH SW	26.1 (2.5–79.3)	2.3	210	15.8
710		100	2.4	0.0009	13.4	CPH SW	2.7 (2.2–3.9)	0.07	177	
710	mw + vb	100		0.32	11.9	CPH SW	33.2 (2.5–86.5)	3.4	145	12.7
710		100	2.4	0.0009	13.4	CPH SW	2.9 (2.4–4.2)	0	127	
Different insulation thickness										
350	CaSi	60		0.32	11.9	CPH SW	19.4 (2.2–125.2)	2.8	354	14.6
350		60	2.4	0.0009	13.4	CPH SW	2.8 (2–4.8)	0.3	303	
350	mw + vb	60		0.32	11.9	CPH SW	37.5 (2.5–148.3)	3.4	259	16.8
350		60	2.4	0.0009	13.4	CPH SW	2.9 (2.2–5.1)	0.16	215	
350	CaSi	300		0.32	11.9	CPH SW	28 (2.5–161)	3.2	146	31.6
350		300	2.4	0.0009	13.4	CPH SW	3.1 (2.3–6)	0.6	99	
350	mw + vb	300		0.32	11.9	CPH SW	56.2 (2.5–178.6)	3.5	65	9.6
350		300	2.4	0.0009	13.4	CPH SW	3.4 (2.3–6.4)	1.7	59	
Different insulation systems										
350	XPS	100		0.32	11.9	CPH SW	57.4 (2.5–174.6)	3.5	122	9.3
350		100	2.4	0.0009	13.4	CPH SW	3.2 (2.3–5.9)	1.4	111	
350	iQ-Therm	100		0.32	11.9	CPH SW	34.5 (2.5–156.8)	3.5	177	20.7
350		100	2.4	0.0009	13.4	CPH SW	3.1 (2.3–5.6)	1.4	140	
350	Multipor	100		0.32	11.9	CPH SW	25 (2.5–147.2)	3.3	218	23.8
350		100	2.4	0.0009	13.4	CPH SW	3.1 (2.1–5.7)	1.4	166	
350	Kingspan	100		0.32	11.9	CPH SW	26.9 (2.5–153.3)	3.4	178	50.2
350		100	2.4	0.0009	13.4	CPH SW	3.3 (2.4–6.2)	1	89	
Weak impregnation										
350	-		2.4	0.033	13.4	CPH SW	52.4 (2.2–222.7)	2.7	876	–18.8
350	CaSi	100	2.4	0.033	13.4	CPH SW	77.7 (2.5–251.2)	3.3	399	–44.5
Default thermal conductivity change between dry and saturated brick (in Delphin)										
350				0.32	11.9	CPH SW	11.9 (2–87.8)	0	693	4.3
350	CaSi	100		0.32	11.9	CPH SW	22.5 (2.5–139.4)	3	268	15.7
350	mw + vb	100		0.32	11.9	CPH SW	45.2 (2.5–161.5)	3.5	170	12.1
Exclude wind driven rain method [13,14]										
350	-			0.32	11.9	CPH SW	2.4 (2–3.3)	0	661	10.3
350	CaSi	100		0.32	11.9	CPH SW	3.3 (2.1–7)	0.5	226	18.0
350	mw + vb	100		0.32	11.9	CPH SW	3.9 (2.5–8.8)	2.3	149	15.0
Impregnation depth										
350	-		40	0.0009	13.4	CPH SW	2.3 (2–3.1)	0	662	10.2
350	CaSi	100	40	0.0009	13.4	CPH SW	2.7 (2.1–4.6)	0.2	225	18.4
350	mw + vb	100	40	0.0009	13.4	CPH SW	2.6 (2.2–4.8)	0	149	15.0
Initial moisture content in the masonry (starting point: the average moisture content of the 5 years simulation)										
350	-		2.4	0.0009	13.4	CPH SW	2.5 (2–11)	0.06	665	9.7
350	CaSi	100	2.4	0.0009	13.4	CPH SW	3.3 (2.1–22)	1.5	230	16.7
350	mw + vb	100	2.4	0.0009	13.4	CPH SW	6.5 (2.5–45.2)	3.4	156	11.3
350	-		40	0.0009	13.4	CPH SW	2.5 (2–10.1)	0.05	665	9.8
350	CaSi	100	40	0.0009	13.4	CPH SW	3.4 (2.1–19.9)	1.8	230	16.7
350	mw + vb	100	40	0.0009	13.4	CPH SW	9.4 (4.1–40.6)	3.4	163	7.1
Initial moisture content in the masonry (starting point: the maximum moisture content of the 5 years simulation)										
350	-		2.4	0.0009	13.4	CPH SW	4.9 (2–79.5)	1.5	683	7.4
350	CaSi	100	2.4	0.0009	13.4	CPH SW	10.3 (22.9–136.2)	3.2	254	7.9
350	mw + vb	100	2.4	0.0009	13.4	CPH SW	27.3 (38.1–159.2)	3.5	171	2.7

**Table A2**  
Numerical simulation results of wooden beam degradation

Wall configuration									Wood beam loss (% of wood loss)	
Msy thick Mm	Insul	Ins thick mm	dp mm	Acap kg/m <sup>2</sup> √s	μ	Clim	Orien		110 mm from the exterior surface %	Interface between Masonry and Internal Insulation %
350	-			0.32	11.9	CPH	SW		63	0
350			2.4	0.0009	13.4	CPH	SW		0	0
350	CaSi	100		0.32	11.9	CPH	SW		85.6	0
350		100	2.4	0.0009	13.4	CPH	SW		0	0
350	mw + vb	100		0.32	11.9	CPH	SW		100	100
350		100	2.4	0.0009	13.4	CPH	SW		0	0

## References

- [1] C.A. Balaras, A.G. Gaglia, E. Georgopoulou, S. Mirasgedis, Y. Sarafidis, D.P. Lalas, European residential buildings and empirical assessment of the Hellenic building stock, energy consumption, emissions and potential energy savings, *Build. Environ.* 42 (2007) 1298–1314, <https://doi.org/10.1016/j.buildenv.2005.11.001>.
- [2] M. Jerman, I. Palomar, V. Koci, R. Černý, Thermal and hygric properties of biomaterials suitable for interior thermal insulation systems in historical and traditional buildings, *Build. Environ.* 154 (2019) 81–88, <https://doi.org/10.1016/j.buildenv.2019.03.020>.
- [3] J. MacMullen, Z. Zhang, E. Rirsch, H.N. Dhakal, N. Bennett, Brick and mortar treatment by cream emulsion for improved water repellence and thermal insulation, *Energy Build.* 43 (2011) 1560–1565, <https://doi.org/10.1016/j.enbuild.2011.02.014>.
- [4] M. Guizzardi, D. Derome, R. Vonbank, J. Carmeliet, Hygrothermal behavior of a massive wall with interior insulation during wetting, *Build. Environ.* 89 (2015) 59–71, <https://doi.org/10.1016/j.buildenv.2015.01.034>.
- [5] E. Vereecken, *Hygrothermal Analysis of Interior Insulation for Renovation Projects*, KU Leuven, 2013.
- [6] E. Vereecken, S. Roels, Wooden beam ends in combination with interior insulation: an experimental study on the impact of convective moisture transport, *Build. Environ.* 148 (2019) 524–534, <https://doi.org/10.1016/j.buildenv.2018.10.060>.
- [7] H. Janssen, B. Blocken, S. Roels, J. Carmeliet, Wind-driven rain as a boundary condition for HAM simulations: analysis of simplified modelling approaches, *Build. Environ.* 42 (2007) 1555–1567, <https://doi.org/10.1016/j.buildenv.2006.10.001>.
- [8] A. Erkal, D. D'Ayala, L. Sequeira, Assessment of wind-driven rain impact, related surface erosion and surface strength reduction of historic building materials, *Build. Environ.* 57 (2012) 336–348, <https://doi.org/10.1016/j.buildenv.2012.05.004>.
- [9] V. Soulios, E.J. de Place Hansen, C. Feng, H. Janssen, Hygric behavior of hydrophobized brick and mortar samples, *Build. Environ.* 176 (2020) 106843, <https://doi.org/10.1016/j.buildenv.2020.106843>.
- [10] V. Soulios, E.J. de Place Hansen, H. Janssen, Hygric properties of hydrophobized building materials. MATEC Web Conf., 2019, pp. 1–6, <https://doi.org/10.1051/mateconf/201928202048>, Prague.
- [11] J. Engel, P. Heinze, R. Plagge, Adapting hydrophobizing impregnation agents to the object, *Hydrophobe VIIth Int. Conf. Water Repel. Treat. Prot. Surf. Technol.* *Build. Mater.* 20 (2014) 141–150, <https://doi.org/10.12900/rbm14.20.6-0042>.
- [12] H.M. Künzel, K. Kießl, Drying of brick walls after impregnation, *Bauinstandsetzen* 2 (1996) 87–100, <https://wufi.de/literatur/Künzel,Kießl.1996-Drying.of.brick.walls.pdf>.
- [13] G.R. Finken, S.P. Bjarlov, R.H. Peuhkuri, Effect of façade impregnation on feasibility of capillary active thermal internal insulation for a historic dormitory - a hygrothermal simulation study, *Construct. Build. Mater.* 113 (2016) 202–214, <https://doi.org/10.1016/j.conbuildmat.2016.03.019>.
- [14] A. Abdul Hamid, P. Wallentén, Hygrothermal assessment of internally added thermal insulation on external brick walls in Swedish multifamily buildings, *Build. Environ.* 123 (2017) 351–362, <https://doi.org/10.1016/j.buildenv.2017.05.019>.
- [15] V. Soulios, E.J. de Place Hansen, R. Peuhkuri, Hygrothermal simulation assessment of internal insulation systems for retrofitting a historic Danish building, *Cent. Eur. Symp. Build. Phys.* (2019) 1–6, <https://doi.org/10.1051/mateconf/201928>.
- [16] J. Carmeliet, G. Hovenaghel, J. Van Schijndel, S. Roels, Moisture phenomena in hydrophobic porous building material Part 1: measurements and physical interpretations/Wechselwirkung hydrophobierter poröser Werkstoffe des Bauwesens mit Feuchtigkeit, Teil 1: messungen und physikalische Interpretationen, *Restor. Build. Monum.* 8 (2002) 165–183, <https://doi.org/10.1515/rbm-2002-5660>.
- [17] H. Kober, Water thinnable silicone impregnating agents for masonry protection. *Hydrophobe I Delft*, 1995, pp. 1–13, [http://www.hydrophobe.org/pdf/delft/I\\_3.pdf](http://www.hydrophobe.org/pdf/delft/I_3.pdf).
- [18] J. Zhao, F. Meissner, Experimental investigation of moisture properties of historic building material with hydrophobization treatment, *Energy Procedia* 132 (2017) 261–266, <https://doi.org/10.1016/j.egypro.2017.09.716>.
- [19] T.K. Hansen, S.P. Bjarlov, R.H. Peuhkuri, K.K. Hansen, Performance of hydrophobized historic solid masonry – experimental approach, *Construct. Build. Mater.* 188 (2018) 695–708, <https://doi.org/10.1016/j.conbuildmat.2018.08.145>.
- [20] E.B. Møller, C. Rode, Hygrothermal Performance and Soiling of Exterior Building Surfaces, Technical University of Denmark, 2004, <https://orbit.dtu.dk/files/5285541/byg-r068.pdf>.
- [21] V. Metavitsiadis, V. Soulios, H. Janssen, S. Roels, Wall hydrophobization and internal insulation: the impact of impregnation strength and depth on moisture levels and moisture damages. *Hydrophobe III*, 2017, pp. 69–76, accessed, <http://www.hydrophobe.org/pdf/hongkong/C-1-1.pdf>. (Accessed 26 April 2020).
- [22] T. Kvist Hansen, S.P. Bjarlov, R. Peuhkuri, Moisture transport properties of brick – comparison of exposed, impregnated and rendered brick. *Proc. Int. RILEM Conf. - Mater. Syst. Struct. Civ. Eng. Segm.*, Moisture Mater. Struct., 2016, pp. 351–360, in: [http://orbit.dtu.dk/ws/files/128040737/Pages\\_from\\_Moisture\\_conf\\_proceedings\\_3.pdf](http://orbit.dtu.dk/ws/files/128040737/Pages_from_Moisture_conf_proceedings_3.pdf).
- [23] A. Nicolai, J. Grunewald, User Manual and Program Reference Delphin, 5, 2015, pp. 1–171, [http://bauklimatik-dresden.de/downloads/documentation/DELPHIN5-reference\\_manual\\_en.pdf](http://bauklimatik-dresden.de/downloads/documentation/DELPHIN5-reference_manual_en.pdf).
- [24] T. Odgaard, S.P. Bjarlov, C. Rode, Interior insulation – experimental investigation of hygrothermal conditions and damage evaluation of solid masonry façades in a listed building, *Build. Environ.* 129 (2018) 1–14, <https://doi.org/10.1016/j.buildenv.2017.11.015>.
- [25] M. Harrestrup, S. Svendsen, Internal insulation applied in heritage multi-storey buildings with wooden beams embedded in solid masonry brick façades, *Build. Environ.* 99 (2016) 59–72, <https://doi.org/10.1016/j.buildenv.2016.01.019>.
- [26] T.K. Hansen, S.P. Bjarlov, R.H. Peuhkuri, M. Harrestrup, Long term in situ measurements of hygrothermal conditions at critical points in four cases of internally insulated historic solid masonry walls, *Energy Build.* 172 (2018) 235–248, <https://doi.org/10.1016/j.enbuild.2018.05.001>.
- [27] M. Morelli, L. Ronby, S.E. Mikkelsen, M.G. Minzari, T. Kildemoes, H.M. Tommerup, Energy retrofitting of a typical old Danish multi-family building to a “nearly-zero” energy building based on experiences from a test apartment, *Energy Build.* 54 (2012) 395–406, <https://doi.org/10.1016/j.enbuild.2012.07.046>.
- [28] N.F. Jensen, T.R. Odgaard, S.P. Bjarlov, B. Andersen, C. Rode, E.B. Møller, Hygrothermal assessment of diffusion open insulation systems for interior retrofitting of solid masonry walls, *Build. Environ.* 2020. Article in press.
- [29] T. Odgaard, S.P. Bjarlov, C. Rode, Influence of hydrophobation and deliberate thermal bridge on hygrothermal conditions of internally insulated historic solid masonry walls with built-in wood, *Energy Build.* 173 (2018) 530–546, <https://doi.org/10.1016/j.enbuild.2018.05.053>.
- [30] J. Sadauskienė, J. Ramanaukas, V. Stankevicius, Effect of hydrophobic materials on water impermeability and drying of finish brick masonry, *Issn Mater. Sci.*, 2003, pp. 1320–1392, [https://www.researchgate.net/profile/Jolanta\\_Sadauskiene/publication/237779777\\_Effect\\_of\\_Hydrophobic\\_Materials\\_on\\_Water\\_Imp permeability\\_and\\_Drying\\_of\\_Finish\\_Brick\\_Masonry/links/53fb1c580cf27c365cf06ef8.pdf](https://www.researchgate.net/profile/Jolanta_Sadauskiene/publication/237779777_Effect_of_Hydrophobic_Materials_on_Water_Imp permeability_and_Drying_of_Finish_Brick_Masonry/links/53fb1c580cf27c365cf06ef8.pdf).
- [31] A.G. Momeni, Silblock Wms Technical Data Sheet, 1–4, 2011, [https://www.momentive.com/docs/default-source/productdocuments/silblock-wms/silblock-wms-mb-indd.pdf?sfvrsn=d50e61c\\_14](https://www.momentive.com/docs/default-source/productdocuments/silblock-wms/silblock-wms-mb-indd.pdf?sfvrsn=d50e61c_14).
- [32] ASTM Int, C518-15: standard test method for steady-state thermal transmission properties by means of the heat flow meter apparatus, *ASTM Int* 4 (2015) 1–15, <https://doi.org/10.1520/C0518-10.2>.
- [33] ISO 15148, Hygrothermal Performance of Building Materials and Products Determination of Water Absorption Coefficient by Partial Immersion, 2002, pp. 1–14. English version of DIN EN ISO 15148.
- [34] C. Feng, A.S. Guimarães, N. Ramos, L. Sun, D. Gawin, P. Konca, C. Hall, J. Zhao, H. Hirsch, J. Grunewald, M. Fredriksson, K.K. Hansen, Z. Pavlík, A. Hamilton, H. Janssen, Hygric properties of porous building materials (VI): a round robin campaign, *Build. Environ.* 185 (2020), <https://doi.org/10.1016/j.buildenv.2020.107242>.
- [35] A. Nicolai, J. Grunewald, J.J. Zhang, Recent improvements in HAM simulation tools: Delphin 5/CHAMPS-BES. *Conf. Proc. 12th Symp. Build. Phys.*, 2007, pp. 866–876, [https://www.researchgate.net/profile/Andreas\\_Nicolai/publication/278673185\\_Recent\\_improvements\\_in\\_HAM\\_simulation\\_tools\\_Delphin\\_5\\_CHAMPS-BES/links/558296eb08aeab1e4666fbad/Recent-improvements-in-HAM-simulation-tools-Delphin-5-CHAMPS-BES.pdf](https://www.researchgate.net/profile/Andreas_Nicolai/publication/278673185_Recent_improvements_in_HAM_simulation_tools_Delphin_5_CHAMPS-BES/links/558296eb08aeab1e4666fbad/Recent-improvements-in-HAM-simulation-tools-Delphin-5-CHAMPS-BES.pdf).
- [36] DTU Climate Station Data, The Technical University of Denmark, Department of Civil Engineering, 2020, <http://climatestationdata.byg.dtu.dk/>.
- [37] Frannhofer, Climate for culture. *www.climateforculture.eu*, 2015.
- [38] T.K. Hansen, S.P. Bjarlov, R. Peuhkuri, The effects of wind-driven rain on the hygrothermal conditions behind wooden beam ends and at the interfaces between internal insulation and existing solid masonry, *Energy Build.* 196 (2019) 255–268, <https://doi.org/10.1016/j.enbuild.2019.05.020>.
- [39] S.E. Viitanen, T. Toratti, L. Makkonen, S. Thelander, T. Isaksson, E. Früwald, J. Jermer, F. Englund, Modelling of service life and durability of wooden structures. 9th Nord. Symp. Build. Phys., Tampere, Finland, 2011.

- [40] H. Viitanen, T. Toratti, L. Makkonen, R. Peuhkuri, T. Ojanen, L. Ruokolainen, J. Räisänen, Towards modelling of decay risk of wooden materials, *Eur. J. Wood Prod.* 68 (2010) 303–313, <https://doi.org/10.1007/s00107-010-0450-x>.
- [41] M. Morelli, E.B. Møller, Energy savings and risk of mold growth in apartments renovated with internal insulation, *Sci. Technol. Built Environ.* 25 (2019) 1199–1211, <https://doi.org/10.1080/23744731.2019.1629241>.
- [42] G. Hilbert, H. Neumann, E. Wendler, Hydrophobization – one target , several possibilities, *Restor. Build. Monum.* 18 (2012) 3–12, <https://doi.org/10.1515/rbm-2012-6495>.
- [43] A.E. Charola, Water repellents and other “ protective ” Treatments : a critical review. *Hydrophobe III. 3rd Int. Conf. Surf. Technolgy with Water Repel. Agents*, Aedif. Publ., 2001, pp. 3–20. [http://www.hydrophobe.org/pdf/hannover/III\\_01.pdf](http://www.hydrophobe.org/pdf/hannover/III_01.pdf).
- [44] R.P.J. van Hees, The performance of surface treatments for the conservation of historic brick masonry, *Compat. Mater. Prot. Eur. Cult. Herit.* 2 (1998) 279–287.



## SUMMARY

Denmark is targeting to be independent of fossil fuels by the year 2050. Although the use of renewable energy sources will be increased, it also requires the energy demand from buildings to be reduced. Further, the maintenance of cultural heritage is of primary importance, which often leaves internal insulation as the only feasible option. However, internal insulation is not necessarily moisture safe in Denmark, mainly due to the high wind-driven rain load. A transparent coating for exterior use in buildings could be the solution.

This PhD thesis investigates whether hydrophobization is able to create a transparent coating against rain by leaving the wall elements, brick and mortar, to breathe. It also investigates whether this transparent coating can stay durable in the long run. Based on these studies it discusses whether a robust energy renovation of solid masonry walls is possible by combining hydrophobization with internal insulation.